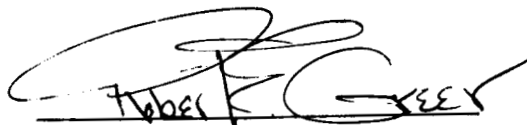SD 69-329
Volume 2

S-II-8 STATIC FIRING
FINAL TEST
REPORT

20 June 1969

Approved by

Robert E. Greer
Vice President and
S-II Program Manager

SPACE DIVISION
NORTH AMERICAN ROCKWELL CORPORATION

SD 69-329
Volume 2

S-II-8 STATIC FIRING
FINAL TEST
REPORT

20 June 1969

Approved by

Robert E. Greer
Vice President and
S-II Program Manager

SPACE DIVISION
NORTH AMERICAN ROCKWELL CORPORATION

FOREWORD

This report presents the results and analyses of
data obtained during the S-II-8 static firing test
program conducted by the Space Division of North American
Rockwell Corporation at the Mississippi Test Facility
under Contract NAS7-200. This document fulfills the
requirements of Line Item 131 of SID 61-366B.

Volume 1 of this report evaluates stage and sub-
system performance during acceptance static firing in
terms of specific test objectives on the basis of a
quick-look analysis of test data.

Volume 2 (this document) presents a more detailed
evaluation of stage and subsystem performance for the
full duration of the S-II-8 acceptance static firing
test. Applicable flight performance predictions also
are presented.

TECHNICAL REPORT INDEX/ABSTRACT

ACCESSION NUMBER						DOCUMENT SECURITY CLASSIFICATION	
						UNCLASSIFIED	

TITLE OF DOCUMENT	LIBRARY USE ONLY
S-II-8 STATIC FIRING FINAL TEST REPORT (VOLUME 2)	

AUTHOR(S)
S-II ENGINEERING

CODE	ORIGINATING AGENCY AND OTHER SOURCES	DOCUMENT NUMBER
QN085057	SPACE DIVISION OF NORTH AMERICAN ROCKWELL CORPORATION, SEAL BEACH, CALIFORNIA	SD 69-329 VOLUME 2

PUBLICATION DATE	CONTRACT NUMBER
20JUN69	NAS7-200

DESCRIPTIVE TERMS
*STATIC FIRING SYSTEM ANALYSIS, *PREDICTED STAGE FLIGHT PERFORMANCE

ABSTRACT

VOLUME 1 OF THIS REPORT PRESENTS THE S-II-8 STAGE AND SUBSYSTEM
ACCEPTANCE TEST PERFORMANCE DURING THE STATIC FIRING CONDUCTED AT
THE MISSISSIPPI TEST FACILITY ON 8 APRIL 1969. THE TEST
CONFIGURATION SIMULATED THE SATURN V COUNTDOWN, S-IC STAGE BOOST,
AND S-II STAGE BOOST AS CLOSELY AS GROUND CONDITIONS WOULD PERMIT.
VOLUME 2 (THIS REPORT) PRESENTS A MORE DETAILED EVALUATION OF
STAGE AND SUBSYSTEM PERFORMANCE. WHERE APPLICABLE, FLIGHT
PERFORMANCE PREDICTIONS ALSO ARE GIVEN.

CONTENTS

ILLUSTRATIONS

TABLES

SUMMARY

This section contains a summation of the S-II-8 stage and individual systems performance during the full-duration acceptance static firing test A2-546-8A-69, conducted at the Mississippi Test Facility on 8 April 1969. This was the first S-II stage firing programmed for cutoff of the center engine prior to outboard engines cutoff. The change was made to obtain data prior to the AS-505 flight mission, on the effects of early center engine cutoff.

Volume 1 of this report presents the stage and systems performance in relation to the static firing test acceptance criteria. Test operations and chronology are also contained in Volume 1.

STAGE PERFORMANCE

The S-II-8 was capable of accepting and responding satisfactorily to inputs from the simulated airborne instrumentation unit (IU) computer event sequencer. A close agreement was obtained between the static firing test sequence and the planned event sequence time for the S-II portion of the AS-508 flight mission.

The AS-508 mission trajectory was simulated using predicted and actual static firing engine thrust and propellant flowrates. A velocity loss at S-II/S-IVB separation of 36.6 feet per second was caused primarily by weight differences between predicted and static firing data at S-II outboard engines cutoff. At engine cutoff the pressurant gas was 246 pounds greater-than-predicted and the propellant residual was 1965 pounds greater-than-predicted.

PROPULSION SYSTEM

Servicing and Conditioning

Engine Purges

The J-2 engine purge requirements were satisfied before propellant loading and during engine conditioning, except for the thrust chamber jacket helium purge. The thrust chamber jacket helium purge pressure was below the required level at the stage umbilical, but met stage/engine interface requirements.

Propellant Loading

The LH_2 tank preconditioning was accomplished satisfactorily during the S-II-8 tanking and static firing tests, although a LOX loading temporary hold at the 40 percent level was performed to fulfill the -50 F preconditioning requirement. The propellant loads, based on flowmeter integration, were 0.2 percent less LOX mass and 1.08 percent higher LH_2 mass than predicted.

Start Tank and Helium Tank Conditioning

The engine start tank temperatures and pressures met the prelaunch and engine start requirements. The engine helium tank conditions at prelaunch and engine start were satisfactory and the new requirement for a continuous purge on the LOX dome after center engine cutoff was satisfied.

Engine Thrust Chamber Chill

Although instrumentation problems developed during the static firing the chamber temperatures at engine start were well within the redline band. Instrumentation problems will be corrected during post-static firing checkout and it is expected that no problems will be experienced during the CDDT.

Propellant Tanks Pressurization

Both the LOX and LH_2 tanks were prepressurized satisfactorily. Auxiliary GH_2 pressure was required due to a failure of the LH_2 prepressurization solenoid valve in the S7-41. LOX and LH_2 tank ullage pressures remained within allowable limits and provided satisfactory NPSH at the engine inlets at simulated liftoff and engine start. The LH_2 tank vent valve cracking test verified proper operation of the vent valves.

Recirculation Systems

The LOX and LH_2 recirculation systems satisfactorily conditioned the engines for simulated liftoff and engine start. The helium injection system performed satisfactorily even though the helium injection regulator and low pressure relief valve has not functioned properly during the pre-static firing checkout operations. The malfunctioned components were replaced after static firing.

Propulsion System Start and Mainstage Operation

Start Transients

All J-2 engines provided satisfactory thrust buildup rates. All parameters responded normally during the transition period.

Mainstage Operation

Engine mainstage performance was satisfactory throughout the engine firing of 384.74 seconds. An average stage thrust level of 1,164,000 pounds was produced during high EMR. This was reduced after center engine cutoff and EMR shift. Although minor problems (i.e., turbine seal drain leak, engine pneumatic regulator pressure measurement) were reported, the operation was considered highly successful.

Engine Cutoff

Analysis of all data gathered during both S-II-7 and S-II-8 acceptance static firing tests has resulted in the following set of conclusions relevant to the results of center engine cutoff.

1. Center engine oscillation buildup encountered during S-II-7 static firing was eliminated during S-II-8 static firing by shutdown of the center engine.

2. Center engine vibration measurements indicated a substantial decrease in oscillation amplitude subsequent to center engine cutoff (CECO).

3. Outboard engine (Engine 1) measurements indicated a decrease in oscillation amplitude subsequent to CECO.

4. All S-II-8 measurements indicated a further decay in oscillation amplitude starting at PU step at 325 seconds and reaching an insignificant level at 340 seconds.

Propellant Management

Open-loop propellant utilization (PU) system operation was successfully demonstrated. Performance of the propellant management system (PU loading mass indication, propellant level indication, and engine cutoff functions) was considered highly satisfactory. PU valve movement off the high EMR and low EMR extreme positions occurred exactly at the predicted times. LOX depletion ECO occurred at ESC+384.74 seconds versus ESC+388.20 predicted, utilizing a nominal 1.0 second time delay. PU system error at engine cutoff was +2350 pounds versus a +4500 pounds tolerance.

Pressurization System

Pressurization System performance was satisfactory throughout. LOX step pressurization was initiated at 100 seconds after engine start to increase NPSH near the end of S-II burn. System operation was as expected and increased LOX tank ullage pressure above the regulator band to just below the vent valve crack pressure. LOX ullage pressure then decreased to within the regulator range after EMR shift when the heat exchangers become saturated. LH_2 tank ullage pressure was also maintained satisfactory throughout the firing. Vent valve operation was as expected during simulated S-IC boost and S-II mainstage operation.

LOX NPSH was below the minimum requirement at engine cutoff due to a planned lower than normal depletion level at engine cutoff.

Propellant Feed System

The propellant feed system operated satisfactorily, however some instances of LH_2 prevalve position signal flickering were observed.

Valve Actuation System

The valve actuation system performance was normal and satisfactory.

ENGINE ACTUATION SYSTEM

The engine actuation system performed satisfactorily throughout the acceptance static firing test. Servoactuator responses to step-position gimbaling commands were both accurate and stable. Frequency response characteristics of the actuators to sinusoidal gimbaling commands showed that the actuator phase lag angles at 1 Hertz were well within the acceptance requirement. The system operating temperatures, pressures and actuator forces were as expected for the static firing environment and gimbaling operations.

ELECTRICAL SYSTEMS

Electrical Power

The electrical power system performed in a normal manner during all phases of the test. All stage bus voltages were within limits during the test and all bus currents were normal and followed predicted load profiles favorably. The LH_2 recirculation system inverters performed within design requirements during the engine chilldown period.

Emergency Detection System

Engine thrust-ok pressure switches were activated by variations in pressure in the main oxidizer injection lines indicating normal switch operation for thrust-ok circuits.

Separation System

The Mod II switch selector was sequenced during the static firing and performed within design requirements with no malfunctions. The electrical portion of the separation system was sequenced during the static firing and performed within design requirements except that it did not receive an all-engine cutoff signal from the LOX 2-out-of-5 dry cutoff circuitry as expected. This cutoff signal is utilized for triggering the two S-II/S-IVB separation and the two S-II/S-IVB retrorocket firing units. The LOX 2-out-of-5 dry cutoff signal went back to off (wet) 0.589 seconds after it came on (dry), which was 0.446 seconds prior to the time of switch selector S-II/S-IVB separation. In flight a backup cutoff signal (switch selector channel 18) would have provided the cutoff signal for triggering the four S-II/S-IVB firing units.

A safe command was sent approximately 32.1 seconds after engine start, which removed the required power from the range safety command receivers and decoders. The safe command was removed approximately 4.0 seconds later and internal power transfer applied, restoring power to the receivers and decoders.

- 4 -

MEASUREMENT, TELEMETRY, AND RF SYSTEMS

Measurements System

The performance of the measurement system was satisfactory. Seven measurement failures occurred. Reasonable data were received on 98.6 percent of the active measurements throughout the static firing test. The requirement that 95 percent of the active measurements present reasonable data was exceeded.

Radio Frequency (RF) Systems

All RF subsystems performed satisfactorily and within specification limits. The RF power output of the three RF assemblies met the requirements for minimum power (28 watts) at the directional coupler.

The antenna system voltage standing wave ratio (VSWR), calculated from forward and reflected RF power outputs measured at the directional coupler, was less than the maximum allowable ratio of 2 to 1.

Telemetry Systems

The performance of the PCM/FM and the two FM/FM telemetry links was satisfactory and within specification limits. The PCM encoding accuracy for 0 and 100 percent of full-scale output was verified on all applicable time division multiplexer (TDM) channels. All 5-volt dc reference power supply outputs and temperature bridge dc power supply outputs were verified to meet amplitude and voltage drift specifications. All five dc voltage levels were received within specification limits during inflight calibration of the FM/FM telemetry links.

INSULATION

S-II-8 was the first stage completely covered with spray foam insulation on the fuel tank sidewall and the forward skirt. Purge circuits were installed only on the forward bulkhead uninsulated area, the common bulkhead, and the J-ring. The leak detection function was deleted from the remaining purge circuits.

Performance of the insulation was excellent during both the cryogenic proof pressure test and the static firing. Some debonding occurred between the cork facing sheet and the foam insulation around fuel feedline elbow cavities, and between the honeycomb rails and the fuel tank wall. All defects were readily repairable.

VIBRATION AND ACOUSTICS

Measurement of the general vibroacoustic environment of the stage was not performed on S-II-8, nor will it be on subsequent stages. Special dynamic instrumentation was installed in and around the aft section of the stage to assess the low frequency (18 Hertz range) oscillations which were first noted on the AS-503 mission. Data showed that the advance cutoff of the center engine successfully eliminated the previous resonance buildups.

SD 69-329

THRUST STRUCTURE COMPLIANCE

The measured change in engine alignment for the S-II-8 during static firing averaged 0.6 degree in a plane for the high EMR thrust level before center engine cut-off (CECO), and 0.4 degree afterwards. The corresponding cross-corner deflections were: at sea level, 0.9 degree before CECO and 0.6 degree afterwards; and at altitude, 1.3 degrees before CECO and 0.9 degrees afterwards. The greatest in-flight compliance deflection is therefore predicted to be 1.3 degrees prior to CECO. These data are applicable to the S-II-6 through -10 stages as well, because the thrust structure design is common to each of these stages. The engine pre-cant angle will be changed to 1.3 degrees from 2.3 degrees for S-II-7 through S-II-10 by authorization of ECP 6348. The 2.3 degrees pre-cant angle was based on the thrust structure design which existed prior to changes implemented by ECP 5644.

1.0 STAGE PERFORMANCE

TEST EVALUATION

Predicted S-II-8 Flight Performance

The nominal AS-508 trajectory is based on a vehicle launch from Cape Kennedy Complex 39 along a 72 degree launch azimuth. Complete burns of the S-IC and the S-II stages and a partial burn of the S-IVB will boost the vehicle into a 100 nautical mile circular parking orbit. An optimal closed-loop uidance system will steer the vehicle into the parking orbit and shut down the S-IVB when orbital velocity has been attained. Automatic adjustment of the S-IVB burning period will compensate for off-nominal performance excursions of the first two stages. After the vehicle has coasted around the parking orbit to await proper lunar alignment geometry, the S-IVB will reignite and boost the payload up to translunar injection velocity.

Propulsion parameters obtained from static firing test A2-546 were used in a computer program to produce a simulated trajectory to verify the ability of the S-II-8 stage to perform the AS-508 mission. Comparisons between this simulated trajectory and the predicted flight were based on the following performance criteria:

1. Vehicle velocity at S-II/S-IVB separation

2. S-IVB propellant required to achieve translunar injection

To assure a realistic comparison, no changes were made in the S-IC predicted data, the S-IVB predicted data, or the S-II iterative guidance pre-settings used for computation of the trajectories. However, other S-II performance parameters were changed to reflect the results of Test A2-546. Static firing values of thrust (corrected to altitude), flowrate histories, residual propellant weight, tank pressurant gas weights and burned propellant weights were used to compute the simulated trajectory. The comparisons between the simulated S-II-8 stage thrust, flowrate, and specific impulse histories and the predicted values are shown in Figure 1-1. The weight statements for the two trajectories are presented in Table 1-1. It has been assumed that the AS-508 flight will include an early S-II center engine cutoff as was done during the S-II-8 static firing.

Use of A2-546 static firing test data resulted in a vehicle velocity at S-II/S-IVB separation that was approximately 36.6 feet per second less than the predicted velocity. To compensate for the S-II stage performance loss, approximately 429 additional pounds of S-IVB propellant were burned to achieve translunar injection (Table 1-2). It should be noted that the lower performance is due primarily to the fact that the amount of propellant burned was 2135 pounds less than predicted and the vehicle weight at S-II cutoff was 2211 pounds greater than predicted (Table 1-2).

Differences between predicted and actual static firing engine thrust and propellant flowrate caused a velocity gain of 26.9 feet per second, as shown in Table 1-2. This velocity increase was caused by the slightly higher-than-predicted static firing thrust values at low mixture ratio (Figure 1-1).

Table 1-1. Saturn V AS-508 Vehicle Weight Comparison

Item	Weight for Trajectory Simulation	
	Predicted Static Test (pounds)	Actual Static Test (pounds)
Saturn V weight at translunar Injection	136615	136083
S-IVB second burn propellant	153103	152506
Weight loss in orbit	5005	5005
Saturn V weight in parking orbit	294723	293593
S-IVB first burn propellant	72353	73479
Saturn V weight at S-IVB ignition	367076	367076
Total weight jettisoned at S-II/S-IVB separation	104510	106721
(S-II stage contribution to total weight jettisoned)	96375	98586
S-II burn propellant	965111	962976
S-IC/S-II interstage	8750	8750
Launch escape system	8900	8900
Saturn V weight at S-II ignition	1454347	1454312
S-IC stage weight total	4948249	4948249
Saturn V weight at S-IC liftoff	6402596	6402561

Table 1-2. Performance Variations

Item	Change in Vehicle Burnout Velocity at S-II/S-IVB Separation (feet per second)	Change in S-IVB Propellant Burned to Translunar Injection (pounds)
Thrust and flowrate history	+26.9	+251
Ignition weight difference (-37 lb gas, +35 lb liquid)	+ 0.0	0
Cutoff weight difference (+246 lb gas, +1965 lb liquid) Propellant burned difference (-2135 lb)	-63.5	-670
Total	-36.6	-429

SEQUENCE OF EVENTS

An autosequence programmer was used to simulate the flight sequence coded commands from the airborne instrument unit computer of the Saturn V timing system. Event times on this programmer have been established using the flight sequence as a guide but modified to satisfy the static firing functional requirements. Use of this programmer resulted in close agreement with the operational flight sequence, including a time allowance for S-IC stage boost. The C7-77 discrete response data have been used to determine the test sequence of event times. The original C7-77 data are listed in real time, making it difficult to examine the relative event sequencing. Therefore, all event times shown in Table 1-3 are referenced to the simulated S-IC liftoff time. The static firing data is compared in Table 1-3 with stage flight sequencing times listed in ICD40M33627 (latest available flight ICD for the S-II-7 stage at the time of static firing). The S-II-8 ICD was not available at the time of static firing.

The test times shown in Table 1-3 are the times that the first switch Selector-read command was given for each event after register verification. Comparison of results show good agreement between the ICD and static firing test sequences. For the static firing, the hydraulic accumulators must be unlocked prior to the J-2 engines start command. In actual flight, the accumulators are unlocked after the J-2 start command. The propellant utilization open-loop concept events, the LOX step pressurization event, and the Center Engine Cutoff used for the static firing had not yet been incorporated into the ICD event listing. The final event, S-II/S-IVB separation, was properly sequenced relative to the early J-2 cutoff time.

Table 1-3. S-II-8 Static Firing Event Sequencing for Inflight Simulation

Event	Time (Seconds)	
	*ICD40M33627	Test A2-546-8A-69
Liftoff simulation	0.0	0.0
Start first PAM FM/FM calibration	148.2	148.3
Stop first PAM FM/FM calibration	153.2	153.3
Arm S-II ordnance	153.4	153.5
LH$_2$ tank high-pressure vent mode	158.5	157.8
Trigger ullage rockets	158.9	158.0
Unlock hydraulic accumulators	161.4	158.1
Stop LH$_2$ recirculation	158.6	158.4
S-II engine cutoff reset	159.4	158.6
Engine ready bypass	159.5	158.8
Prevalves lockout reset	159.6	159.0
S-II engine start command	159.8	159.8
Engine ready bypass reset	160.2	160.4
Chilldown valves closed	164.8	165.0
Start phase limiter arm	165.1	165.3
High EMR on		165.4
Start phase limiter reset	166.1	166.3
Prevalves close arm	166.2	166.5
Trigger second-plane separation	189.1	189.3
LOX step pressurization		263.0
Start second PAM FM/FM calibration	283.4	283.6
Stop second PAM FM/FM calibration	288.4	288.6
Start third PAM FM/FM calibration	383.4	383.6
Stop third PAM FM/FM calibration	388.4	388.6
Center engine cutoff		457.6
LH$_2$ step pressurization	458.4	458.6
High EMR reset		484.8
Low EMR on		485.0
S-II/S-IVB ordnance arm	506.4	506.6
LOX depletion cutoff arm	507.2	507.4
LH$_2$ depletion cutoff arm	507.4	507.5
S-II cutoff	542.2	544.6
S-II/S-IVB separation	543.0	545.6

*Latest available ICD at time of static firing.
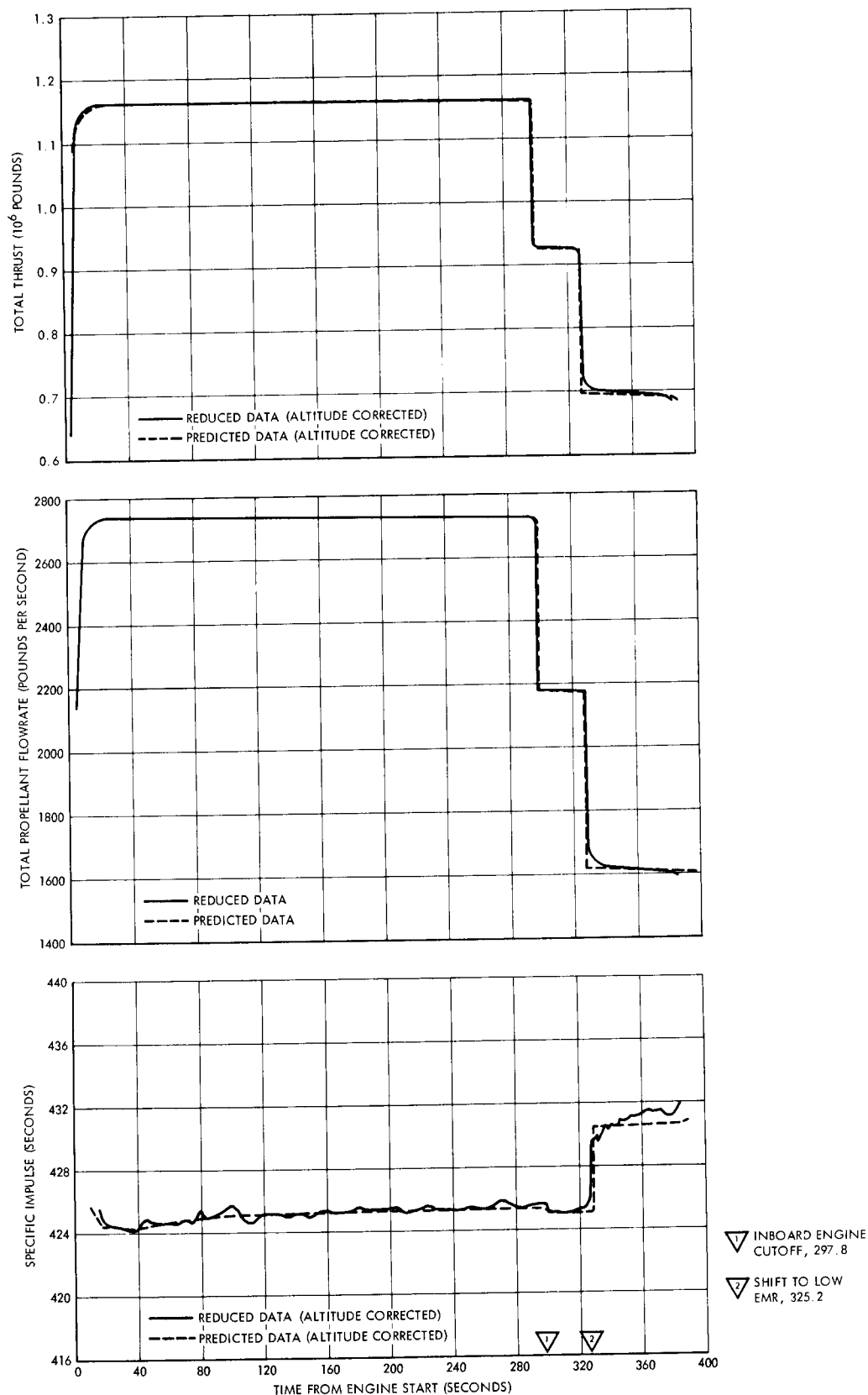
Figure 1-1. Comparison of Static Firing Performance and
Flight Predictions

1-5

2.0 PROPULSION SYSTEM

2.1 SYSTEM DESCRIPTION

The S-II propulsion system consists of five liquid-bipropellant J-2 engines, engine servicing, propellant fill, propellant feed, propellant management, pressurization, valve actuation, and propellant recirculation systems. The five engines are functionally independent but are clustered and controlled to form an integrated main propulsion system for the S-II stage.

ENGINE SYSTEMS

The configuration of the J-2 engines installed on the S-II-8 stage is defined in R-5788 (Saturn J-2 Configuration Identification and Status Report). The following engines were employed for Test 546:

Engine	Serial No.
1	J-2082
2	J-2099
3	J-2102
4	J-2098
5	J-2100

Beginning with the S-II-4 stage, all J-2 engines in use are of the uprated, J-2060 and subsequent configuration delivering a nominal 230,000 pounds of thrust at altitude.

Center Engine Early Cutoff

Modifications to the stage, GSE and facility were required to terminate center engine operation during S-II stage operation prior to the 18 Hertz oscillations buildup as experienced in previous flights. The major changes required to perform early center engine cutoff were as follows:

1. Modification to the stage circuitry and addition of a new switch selector command.

2. Replacement of engine 5 LAD prevalve with a Parker valve.

3. Engine 5 electrical control assembly was insulated.

4. Removal of engine 5 thrust chamber diffuser.

5. Addition of a water spray heat shield system around the exit plane of engine 5.

6. Added instrumentation:

Measurement Number	Title	Measurement Range
BC005-203	E3 Electric Control Box T	M300-200 F
BC005-205	E5 Electric Control Box T	M300-200 F
WB043-206	E5 Hat 5 Area Acoustic 1	0-175 DB
WB044-206	E5 Hat 5 Area Acoustic 2	0-175 DB
WC1115-205	E5 Thrust Chamber Exit-Hat 1 T FIN A	0-1200 F
WC1116-205	E5 Thrust Chamber Exit-Hat 1 T FIN C	0-1200 F
WC1117-205	E5 Thrust Chamber Hat 8-Fuel Manif T.	0-1000 F
WC1118-205	E5 Thrust Chamber Hat 1 T FIN A	0-1200 F
WC1119-205	E5 Thrust Chamber Hat 1 T FIN C	0-1200 F
WC1123-205	E5 PU Valve Surf T 1	0-500 F
WC1124-205	E5 PU Valve Surf. T 2	0-500 F
WC1125-203	E3 Thrust Chamber Hat 1 INB T 1	0-1000 F
WC1126-203	E3 Thrust Chamber Hat 1 INB T 2	0-1000 F
WC1127-205	E5 Pneu Accum. Surf T.	0-500 F
WC1128-205	E5 Thrust Chamber Diff Ring T 1	0-1200 F
WC1129-205	E5 Thrust Chamber Diff Ring T 2	0-1200 F
WC1132-203	E3 Thrust Chamber Hat 1 INB T 3	0-1000 F
WC1130-205	E5 Thrust Chamber Hat 1 - 2 T FIN C	0-1200 F
WC1131-205	E5 Thrust Chamber Hat 1 - 2 T FIN A	0-1200 F
WD264-205	E5 LOX Pump Inlet Hi Pressure	0-200 PSIG
WD265-205	E5 LH_2 Pump Inlet Hi Pressure	0-200 PSIG
D9260-GND	Water Spray Nozzle Pressure	0-250 PSIS
D9259-GND	Water Spray Heat Shield Pressure	0-250 PSIS
WE355-206	Long Vib Thrust Pad E2	M50-50 GPK
WE359-206	Long Vib Thrust Pad E3	M50-50 GPK
WE360-206	Long Vib Thrust Pad E4	M50-50 GPK

Measurement Number	Title	Measurement Range
WE371-205	E5 Thrust Chamber Hat 1 VIB	0-200 GRMS
WE372-205	E5 Thrust Chamber Hat 1 VIB	0-200 GRMS
WE373-205	E5 Main Fuel Valve VIB	0-150 GRMS
WE374-205	E5 OTBV Vib.	0-150 GRMS

7. Instrumentation requiring range changes:

Measurement Number	Title	Range (was)	Range (is)
BD091-205	E5 Engine Inlet LOX P.	0-50 PSIG	0-200 PSIG
WD091-205	E5 Engine Inlet LOX P.	0-50 PSIG	0-200 PSIG
BD092-205	E5 Engine Inlet LH$_2$ P.	0-50 PSIG	0-200 PSIG
WD092-205	E5 Engine Inlet LH$_2$ P.	0-50 PSIG	0-200 PSIG
WD261-205	E5 Close Couple Lox Inlet P.	0-50 PSIS	0-100 PSIS

Special Low Frequency Oscillation Instrumentation
===

Special instrumentation was installed for both S-II-7 and S-II-8 static firings in order to provide better correlation between accelerometers and pressure measurements as related to the low frequency oscillation problem. These consisted of accelerometers at the thrust pad on engines 1 and 5 and another on the LOX tank sump. Close-coupled pressure transducers were mounted on the LOX feedlines for engines 1 and 5 and on the aft bulkhead of the LOX tanks. Installation of the transducers is shown in Figures 2.1-1 through 2.1-3.

ENGINE SERVICING

The engine servicing system consists of subsystems which perform the following functions:

Engine purge
GH$_2$ start tank fill
GH$_2$ start tank vent and relief
GH$_2$ start tank vent control
Engine helium tank fill
Thrust chamber chill

Each subsystem consists of a disconnect at umbilical panel 3A and a rigidly mounted common manifold connected to five stage-mounted engine connect panels.

Engine purge systems transfer gases at specified conditions from the GSE facilities to the appropriate engine area. The purge gases are heated (at MTF only) by the S7-49 heater unit and controlled by the S7-41 pneumatic

control unit. The primary engine purges are the turbopump purge, the LOX dome purge (which utilizes the helium tank and fill system), and the thrust chamber purge. In addition, the start tanks are purged prior to propellant loading via the pressurize-vent cycle method. The drag-in waterline to the thrust chamber diffuser is purged with GN_2 shortly before thrust chamber chill.

In addition, the start tank vent control system contains five solenoid valves. The configuration for static firing does not include the disconnects that are installed after the final static firing. A start tank emergency vent system was added for the S-II-3 and subsequent stages (S-II-6 and subsequent stages at MTF). This system consists of a solenoid valve and line routed from the start tank to the LH_2 pump seal drain on the engine side of the engine connect panel.

PROPELLANT MANAGEMENT

The configuration of the S-II-8 propellant management system is identical to S-II-7 stage's configuration reported in SD 69-80, Volume II. The propellant utilization (PU) system consists of a full-length capacitance probe in each tank that furnishes propellant mass information to an electronics package located in stage container 214. This package contains an analog computer/power supply which provides power and control signals to the PU valves on each engine for engine mixture ratio (EMR) control. Loading control and propellant mass indication data are also provided to GSE and the telemeter system.

Also included in the propellant management system are the propellant-depletion engine cutoff subsystem and the propellant level monitoring subsystem. These subsystems are identical to those described in the S-II-5 Static Firing Report (Volume 2 of SD 68-377), except that the propellant level monitoring point sensors are not telemetered, but rather are only hardwired on S-II-6 and subsequent stages. The propellant-depletion engine cutoff subsystem used 1.0 second LOX ECO time delays for all engines except number one which used zero seconds time delay module.

The calibration criteria used for the PU computer adjustment are presented in Table 2.1-1. This calibration is also programmed for use with the AS-508 flight. The open-loop capability was utilized with EMR controlled by discrete GSE commands rather than feedback signals from the capacitance probes (closed-loop). ''Low EMR ON'' command was programmed for engine start plus 325 seconds. The previous static firing with S-II-7 used a ''Low EMR On'' signal at engine start command (ESC) plus 280 seconds followed by ''Open-loop Reset On'' at ESC plus 320 seconds for a final closed-loop portion of control.

PROPELLANT TANK PRESSURIZATION SYSTEM

The pressurization system serves two separate functions on the S-II stage: it supplies ullage pressure to meet the engine propellant pump requirements, and it contributes to the structural integrity of the stage.

Table 2.1-1. PU System Calibration Criteria

Item	LOX		LH$_2$	
	Pounds	Fine Mass (Percent)	Pounds	Fine Mass (Percent)
Empty calibration point	0	2.000	2,429	2.00
Probe bottom (flight)	2,465	2.281	901	1.090
Probe bottom (ground)	2,526	2.281	901	1.090
Full calibration point	705,436	82.50	154,467	92.500
Bridge gain (calibration)	1.14114×10^{-4} percent/pound		5.95246×10^{-4} percent/pound	
Bridge gain (loading for static firing	1.14449×10^{-4} percent/pound		5.98503×10^{-4} percent/pound	
Bridge gain (flight)	1.14166×10^{-4} percent/pound		5.96749×10^{-4} percent/pound	
Reference mixture ratio [1,2]	4.64			
Engine mixture ratio [2]	4.67			
PU Bias for static firing [3]	1917 pounds LH$_2$			

[1]Based on total tank flowrate.
[2]Based on a linear simulation of a flight. (Closed-loop)
[3]Based on LOX ECO with 1.0 second time delay.

Both propellant tanks are initially pressurized by ground-supplied gaseous helium. The LH_2 and LOX tank pressure switches for controlling prepressurization are set to operate at 34 to 36 psia and 37 to 39 psia, respectively.

During S-II boost, the LOX tank is pressurized by gaseous oxygen produced by passing liquid oxygen through the heat exchangers located in the turbine exhaust system of each J-2 engine. The LH_2 tank is pressurized by gaseous hydrogen bled from the four outboard J-2 engines at points downstream of the thrust chamber cooling jackets. The propellant tank ullage pressure levels are kept within the required limits by pressure regulators during S-II boost.

Two parallel-connected vent valves for each tank act as relief valves to prevent tank overpressurization. The LH_2 tank vent valves are gauge (differential) sensing valves with a low-pressure sensing mode set at 27.5 to 29.5 psid for the S-IC boost period and with a high-pressure sensing mode set at 30.5 to 33.0 psid for the S-II boost period. The differential pressure is between the LH_2 tank ullage pressure and the external ambient (reference) pressure. The LOX tank vent valves are absolute single mode type (sensing ullage pressure only) set at 40 to 42 psia.

Prior to S-II-7 static firing, and AS-504 launch the LOX tank vent valves served solely as safety, pressure-relief mechanisms. However, for S-II-7 static firing the LOX tank ullage step pressurization was initiated at ESC plus 150 seconds as a special test to provide higher LOX NPSH in design support of the AS-504 launch. AS-504 initiated LOX step pressurization at S-IC outboard engines cutoff (T_3) plus 100 seconds and S-II-8 was the initial static firing to use this sequence. All future flights and static firings are scheduled to continue LOX step pressurization which will cause the LOX tank ullage pressure to reach the normal venting range of 40 to 42 psia with a good possibility of venting.

RECIRCULATION SYSTEMS

Fuel Recirculation System

The LH_2 recirculation system is required to precondition the S-II stage and engine LH_2 systems by removing heat from the feed ducts and engine LH_2 pumps prior to engine start so that J-2 LH_2 engine inlet temperature conditions for engine start will be within the requirements envelope. To assure satisfaction of this inflight engine start requirement, the LH_2 engine inlet temperatures and pressures must meet prelaunch redline limits. This is achieved by pumping LH_2 around the prevalve through the feed duct, the LH_2 engine pump, and the gas generator bleed circuit of each engine and then back into the LH_2 tank through a common return manifold. The stage portions of the LH_2 recirculation system are insulated by vacuum jacketing and polyurethane foam. The engine portions of the system are insulated in part by vacuum jackets and in part by a silicone elastomer (Larodyne).

Prior to initiating LH_2 recirculation, the pump discharge valves and return line valve are opened to allow flow. Five to 10 minutes prior to liftoff, the recirculation pumps are turned on and the prevalves closed. During first stage boost, the recirculation system operates as it did on the launch pad, except that airborne battery power is used to operate the pumps. LH_2 recirculation is terminated 1.2 seconds prior to S-II engine start by removing power from the recirculation pumps and opening the LH_2 S-II-8 static prevalves. Five seconds after S-II engine start, the pump discharge valves and the return line valve are closed to provide tank isolation in case of an emergency.

The configuration of the stage fuel recirculation system for S-II-8 static firing was the same as for S-II-6 and S-II-7. Improved vacuum line maintenance procedures using CO_2 during the backfill and purge of the LH_2 feed and recirculation lines, were employed by the vendors at Seal Beach during installation of the new design evacuation valves.

<u>LOX Recirculation and Helium Injection System</u>

The LOX feed and engine systems are conditioned before engine start by the recirculation of LOX through the feed duct, LOX engine pump, and gas generator bleed circuit of each engine and then back into the LOX tank through individual return lines. The driving force for this recirculation is provided by the difference in density between the fluid in the engine feed ducts and the warmer, less dense fluid in the uninsulated return lines. An inflight helium injection system supplements natural convection recirculation. This system injects ambient helium into the bottom of the return lines to decrease the return line fluid density and thereby increase the driving force.

The configuration of the stage LOX recirculation and inflight helium injection systems were the same as that of the S-II-6 and S-II-7 stages for static firing.

VALVE ACTUATION SYSTEM

The valve actuation system provides the actuation gas for the stage prevalves and recirculation system valves. The system consists primarily of a fill disconnect, a receiver, a pressure regulator, and various check valves and test disconnects. Relief valves prevent overpressurization of the system.

The system provides stored helium gas at an initial pressure and temperature of 3000 psig and 70 F nominal. The pressure of the stored gas in the receiver is reduced by the regulator to an operating band of 675 to 750 psig (690 to 765 psia).

The LH_2 prevalves, LH_2 recirculation valves, LH_2 return line valve, LOX prevalves, and LOX return line valves are all spring-loaded open. In the hydrogen leg of the actuation system, the helium gas closes the five

LH$_2$ prevalves, five LH$_2$ pump discharge valves, and the LH$_2$ return line valve. Teh helium gas flow to the recirculation system valves is controlled by a single three-way normally closed solenoid valve, and each prevalve is controlled by a separate three-way normally closed solenoid valve.

In the LOX leg of the actuation system, the helium gas closes the five LOX prevalves and the five LOX return line valves. The helium gas flow to the LOX return valves is controlled by a single three-way normally closed solenoid valve. Each prevalve is controlled by a separate three-way normally-closed solenoid valve.

PROPELLANT FEED SYSTEM

The LH$_2$ servicing subsystem consists of the fill valve and the airborne part of the fill disconnect coupling. The LOX servicing subsystem consists of the fill valve mounted to the LOX sump interface, approximately 16 feet of 8-inch line with a pressure-compensating bellows, one free bellows and two universal bellow ball-joints to provide movement, and the airborne part of the fill disconnect coupling. These propellant servicing subsystems are designed to both fill and drain the S-II stage propellant tanks.

After tanking is completed, the LOX fill line is drained and inerted by purging with helium gas injected through the high point of the fill disconnect coupling. A 1-inch drain line that exists at the low point of the fill disconnect is routed overboard to the GSE/facility. A temperature measurement in the GSE facility indicates (by an increase in temperature) when the LOX purge has been completed.

The engine feed subsystem consists of 10 prevalves: five mounted on the LOX sump and five mounted adjacent to the LH$_2$ tank outlet in the associated engine feed ducts. All outboard engine prevalves are commanded to close approximately 430 milliseconds after the dropout of the engine mainstage pressure switches. The center engine prevalve closure is delayed 2.5 seconds after the dropout of the engine mainstage pressure switches.

The feed system for S-II-8 static firing differed from S-II-7 in that a ME284-0358 prevalve had been installed on engine 5 LOX feedline. ME284-0358 prevalves will be installed on the outboard engine's LOX feedlines prior to CDDT. These valves replace the V7-480700 prevalves.
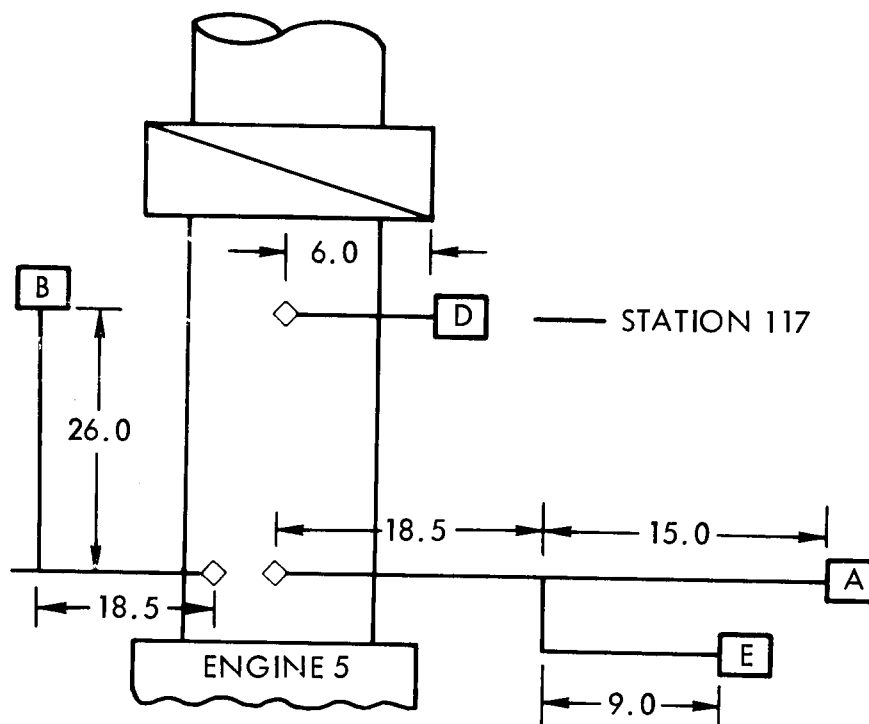
TRANSDUCER	MEASUREMENT NUMBER	RANGE
A	WD091-205A	0-50 PSIG
B	BD091-205	0-50 PSIG
C	N/A	N/A
D	WD261-205	0-50 PSIG
E	D091-205	20-55 PSIA

NOTE: ALL DIMENSIONS ARE IN INCHES
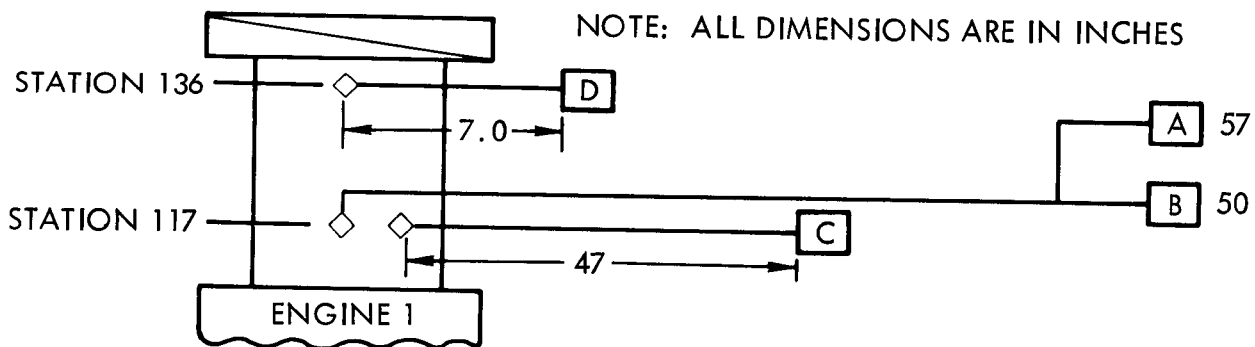
TRANSDUCER	MEASUREMENT NUMBER	RANGE
A	WD091-201A	0-50 PSIG
B	BD091-201	0-50 PSIG
C	D091-201	20-55 PSIA
D	WD261-201	0-50 PSIG

Figure 2.1-1. LOX Feedline Instrumentation Location, S-II-7

SPACE DIVISION of NORTH AMERICAN ROCKWELL CORPORATION
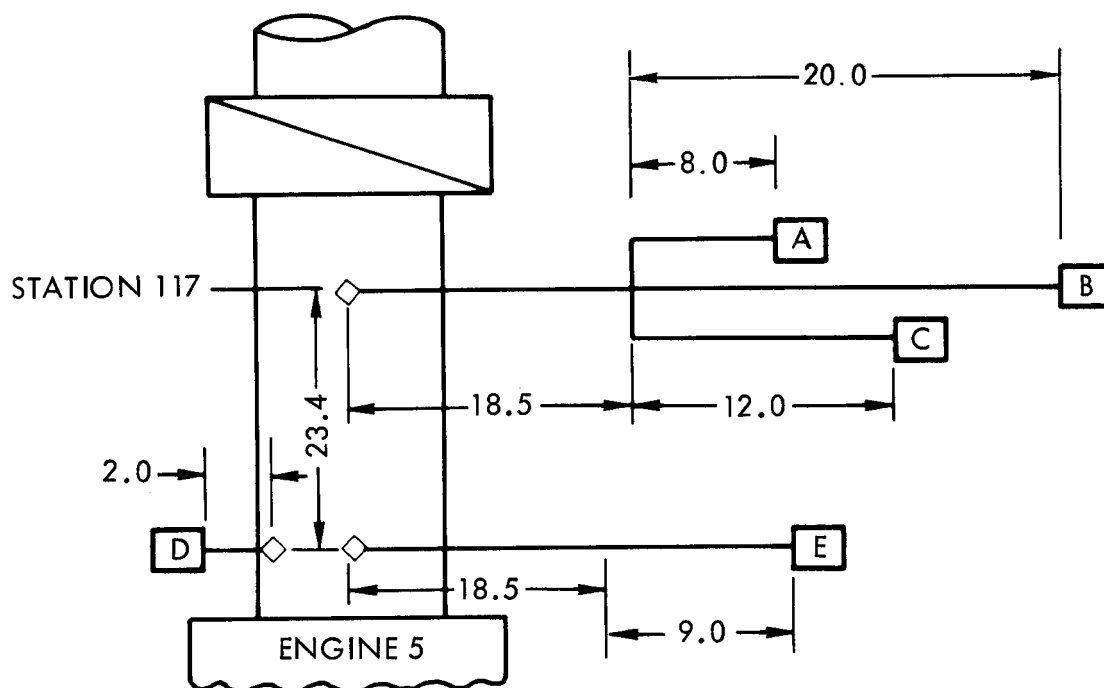
TRANSDUCER	MEASUREMENT NUMBER	RANGE
A	WD091-205	0-200 PSIG
B	BD091-205	0-200 PSIG
C	WD264-205	0-200 PSIG
D	WD261-205	0-100 PSIS
E	D091-205	20-55 PSIA

NOTE: ALL DIMENSIONS ARE IN INCHES
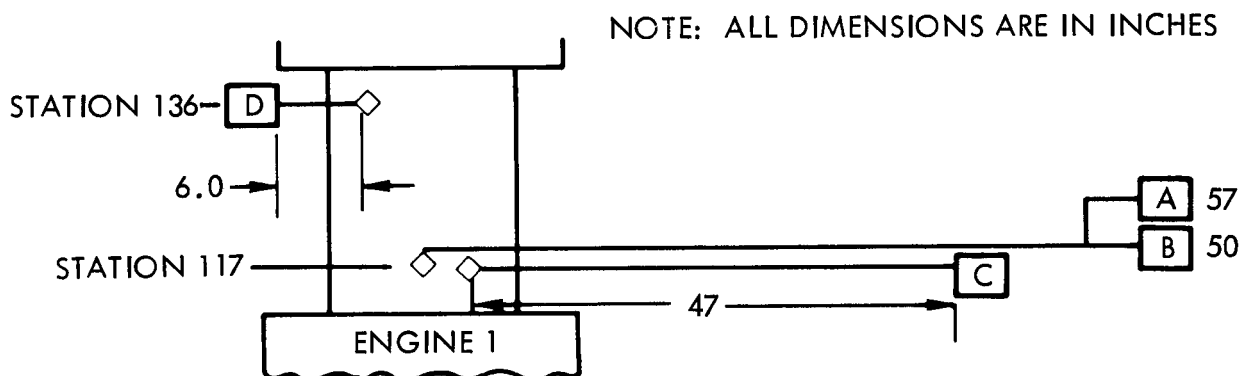
TRANSDUCER	MEASUREMENT NUMBER	RANGE
A	WD091-201	0-50 PSIG
B	BD091-201	0-50 PSIG
C	D091-201	20-55 PSIA
D	WD261-201	0-50 PSIS

Figure 2.1-2. LOX Feedline Instrumentation Location, S-II-8

2-10

CRUCIFORM BEAM

THRUST BLOCK

STAGE ℄

2.0 IN.

2.0 IN.

WE358-206
WA022-206

ENGINE 5 THRUST PAD TRANSDUCER LOCATION

WE357-206
WA021-206
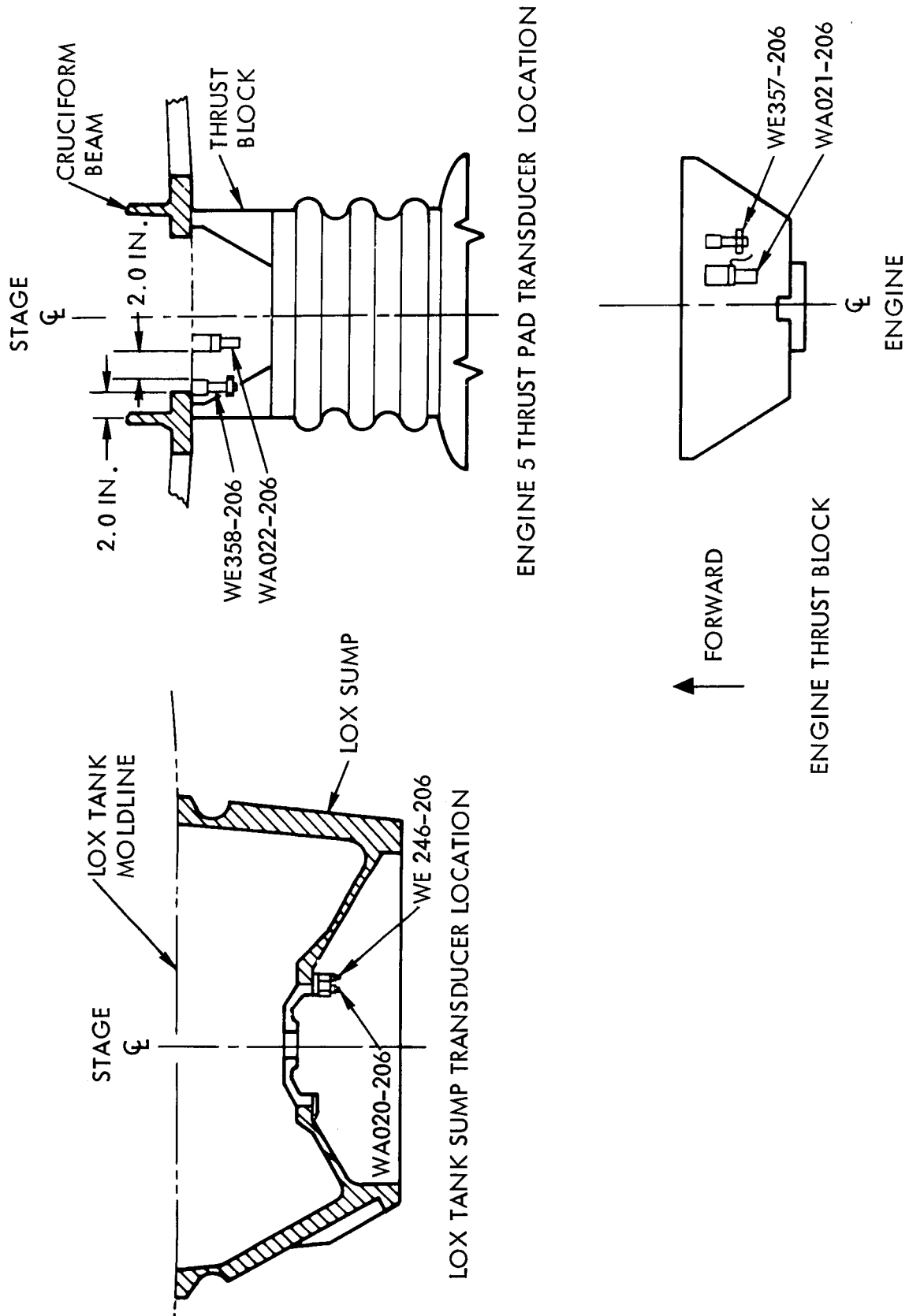
℄ ENGINE

ENGINE 1 THRUST PAD TRANSDUCER LOCATION

FORWARD

ENGINE THRUST BLOCK

LOX SUMP

LOX TANK MOLDLINE

STAGE ℄

WE 246-206

WA020-206

LOX TANK SUMP TRANSDUCER LOCATION

Figure 2.1-3.   Vibration Transducer Locations

2-11

2.2 PROPULSION SYSTEM SERVICING AND
CONDITIONING EVALUATION

This section contains an evaluation of all propulsion system performance during S-II-8 static firing test 546 prior to engine start. All acceptance requirements imposed upon the propulsion system prior to engine start were satisfied. Evaluation and supporting data for the acceptance requirements are presented in Volume I of this report.

ENGINE PURGES

The engine purge parameters were essentially constant during the periods of operation. The evaluation consists of verifying that the purge gas conditions satisfy the requirements of Table 2.2-1. Actual purge data are also presented in Table 2.2-1 to illustrate performance.

Turbopump and GG Purge

The turbopump purge system supply pressure was 137 psia during both the prepropellant loading and the fuel tank pressurization intervals. ICD 13M50097, stage-GSE requirements, specify a range of 87 to 140 psia at the umbilical panel. Based on these data, it may be concluded that the turbopump purge pressure requirements were satisfactory. During S-II-6 acceptance on the A2 test stand the supply pressure was 90 psia. The S7-41 pneumatic servicing console regulator and solenoid valve were revised to components of higher flow capacity and pressure in accordance with MCR 5553 for S-II-7 and subs at MTF. The purge temperature was adequate at 80 F.

Thrust Chamber Purge

Thrust chamber GN_2 purge requirements were marginal with a pressure of 214 psia and a temperature of 150 F. The helium (GHe) purge pressure of 190 psia continues to be below the requirement range of 215 to 265 psia. However, based on the engine manufacturer's minimum requirement of 55 psia (ICD 13M07005) at the engine/stage interface, it may be concluded that the purge flowrate is satisfactory.

Engine Diffusers Purge

The outboard engine diffusers were purged as planned for five minutes prior to thrust chamber chill to eliminate moisture in the diffuser. The system performance was satisfactory.

Start Tank Purge

Beginning with S-II-5 at MTF and AS-503 at KSC a pressure/vent cycle procedure to ensure adequate purging of all start tanks in place of the previous flow through method was incorporated in test procedures. The start tank purge is completed prior to initiation of the other system purges in order to meet the pressure requirements. No data are available from this early time period.

Helium Tank/Gas Generator Purge

Purging requirements of the helium tank are satisfied by the high pressure purge through the LOX dome, GG LOX injector, and turbopump intermediate seal.

In operation, the helium tank hi-press mode is selected resulting in a pressure level of 3000+200 psig at the outlet of the S7-41 GSE unit. The components and systems of concern were then purged through the helium control solenoid with a pressure in the helium tank of 2215 psia.

For the S-II-8 static firing operation employing early center engine cutoff the helium purge of the LOX dome and GG LOX injector were reinitiated to protect the center engine from moisture contamination. To provide adequate purge gas flow the engine helium bottles were recharged through the GSE supply at engine start + 270 seconds and remained in the continuous recharge configuration until termination of test operations.

PROPELLANT LOADING

LH$_2$ Tank Preconditioning

The LH$_2$ preconditioning was accomplished satisfactorily during the S-II-8 tanking and static firing tests, although a LOX loading temporary hold at the 40-percent level was performed on Test 546 to fulfill the -50 F preconditioning requirement. The maximum allowable temperature differentials of the common bulkhead forward and aft facing sheets in the J-ring area were not exceeded during S-II-8 stage propellant loading sequence. The -160 F LH$_2$ tank cylinder 1 temperature limit was met before start of LH$_2$ loading on both tests.

The LH$_2$ tank chilling procedure stated below was followed during LN$_2$/LH$_2$ tanking test 545 and the acceptance static firing test 546.

1. After initiation of LOX barge pump chilldown, initiate LH$_2$ tank preconditioning with a precool controller setting of 100 percent. When the LH$_2$ fill line temperature (C9122) indicates 0 F, decrease the precool controller setting to 60 percent until LOX is at 5 percent level.

2. Increase precool controller setting to 80 percent until completion of LOX loading.

3. Increase precool controller setting to 85 percent until the LH_2 tank sidewall temperature (WC104-218) decreases to less than -160 F.

There are only two temperature measurements on S-II-8 in the vicinity of the J-ring structure that can be used in the test evaluation. They are measurements WC104-218 and WC105-218 which are installed on the LH_2 tank sidewall at station 320 and 356, respectively. Lack of the aft facing sheet temperature data creates a difficulty in evaluation of the temperature differential across the common bulkhead during initial phase of the chilling procedure. However, based on the thermal analysis which involves a comparison with S-II-5 and other previous data, the temperature differential across the common bulkhead was within the allowable limit. The LH_2 tank preconditioning procedure employed on S-II-8 was similar to ones that performed satisfactorily during the two static firings on S-II-5.

Figures 2.2-1 and 2.2-2 present the temperature variation of LH_2 tank cylinder 1, as measured by measurement WC104-218, for tests 545 and 546, respectively. They also show the prechill gas temperatures as measured by measurement C9122-GND, which is located on the ground half of LH_2 fill and drain disconnect at the stage interface.

LH$_2$ Tank Cylinder 1 Temperatures

Event	Test 545	Test 546	Limit
40 percent LOX	-83.5 F	-35 F	-50 F maximum
Start LH$_2$ Load	-245 F	-280 F	-160 F maximum

During test 546, loading of the LOX tank above the 40-percent level was temporarily halted until a temperature reduction below -50 F was indicated on WC104-218. The slow LH_2 tank sidewall temperature reduction appears to be attributed to a faulty calibration of the precool controller to set the open position of prechill gas flow valve for required gas flow rates, or the prechill gas flow valve response failure to the precool controller command signal. The faulty precool controller calibration is suspected because a slow chilldown has been experienced during tests on previous stages where this particular valve was used. The valve response failure to the precool controller command signal is apparent because there is no significant change in the prechill gas temperature reduction rate as measured by C9122-GND in response to the 80 percent valve open command (see Figure 2.2-2.)

LH$_2$ Boiloff Rate

Predicted and experimental estimates of LH_2 boiloff rate for the spray foam insulated S-II-8 vehicle are presented in Figure 2.2-3. The predicted estimate of LH_2 boiloff rate of 2.1 percent per hour was calculated for

2-15

nominal day conditions. The experimental estimate of LH$_2$ boiloff rate was determined from fine mass level sensor data recorded at MTF during test 545. The average LH$_2$ boiloff rate over the 30 minute period for which the data was observed is 1.84 percent per hour compared to a predicted 2.1 percent per hour. The environmental conditions used in the calculations is nearly the same for both the predicted and experimental LH$_2$ boiloff rates. These results indicate a good correlation between analysis and experiment, and thereby, verify theoretical thermal conductivity values used in the predictive analysis.

LOX Loading

The LOX tank fill was initiated with the LOX vent valves and the LOX return line valves open. The LOX tank was filled at the slow-fill rate to the 5-percent level. At the 1-percent level, the LOX prevalves were opened; at the 5-percent level, the LOX tank fast-fill was started but halted at the 40-percent level for about 13 minutes to allow the J-ring temperature limitation to be satisfied. The average fast-fill rate was 3780 gpm from 40-percent level to the overfill shutoff level. The fast-fill and overfill LOX tank point sensors operated satisfactorily. The LOX tank was then drained to a mission load at engine start command of 95.85 percent fine mass.

LH$_2$ Loading

The LH$_2$ tank loading was initiated at the slow-fill rate with the vent valves open and the LH$_2$ prevalves and LH$_2$ recirculation valves closed. The LH$_2$ tank was filled at the slow-fill rate to the 5-percent level and the LH$_2$ prevalves were opened. LH$_2$ tank fast-fill was initiated and continued to the automatic fast-fill shutoff. The average fast-fill flowrate was 9950 gpm. At the 10-percent level, the LH$_2$ recirculation valves were opened. The LH$_2$ tank level was reduced to a mission load at engine start command of 95.63 percent fine mass. Both the fast-fill and overfill cutoff sensors were verified for proper operation.

Geysering, which is suspected of causing erratic behavior of the S-II-7 LH$_2$ fine mass measurement, did not recur during the S-II-8 loading.

Loading Termination

Proper operation of all point sensors and capacitance probe mass indication systems were verified with no anomalies. Propellant loadings, as indicated by the capacitance probes (mass) were 0.02 percent greater than predicted for LOX and 0.43 percent higher than predicted for LH$_2$ at liftoff (simulated). Best estimates of loaded propellants are 818,866 pounds of LOX and 159,701 pounds of LH$_2$, based on integration of engine flowmeter data. These estimates compare to predicted values of 820,529 pounds of LOX and 158,000 pounds of LH$_2$ (Table 2.3-1). Figures 2.2-4 and 2.2-5 show the PU probe error during tanking.

The propellant fill valves were closed at the completion of propellant loading and topping operations. The LOX fill valve closed in 8.42 seconds, and the LH$_2$ fill valve closed in 16.18 seconds. The fill valve actuation times are presented in Table 2.3-8. The closing times for both valves were within the required time of 5 to 20 seconds. The LOX fill line was drained in approximately 80 seconds in sufficient time to meet the requirement that it be drained prior to engine start.

ENGINE START TANK AND HELIUM TANK CONDITIONING

Engine Start Tank Conditioning

Both temperature and pressure conditions of the engine start tanks were within the required prelaunch and engine start boxes as shown in Figure 2.2-6. The start tank conditioning test results are summarized in Table 2.2-2 and Figures 2.2-7 and 2.2-8. Start tank temperatures at the conclusion of chilldown ranged from -289 to -283 F. The start tanks were pressurized to the nominal requirement of 1175 psia in 72 seconds resulting in a temperature warmup of 21 to 28 F.

Heat-up rates (completion of pressurization to engine start) were similar to previous tests averaging 15.2 psi/min and 2.7 F/min.

A comparison of hardwire and telemetry data at engine start for start tank pressure (D016) indicates a maximum difference of 34 psi on Engine 4. All other engines were within 16 psi.

The redundant start tank pressure measurement (D022) was within 26 psi maximum of the standard flight measurements. These differential values were well within the measurement system accuracies.

The center engine start tank pressure and temperature increased 64 psi and 25 F respectively from center engine cutoff (CECO) to outboard engine cutoff. The outboard engines pressure and temperature increased an average of 20 psi and 13 F over the same time period.

Engine Helium Tank Conditioning

The helium tank prelaunch and engine start limits were satisfactory. The helium tank pressure at engine start was 3273 to 3311 psia. The engine helium tank conditioning test results are presented in Table 2.2-2 and Figures 2.2-9 and 2.2-10. Helium tank temperatures at completion of chill (liftoff (T_o) - 277 seconds) were -242 to -248 F. At T_o - 20 seconds the temperature differential between the hydrogen start tank and helium tank was 7 to 13 F. At engine start (T_o + 159) the temperature differential was 5 to 8 F.

A comparison of hardwire and telemetry data for helium tank pressure (D015) at prelaunch and engine start indicates a maximum difference of 50 psi on Engine 2. The redundant helium tank pressure measurement (D021) varied 6 to 80 psi from the standard flight measurement (D015). These differential values were well within the measurement system accuracies.

Because of early center engine cutoff, the requirement of a continuous LOX dome purge on the center engine following cutoff was initiated. This requires repressurizing and maintaining the ground helium supply to all five engine helium tanks. Since one engine cannot be serviced by itself, all engines require the servicing. The tanks were repressurized to between 3033 and 3103 psia (increase of 340 to 525 psi) in 11 seconds. This repressurizing resulted in helium tank temperature increases of 25 F maximum. Subsequent to center engine cutoff, with engine 5 LOX dome purge on and the S7-41 supplying ambient helium to the tank, the helium tank temperature increased from -235 F to -70 F at outboard engines cutoff. Engine 5 helium tank pressure decreased 138 psia, outboard engines pressure decreased 35 psi, and the temperature remained constant during the same period of time.

Engine Thrust Chamber Chill

Prior to S-II-6 acceptance testing the sequence of operations for the thrust chamber chill was changed so as to provide for a full eight (8) minutes of chilldown. Previous static test operations had limited thrust chamber chill duration to 5 minutes, 30 seconds to preclude the possibility of violating the original redline of -250 F minimum at engine start. This redline has since been changed to -300 F for both static test and flight. In order to provide greater confidence in the chilldown of the thrust chamber nozzle bell (there is no instrumentation located on the bell) the time was extended to the eight minute duration similar to the procedure used for prelaunch operations.

Chilldown was initiated and terminated in accordance with pre-planned countdown event times. The resulting chamber temperatures at engine start were -213 to -250 F, well within the -300 to -150 F redline band. The chamber chilldown hardwire data for all five engines are presented in Figure 2.2-11.

Immediately following engine start, two thrust chamber jacket temperature measurements on the hardwire system were lost. Post-test investigation revealed that this was due to faulty drag-in cabling. Since the transducers reacted properly during chamber chilldown, it is presumed that they are in satisfactory working order.

In data received over the telemetry system, however, three measurements exhibit unsatisfactory operation during both chilldown and static firing portions of the test. The observed characteristic was a lag in response to chilldown of the thrust chamber structure and a high degree of sensitivity to environmental changes. These characteristics imply a lack of adequate contact between transducer and thrust chamber. Pretest examination, however, has indicated that a satisfactory contact situation existed between the thrust chamber, mounting pad, and transducer.

Equating the eight minute chilldown interval to prelaunch conditioning, two thrust chamber temperatures (1 and 5) would have failed to satisfy either the autosequence permit level of -170 F or the liftoff commit of -200 F. Both of these transducers will be replaced. Engine 4 was marginal at both simulated KSC redline verification points. These data are shown in Figure 2.2-11.

2-18

During the modification and checkout period at MTF all of the transducer mounting pads will be x-rayed to verify adequate braze bond between pad and thrust chamber. If necessary, the Eccobond compound will be injected beneath the mounting pad in order to fill any braze voids and improve thermal contact. In addition, the transducer, mounting pad contacts on all engines will be re-examined and relubricated.

Completion of these inspection and repair procedures plus the normal KSC checkout should be sufficient to result in satisfactory CDDT system performance. In the event that the transducers connected to the telemetry system fail to operate properly during CDDT, it is possible to switch the connectors to the alternate transducers used for static test ground measurements at MTF. Since these operated properly at MTF they should be capable of supporting launch operations.

PROPELLANT TANK PRESSURIZATION

LOX Tank Prepressurization

The LOX tank ullage pressure from the start of LOX prepressurization system chilldown (T_0-307 seconds) to S-II engine start is presented on Figures 2.2-12. The surge in ullage pressure at the start of the two-minute chilldown period was a result of temperature transients in the A7-71 heat exchanger, the prepressurization line, and the vent ducts. LOX tank prepressurization helium temperature presented on Figure 2.2-13 shows the chilldown characteristics at the stage LOX prepressurization disconnect. The system chilldown requirements were marginal because of a problem with supplying LH_2 to the heat exchanger.

The LOX tank vent valves were commanded closed at T_0-187 seconds and the LOX tank was prepressurized to a LOX tank pressure switch cutoff at 38.3 psia, which was within the pressure switch range of 37 to 39 psia. LOX tank prepressurization flow rate during LOX ullage prepressurization was 1.6 pounds per second.

After the initial pressure switch cutoff, the LOX tank ullage pressure decay required one pressure makeup cycle. The LOX tank ullage pressure increased during LH_2 tank ullage prepressurization as a result of common bulkhead deflection. LOX tank ullage pressure stabilized at 38.6 psia prior to S-II engine start and was well above the prelaunch and engine start minimum redlines of 36.5 psia and 33.0 psia, respectively (see Figure 2.2-12).

LH$_2$ Tank Prepressurization

The LH_2 tank ullage pressure during prepressurization and simulated S-IC boost is presented on Figure 2.2-14. LH_2 tank pressurization was initiated at T_0-97 seconds. The LH_2 tank ullage prepressurization rate was slow; therefore the auxiliary GH_2 pressure system was initiated at T_0-59 seconds. With the auxiliary GH_2 pressure system the LH_2 tank ullage pressure responded to a more normal prepressurization rate. The LH_2 tank pressure switch cut off the pressurant supply at an LH_2 tank ullage pressure of 35.7 psia.

Vent valve 1 closed indication switch did not indicate closed until T_o-83.8 seconds as compared to T_o -94.8 seconds for vent valve 2. The increase in ullage pressure verifies that the indicating switch was in error and the valve closed normally as commanded.

The initial slow ullage pressure increase rate was traced to the LH_2 prepressurization supply solenoid valve in the S7-41. This was verified by the supply pressure both upstream and downstream of the stage main solenoid valve. The upstream and downstream pressure data are presented in Figure 2.2-15 and 2.2-16, respectively. A schematic diagram indicating the pressure measurement locations is presented in Figure 2.2-17. Shortly after the LH_2 tank vent valves were closed, the ullage pressure increased approximately 1 psi during the initial 35 seconds indicating an insufficient supply of prepressurant gas. Also, the pressure at the prepressurization disconnect was about 65 psia. LH_2 tank auxiliary GH_2 pressure was then applied increasing the pressure at the positive pressure disconnect to 245 psia, and then increasing ullage pressure to the pressure switch cutoff. Pressure switch cutoff terminated auxiliary GH_2 pressurization in the normal manner at T_o-41 seconds. As shown in Figure 2.2-15, the prepressurization disconnect pressure continued to increase slowly. This increase was due to leakage past the S7-41 prepressurization supply valve and the blockage of the stage solenoid valve. The vent GSE pressure command relieved the pressure in the system just prior to simulated liftoff.

The prepressurization helium flowrate is normally derived utilizing the pressure measurement at the positive pressure disconnect and the LH_2 tank helium fill temperature measurement. However, due to the use of the auxiliary pressurization, the flowrate will not be determined. The LH_2 tank ullage pressure was well above the prelaunch (at T_o-33 seconds) and engine start minimum redlines of 33 psia and 27.5 psid, respectively (see Figure 2.2-14).

Common Bulkhead Evacuation

The common bulkhead was evacuated without incident to well below the required level of 3 psia prior to T_o-30 seconds. This evacuation minimized the heat transfer between the LOX and LH_2 tanks.

LH_2 Tank Vent Valve Operation

Venting of the LH_2 tank ullage is anticipated during the S-IC boost period for a normal mission. The venting process is tested during the static firing countdown by evacuating the LH_2 vent valve reference pressure line at a rate which simulates the atmospheric pressure change rate during S-IC boost. A differential pressure transducer is used to directly measure the difference between LH_2 tank ullage pressure and the LH_2 tank vent valve reference pressure. LH_2 tank vent valve differential pressure presented on Figure 2.2-18 shows that venting was accomplished as anticipated within the required vent range as noted. Analysis of discrete data indicates that only vent valve 1 cracked at T_o+82.8 seconds.

2-20

RECIRCULATION SYSTEM PERFORMANCE

LOX Recirculation and Helium Injection System

For test 546, the LOX recirculation and inflight helium injection systems adequately preconditioned the engine and LOX feed systems to meet engine start requirements. LOX pump inlet and LOX pump discharge temperatures at engine start are presented in Figure 2.2-19. Figures 2.2-20 and 2.2-21 present the LOX pump discharge and inlet temperatures, plus the predicted temperature bands. These parameters were within the predicted bands. The LOX pump discharge and inlet temperatures at simulated liftoff were -291.10 ± 0.90 F and -295.60 ± 0.30 F, respectively. Evaluation of all parameters indicates that system performance was satisfactory.

The helium injection system performance for Test 546 is presented in Figure 2.2-22. The figure presents the histories of the supply bottle, regulator outlet and primary orifice outlet pressures from engine start minus 220 seconds to the end of simulated S-IC boost. As can be seen, the primary orifice outlet pressure limit of 250 ± 50 psia was met satisfactorily, and also the expected decrease in the regulator outlet pressure at approximately engine start minus 30 seconds is shown. Regulator outlet pressure decreases when regulator inlet pressure decreases to approximately 1000 psia.

The total helium flowrate for test 546 was calculated by using the initial supply bottle pressure and the supply bottle pressure after 185 seconds (time from pressure lines vent to 1.2 seconds prior to S-II engine start). Total system flowrate was 68.4 scfm.

The results of the ambient flow distribution test for S-II-8 (conducted at Seal Beach) is shown in Table 2.2-3. As can be seen, all five engines were within allowable limits.

During the S-II-8 prestatic firing checkout at MTF, it was found that the helium injection regulator and low pressure relief valve were not functioning properly. Further investigation revealed that these components malfunctioned only during system lock-up (supply bottle pressurized and the solenoid valves closed), and performed satisfactorily when the system was flowing. For this reason, it was decided to proceed with the static firing without replacement of these components.

No data were recorded during the S-II-8 prestatic firing checkout; therefore, Figure 2.2-23 was constructed to show the results of the malfunctioning regulator and low pressure relief valve when the system is locked-up at 1.2 seconds prior to engine start.

Figure 2.2-23 compares the locked-up systems of the S-II-6, S-II-7, and S-II-8 stages. For the S-II-6 and S-II-7 stages, regulator inlet pressure is higher than the outlet pressure. This indicates that the regulator is

closed and leakage is within limits. Regulator outlet pressure further indicates that the relief valve is functioning properly. For the S-II-8 stage, however, regulator inlet pressure continued to decrease until 40 seconds after lock-up due to excessive regulator leakage. During this same time period, the relief valve continuously vented until the regulator outlet pressure decreased to 680 psia. This is abnormal because the relief valve crack and reseat setting is 760 to 825 psia.

Although the S-II-8 regulator and relief valve malfunctioned, it has been clearly shown that these malfunctions did not impair helium injection system performance. The components have been replaced and no future problems are anticipated. Analysis of the removed components revealed physical regulator seat damage and a broken belleville spring in the relief valve check valve. Additional analysis is presently being conducted to determine the cause of the component damage. Therefore, all indications are that the S-II-8 LOX recirculation and inflight helium injection systems will be satisfactory for the flight of AS-508.

Fuel Recirculation System

Figure 2.2-24 shows that the LH_2 recirculation system adequately preconditioned the engine and feed systems to meet static firing engine start requirements. It should be noted that biased telemetry data have been used for this evaluation. Figure 2.2-25 presents a comparison of the five engine inlet temperatures versus their prediction band for the S-II-8 static firing. All temperatures are within the predicted band. Also shown for reference is the saturation temperature for the pressure at the engine inlet. As shown in Figure 2.2-25, prior to recirculation start, the hydrogen is at saturation temperature. There is essentially no flow in the system and the hydrogen is boiling. At recirculation start, the LH_2 recirculation pumps are activated and flow through the system begins. The additional recirculation pump head pressure establishes a higher saturation temperature, with a resulting increase in LH_2 temperatures.

The engine inlet temperatures, Figure 2.2-25, are somewhat higher than were the corresponding temperatures for stages S-II-6 and S-II-7, but are still below the maximum allowable at engine start. This is attributed to higher vacuum levels recorded for the LH_2 feed ducts as shown in Figures 2.2-26 and 2.2-27 at simulated liftoff -22 seconds, and at S-II engine start. The data show, however, that all vacuum levels were within the maximum allowable limit for static firing.

Figures 2.2-26 and 2.2-27 present LH_2 temperature differentials between the tank and engine inlet versus feed duct vacuums measured pretest at ambient temperature. A comparison is made between static firing test results of S-II-6 (test 542) and S-II-7 (test 544). The results show that the vacuum levels and corresponding differential temperatures of the feed lines were higher for S-II-8 than for S-II-6 and S-II-7, except for engine 5 on S-II-7.

2-22

The allowable LH$_2$ temperature differentials shown in Figures 2.2-26 and 2.2-27 are based on the following:

1. The LH$_2$ bulk temperature based on past KSC experience, is -422.7 F at prelaunch constraint time (T$_o$-22 seconds).
2. Instrumentation error is ±0.2 F.
3. The bulk temperature rise from vent valve close to S-II inflight engine start is +0.2 F.
4. The LH$_2$ engine inlet prelaunch redline is -420.5 F.
5. The LH$_2$ engine inlet inflight engine start requirement at the minimum predicted ullage pressure of 27.5 psia is -420.3 F.

Subtracting (1) and (2) from (4) results in a 2.0 F maximum allowable temperature differential at the prelaunch constraint time. Subtracting (1), (2), and (3) from (5) results in a 2.0 F maximum allowable temperature differential at engine start. The maximum temperature differentials experienced were 1.8 F at the prelaunch constraint time and 1.5 F at engine start.

Data from the S-II-8 cryogenic proof pressure test revealed an apparent discrepancy in engine 5 recirculation pump buildup speed. It took approximately 80 seconds for the pump to reach a stabilized speed of 11,000 rpm compared to the normal buildup speed time of approximately one second. Evaluation of the sequence of events prior to energizing the LH$_2$ pumps indicates the recirculation system was in a static condition for an extended period of time while an attempt was made to vent the engine helium bottles by turning on the engine purges. The LH$_2$ bleed valve closes when the helium control solenoid is energized, thus stopping any natural recirculation flow from occurring prior to energizing the recirculation pumps. This static condition probably caused a gas bubble to develop in the feedline and resulted in reduced resistance to pumped flow until the bubble was dissipated and the system returned to normal flow conditions. Subsequent to the cryogenic test, a dry spin test was performed on engine 5 recirculation pump. The speed buildup and coastdown time data indicate normal pump operation. This discrepancy did not re-occur during the static firing test.

From the time of arrival of the S-II-8 at MTF until 25 April 1969, vacuum jacketed lines were serviced a total of 14 times in accordance with current maintenance requirements. Three of these lines required replacement of the evacuation valve, one line required replacement of the gauge tube, and one line was replaced. THe remaining evacuations were required to eliminate normal leakage and to satisfy precryogenic vacuum level requirements.

All indications are that the S-II LH$_2$ recirculation system flight performance will be satisfactory.

Table 2.2-1. S-II-8 Purge Requirements and Operations Summary for MTF

Purge	Gas	Stage-GSE Interface Pressure (psia)		Stage-GSE Interface Temperature (F)		Time Period
		Required	Actual	Required	Actual	
Turbopump and gas generator	He	140 maximum 87 minimum	137	160 maximum 50 minimum	80	(1) 10 minutes prior to loading (2) 2 minutes at fuel tank pressurization
LOX dome, gas generator, LOX injector, LOX pump intermediate seal	He	1400 to 3200 in helium tank	2215	160 maximum 50 minimum	150	15 minutes prior to propellant loading
Helium tank	He	1400 to 3200 in helium tank	2215	160 maximum 50 minimum	150	During LOX dome and GG LOX purge
Thrust chamber	GN$_2$	265 maximum 215 minimum	214	160 maximum 80 minimum	150	From propellant loading to thrust chamber He purge
	He	265 maximum 215 minimum	190	160 maximum 50 minimum	92	5 minutes prior to thrust chamber chill
Diffuser	GN$_2$	No pressure requirement	20	40 minimum at diffuser	65	5 minutes prior to thrust chamber chill
Start tank	He	165 maximum 75 minimum	NA	160 maximum 50 minimum	NA	For 10 minutes prior to propellant loading minimum of 3 pressurize vent cycles.

NA - Not Available

Table 2.2-2. GHe/GH2 J-2 Engine Tank Conditioning Summary

	Engine									
	1		2		3		4		5	
	Temp. (F)	Press. (psia)	Temp. (F)	Press. (psia)	Temp. (F)	Press. (psia)	Temp. (F)	Press. (psia)	Temp. (F)	Press. (psia)
GH$_2$ Start Tank										
Begin chilldown (To -1320)	70	22	75	21	64	21	58	20	74	16
Begin pressurization (To -277)	-289	402	-289	392	-283	398	-289	401	-288	392
Complete pressurization (To -205)	-268	1175	-262	1176	-255	1176	-263	1177	-262	1175
Prelaunch verification (To -30)	-259	1220	-255	1223	-249	1211	-256	1213	-253	1219
S-II engine start (To +159)	-251	1270	-246	1278	-242	1258	-250	1254	-245	1270
GH$_e$ Control Bottle										
Begin chilldown (To -1320)	(1)	3070	(1)	3071	(1)	3070	(1)	3070	(1)	3069
Begin auto sequence (To -187)	-246	3078	(2)	3106	-243	3109	-249	3098	-246	3102
Prelaunch verification (To -19)	-246	3153	(2)	3211	-242	3212	-248	3190	-244	3201
S-II engine start (To +159)	-243	3232	(2)	3311	-237	3301	-244	3273	-239	3292
S-II engine cutoff command	-229	3049	-215	3007	-220	3017	-227	3047	-70	2970

(1) Data not available until T$_o$ -882 seconds.
(2) Measurement malfunction

SD 69-329

Table 2.2-3. S-II-8 Helium Injection Ambient Flow Distribution Test Results, Seal Beach

| Engine	Flowrate (scfm)	Primary Orifice Outlet Pressure D209-206 (psia)	Regulator Outlet Pressure, D128-206 (psia)	Supply Bottle Pressure, D127-206 (psia)	Measured Flowrate Vs. System Flowrate Requirements
1	11.3	225	655	915	Total Flowrate 59.4
2	11.4	225	655	915	Average Flowrate 11.88
3	12.4	225	655	915	Maximum Allowable 13.07 (+10 percent of average)
4	12.9	225	655	915	Minimum Allowable 10.70 (-10 percent of average)
5	11.4	225	655	915	
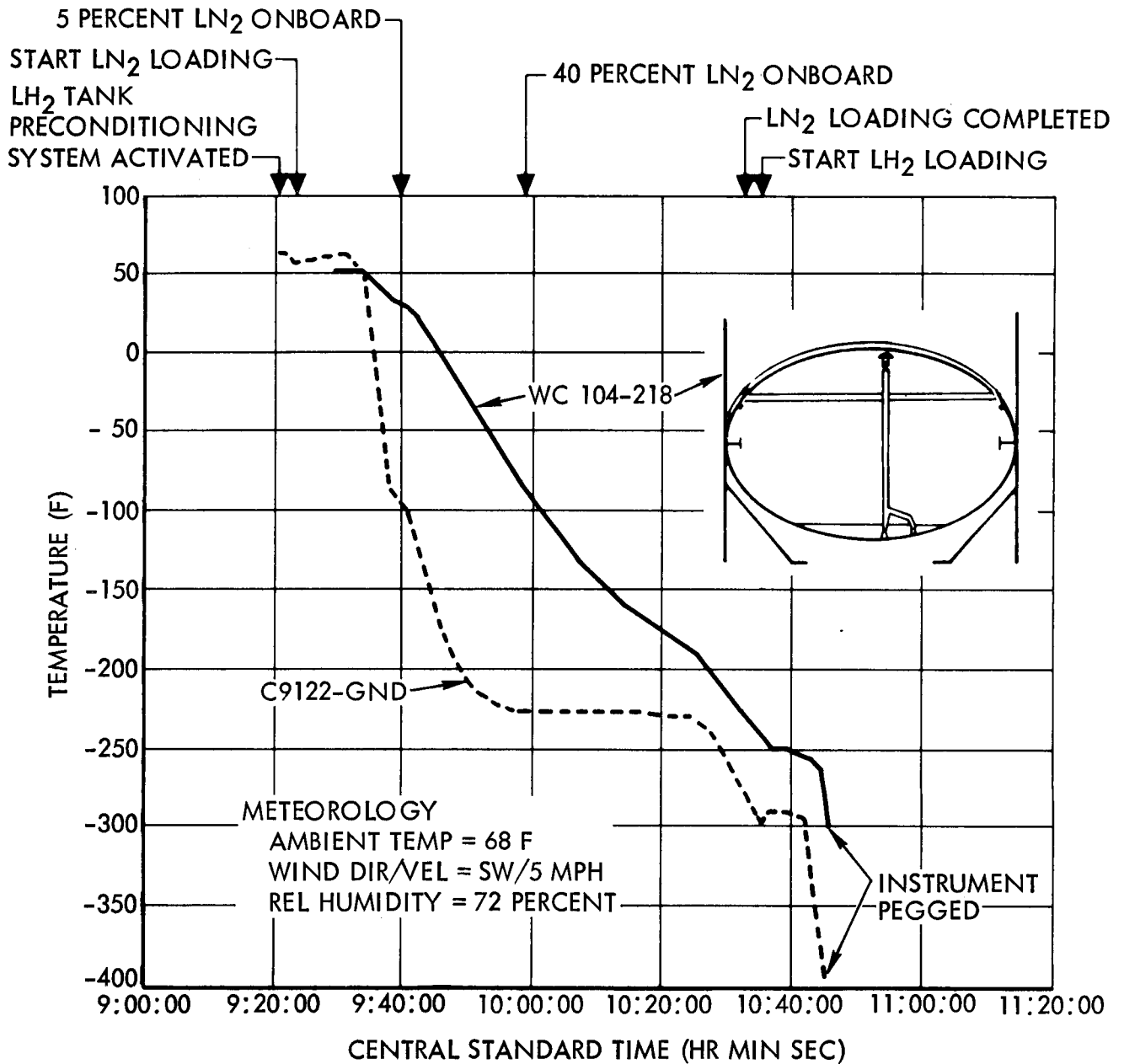
Figure 2.2-1. LH$_2$ Tank Lower Cylinder Temperature During LOX Tank Loading (Test 545)

SPACE DIVISION of NORTH AMERICAN ROCKWELL CORPORATION
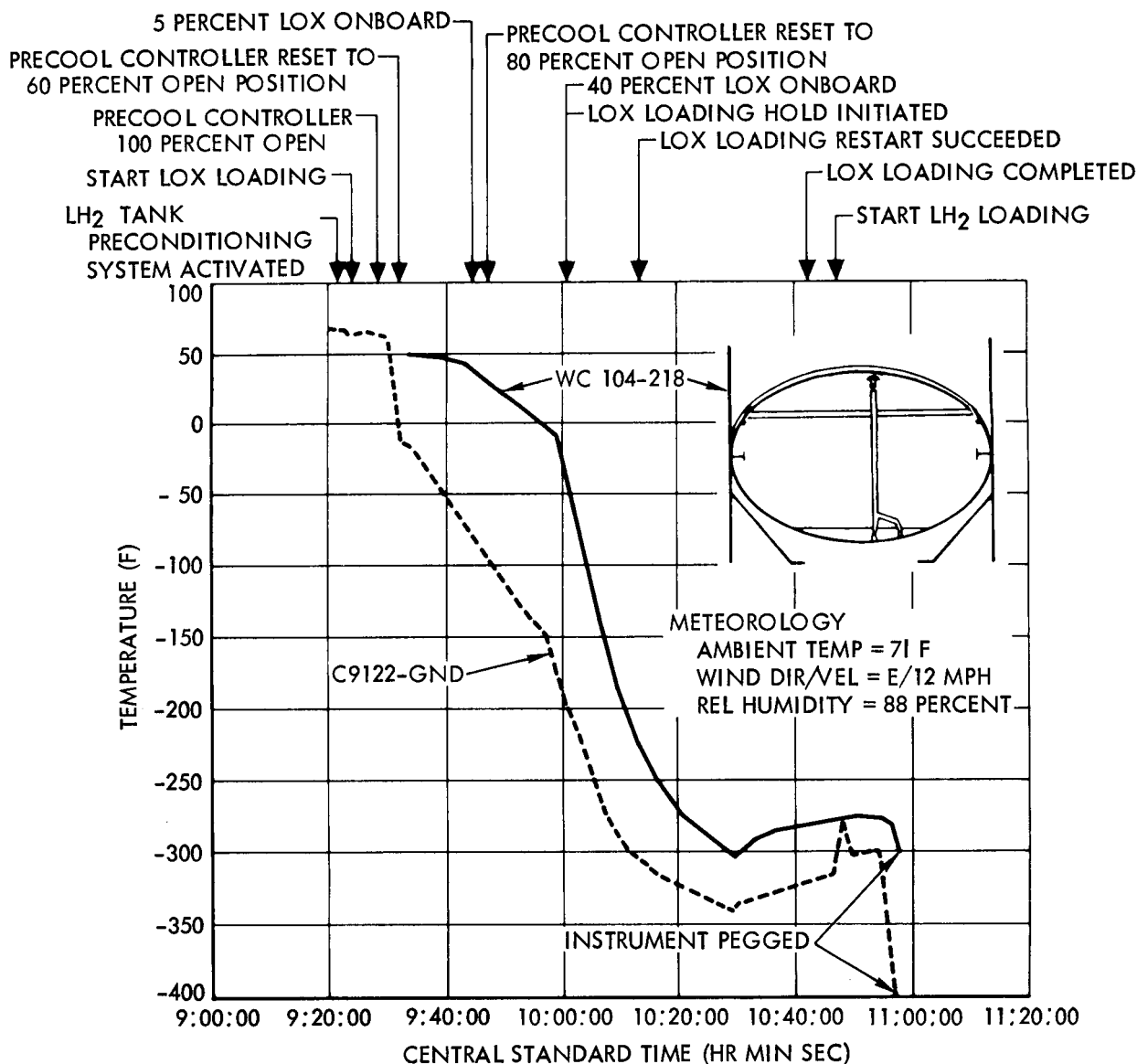

Figure 2.2-2.   LH₂ Tank Lower Cylinder Temperature During
              LOX Tank Loading (Test 546)
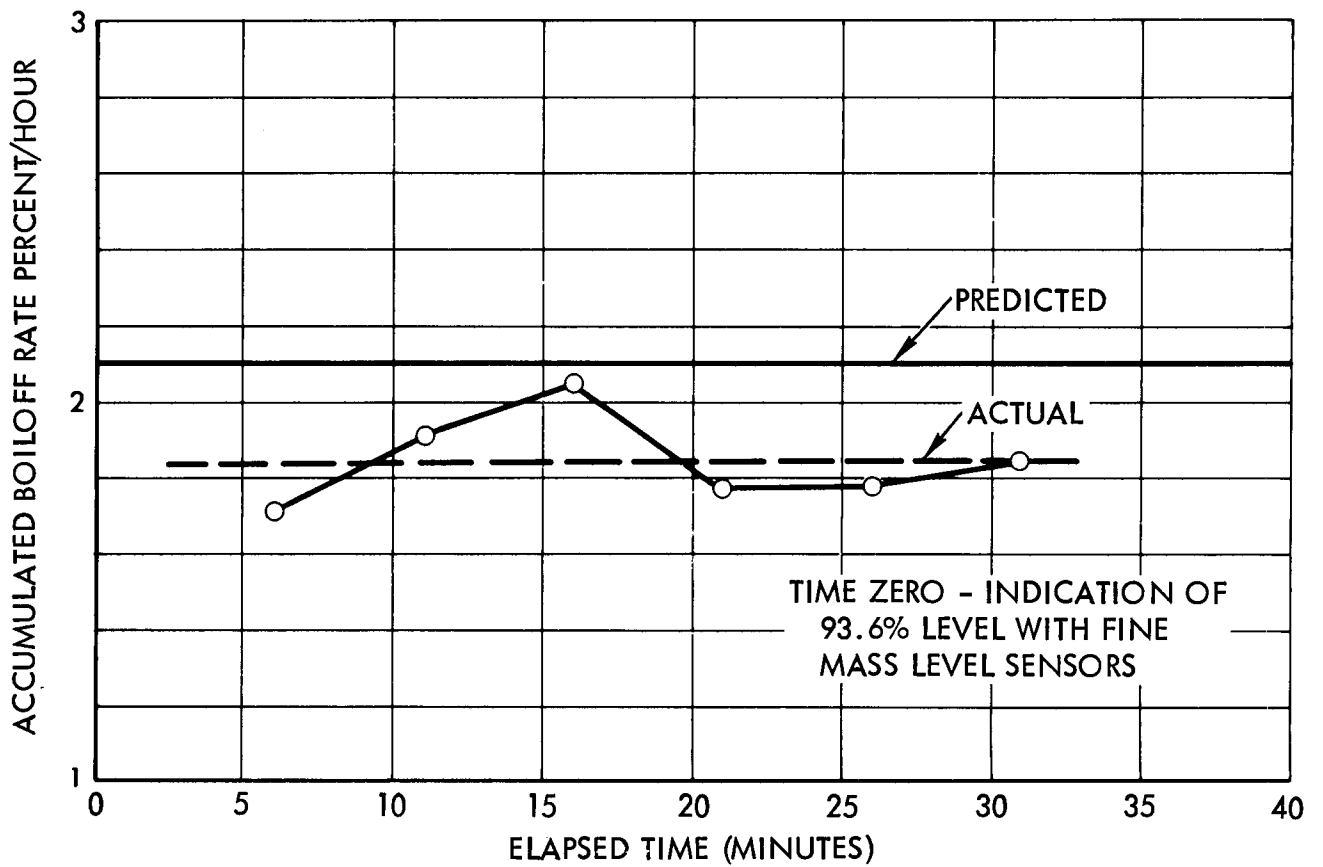
2-28

SD 69-329

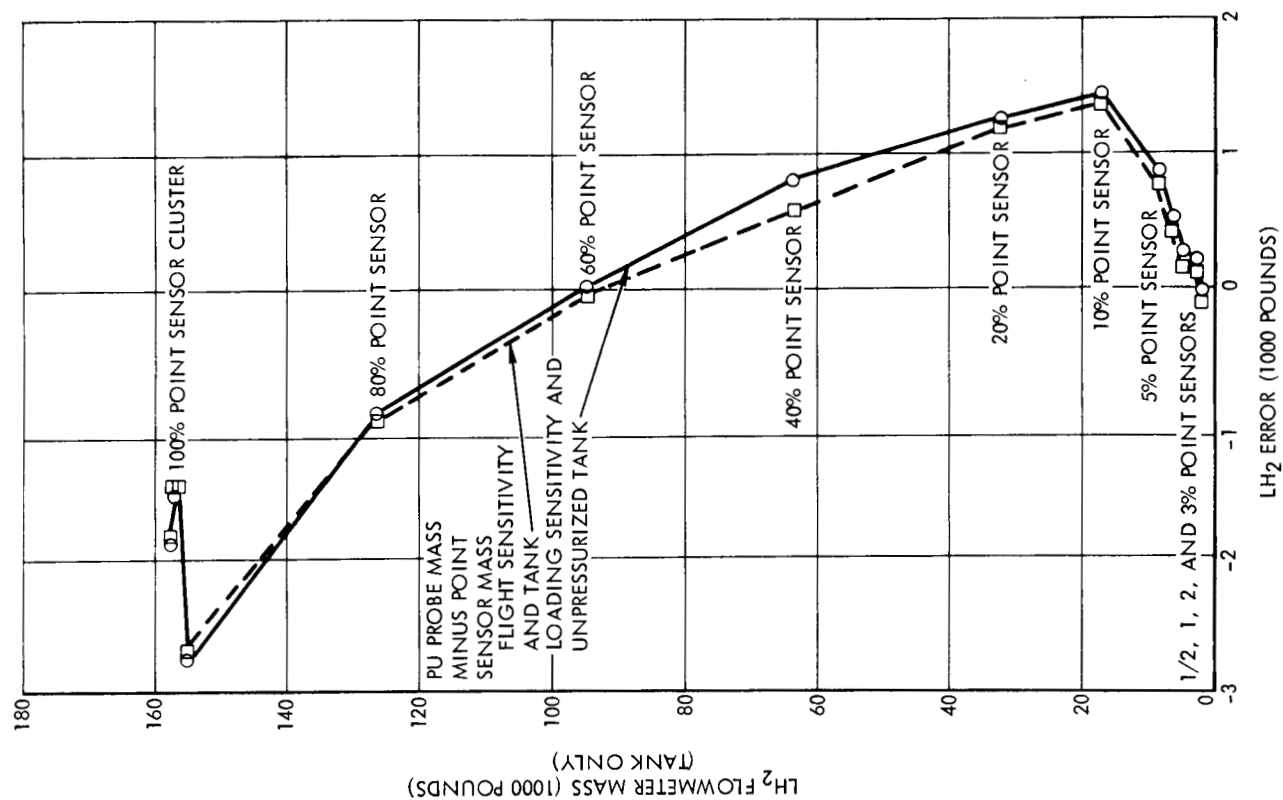Figure 2.2-3. LH$_2$ Boiloff Rate (Test 545)

Figure 2.2-5. LH₂ Probe Error (Unpressurized Tanking)
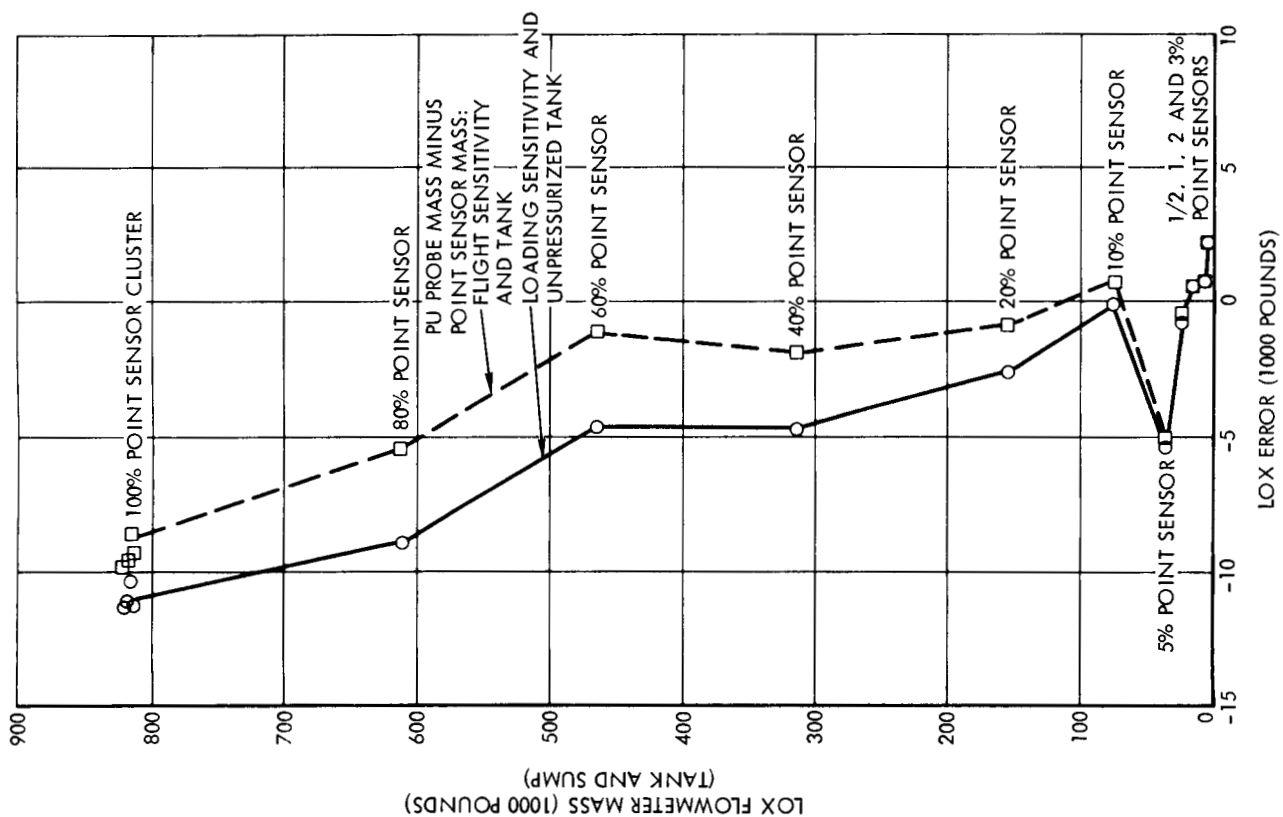

Figure 2.2-4. LOX Probe Error (Unpressurized Tanking)
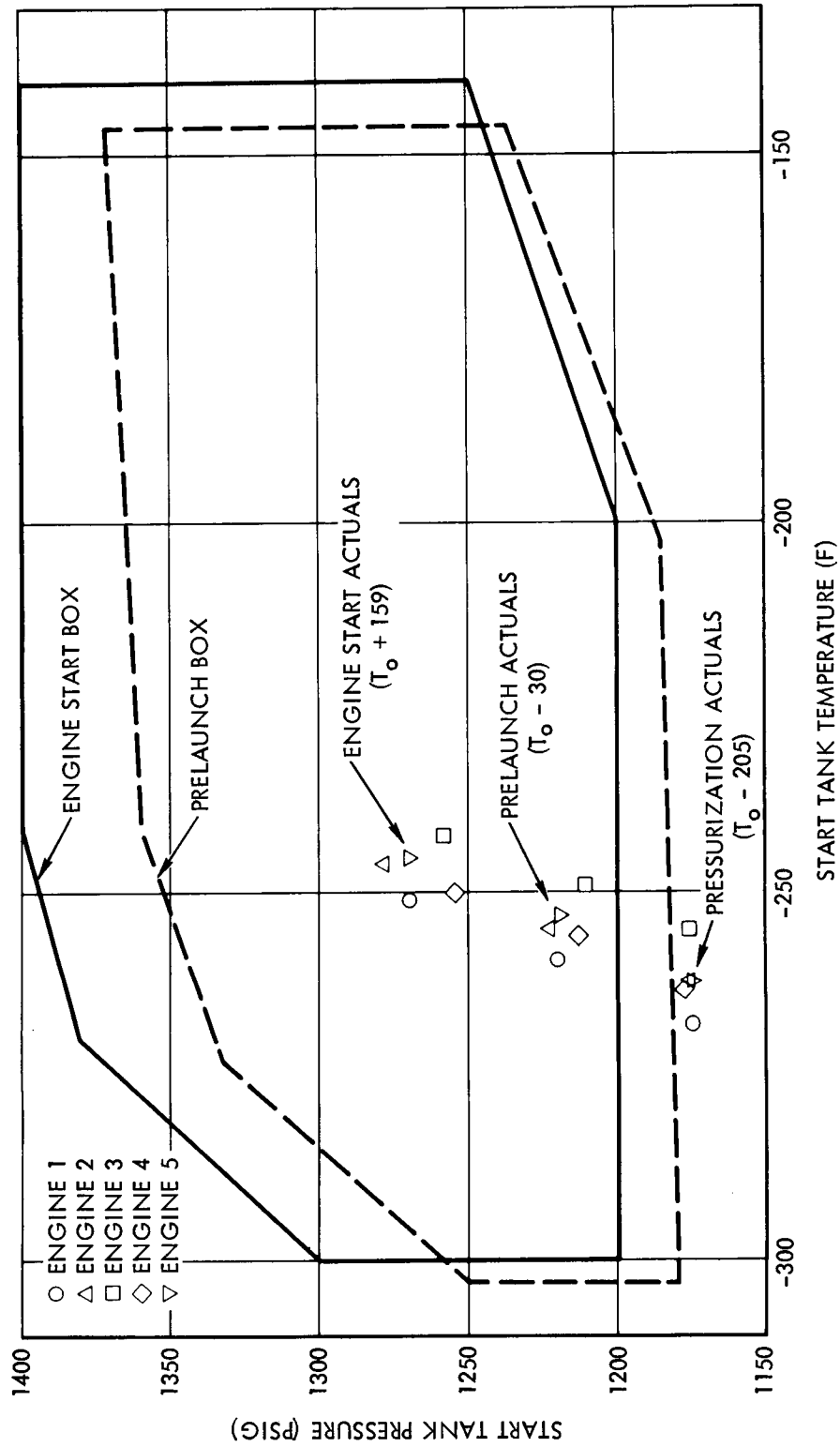
Figure 2.2-6. Engine Start Tank Conditions

Figure 2.2-7. Engine Start Tank Temperature
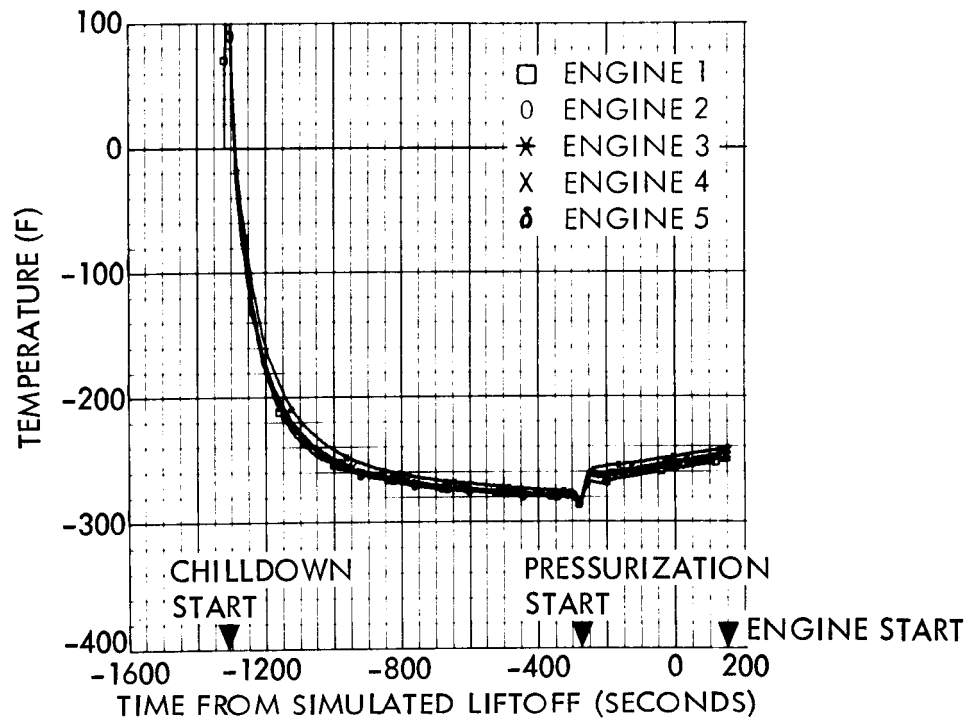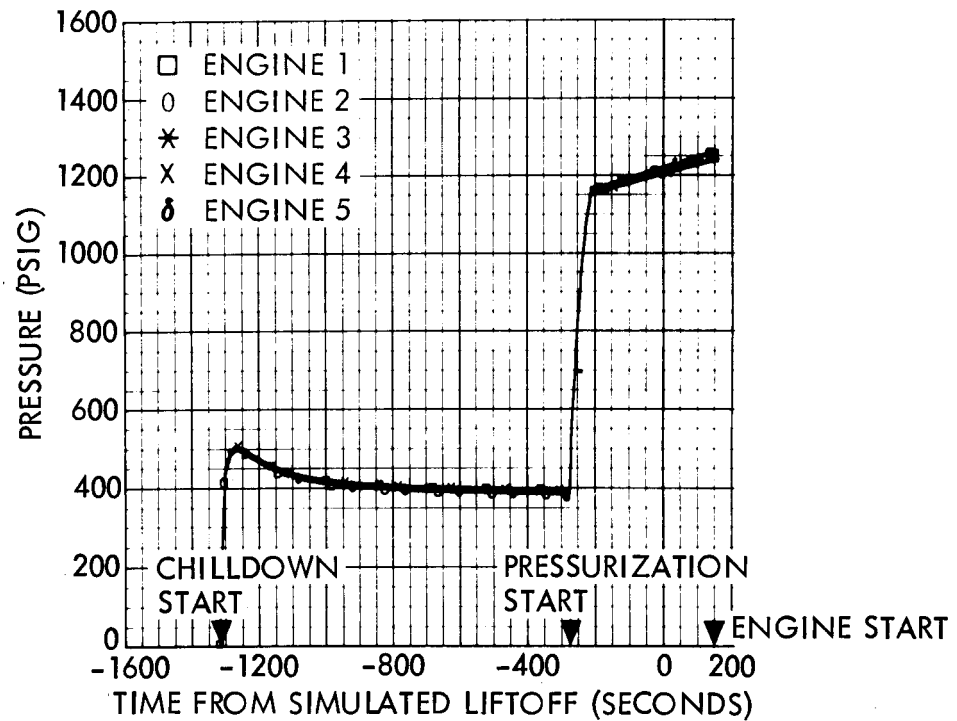

Figure 2.2-8. Engine Start Tank Pressure
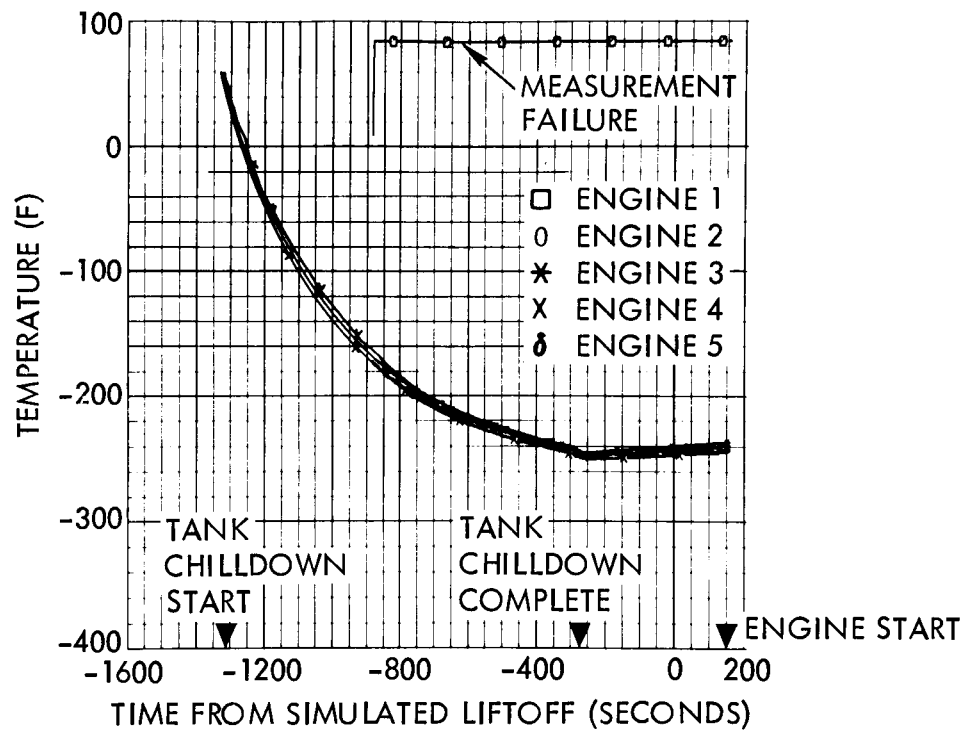
Figure 2.2-9. Engine Helium Tank Temperature
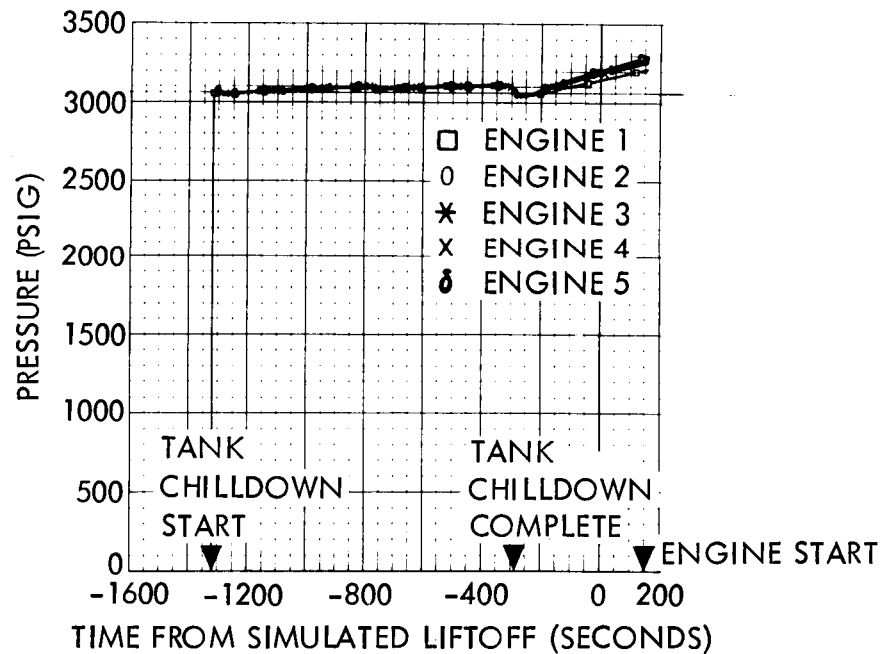
Figure 2.2-10. Engine Helium Tank Pressure
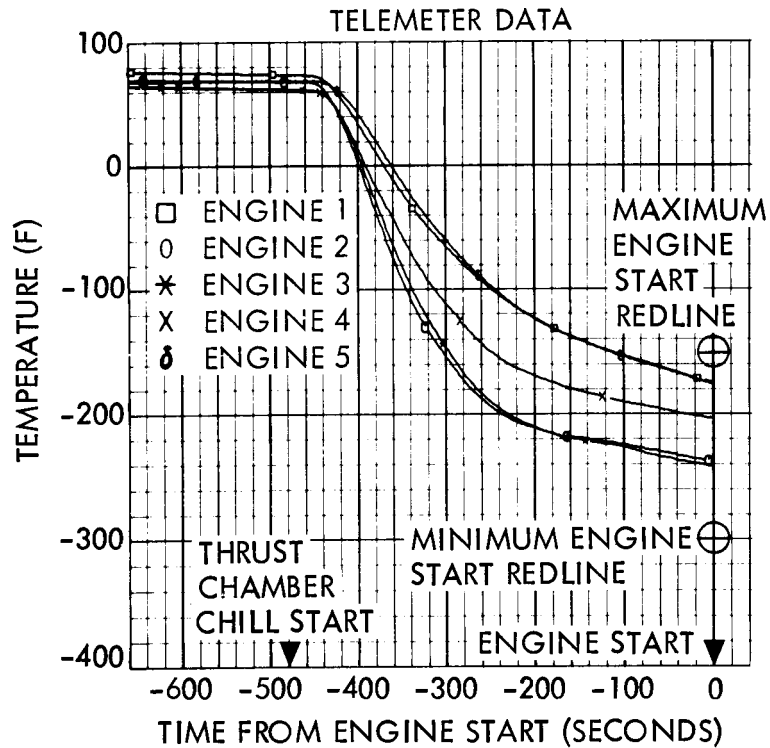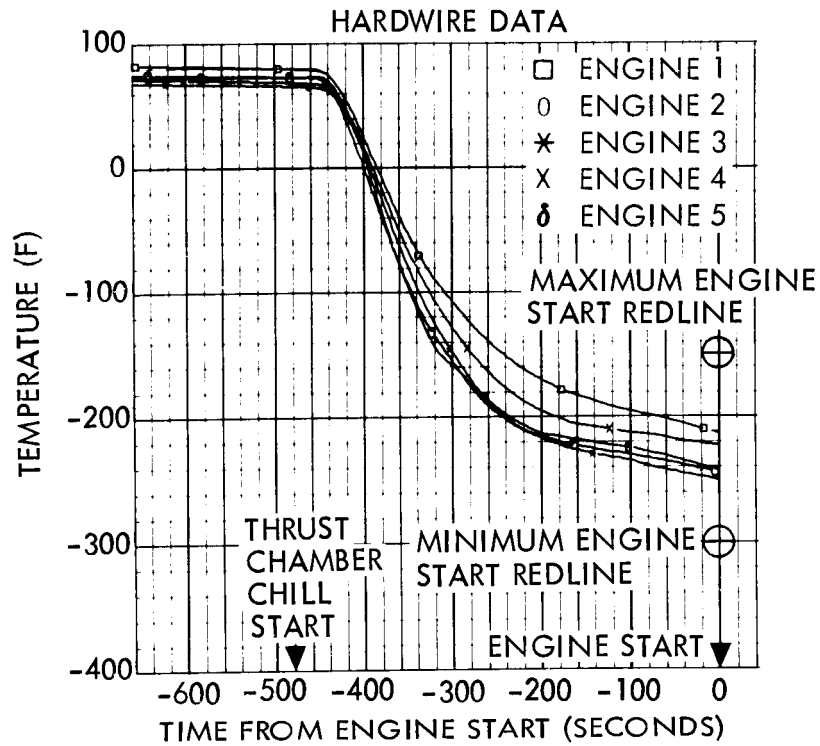
Figure 2.2-11.   Engine Thrust Chamber Temperature
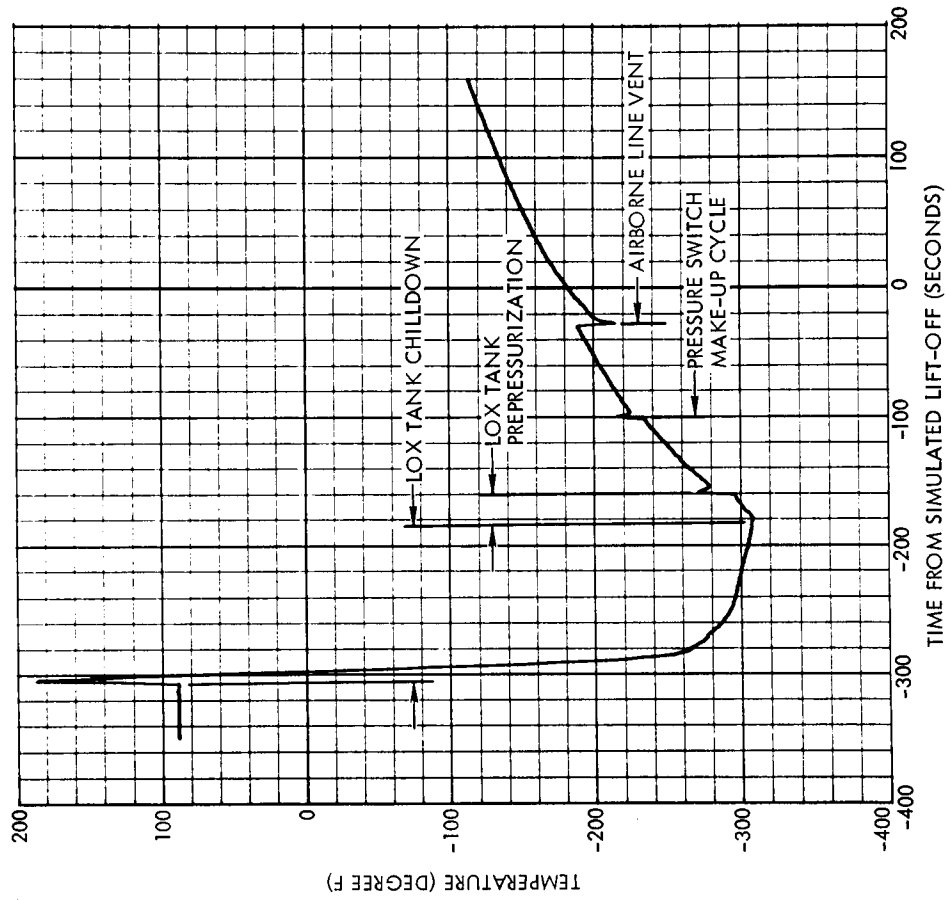
Figure 2.2-13. LOX Tank Prepressurization
Helium Temperature
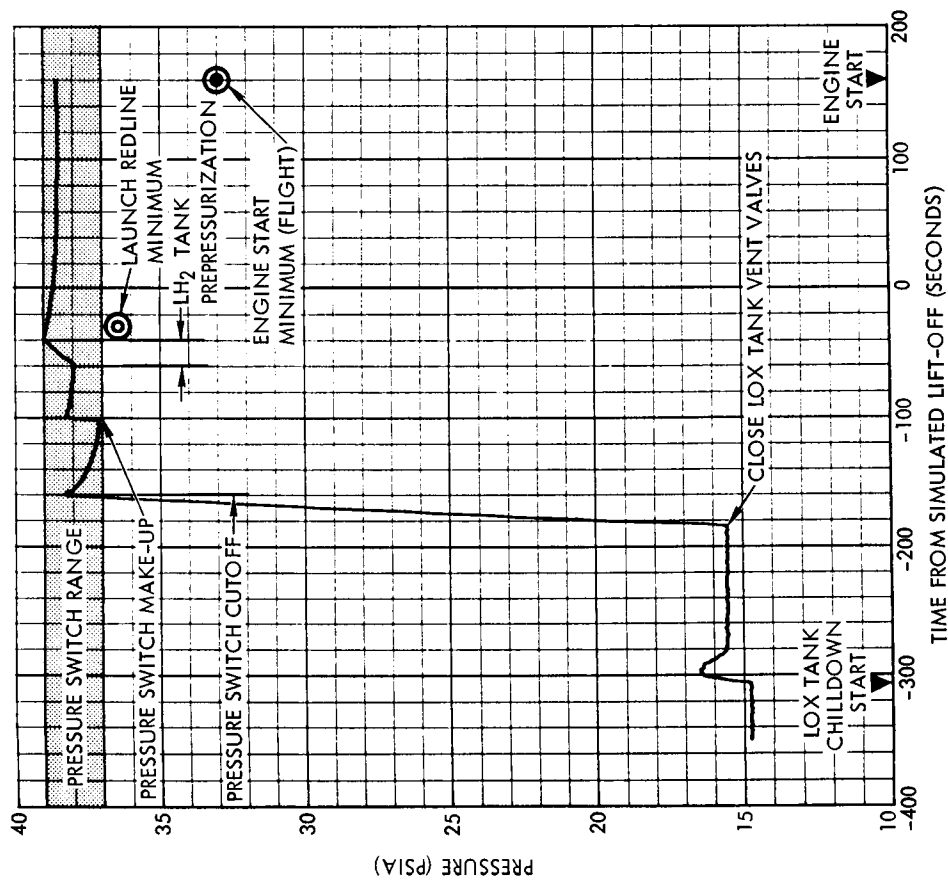
Figure 2.2-12. LOX Tank Prepressurization
Ullage Pressure
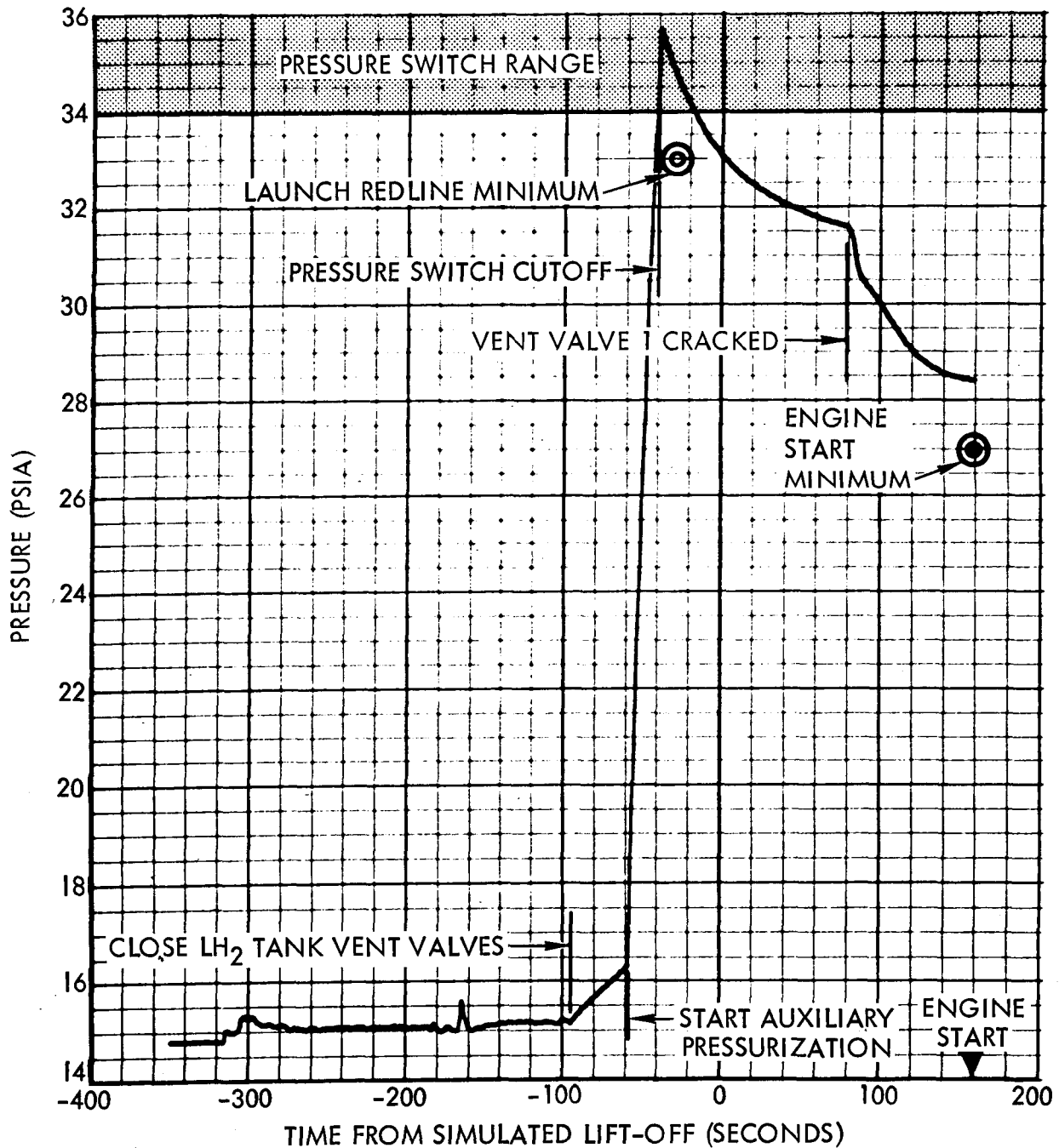
Figure 2.2-14. LH$_2$ Tank Prepressurization Ullage Pressure
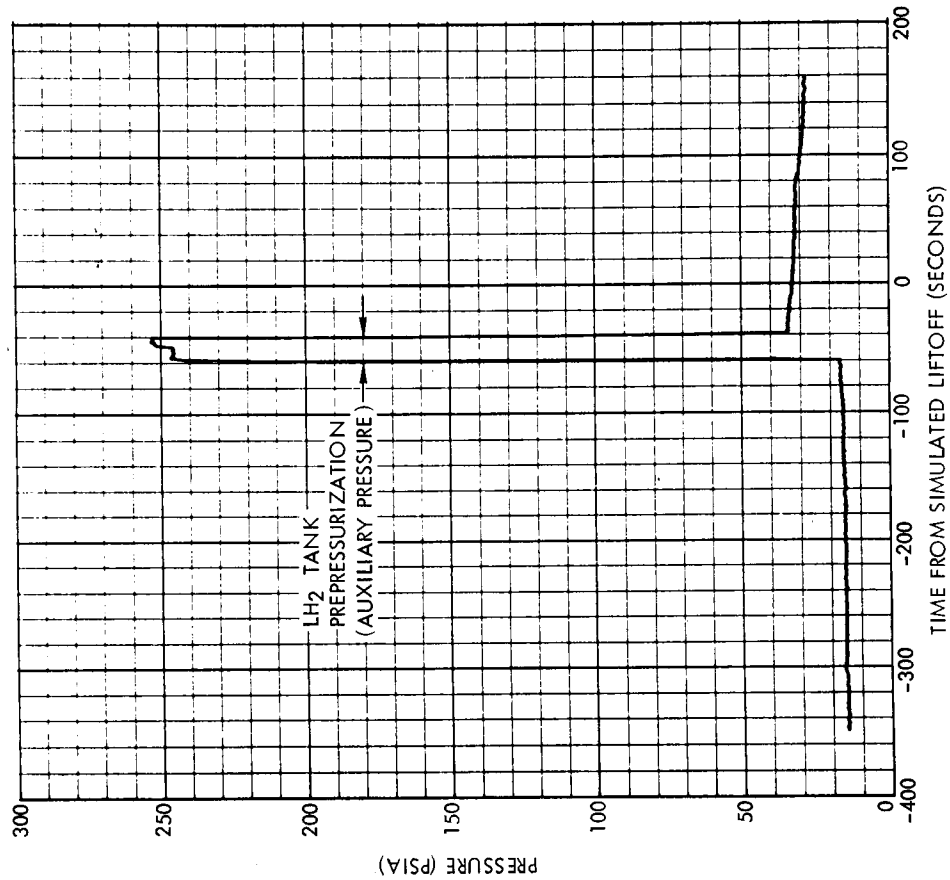
Figure 2.2-16. LH$_2$ Tank Positive Pressure
Disconnect Pressure
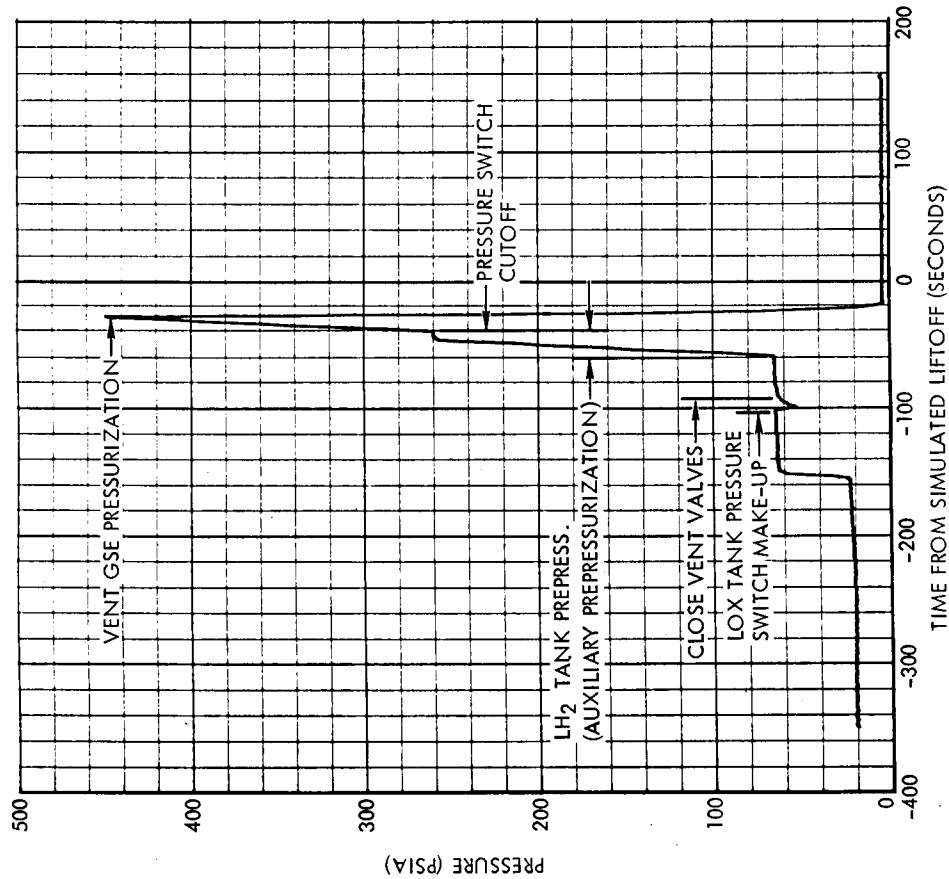
Figure 2.2-15. LH$_2$ Tank Prepressurization
Disconnect Pressure

2-37
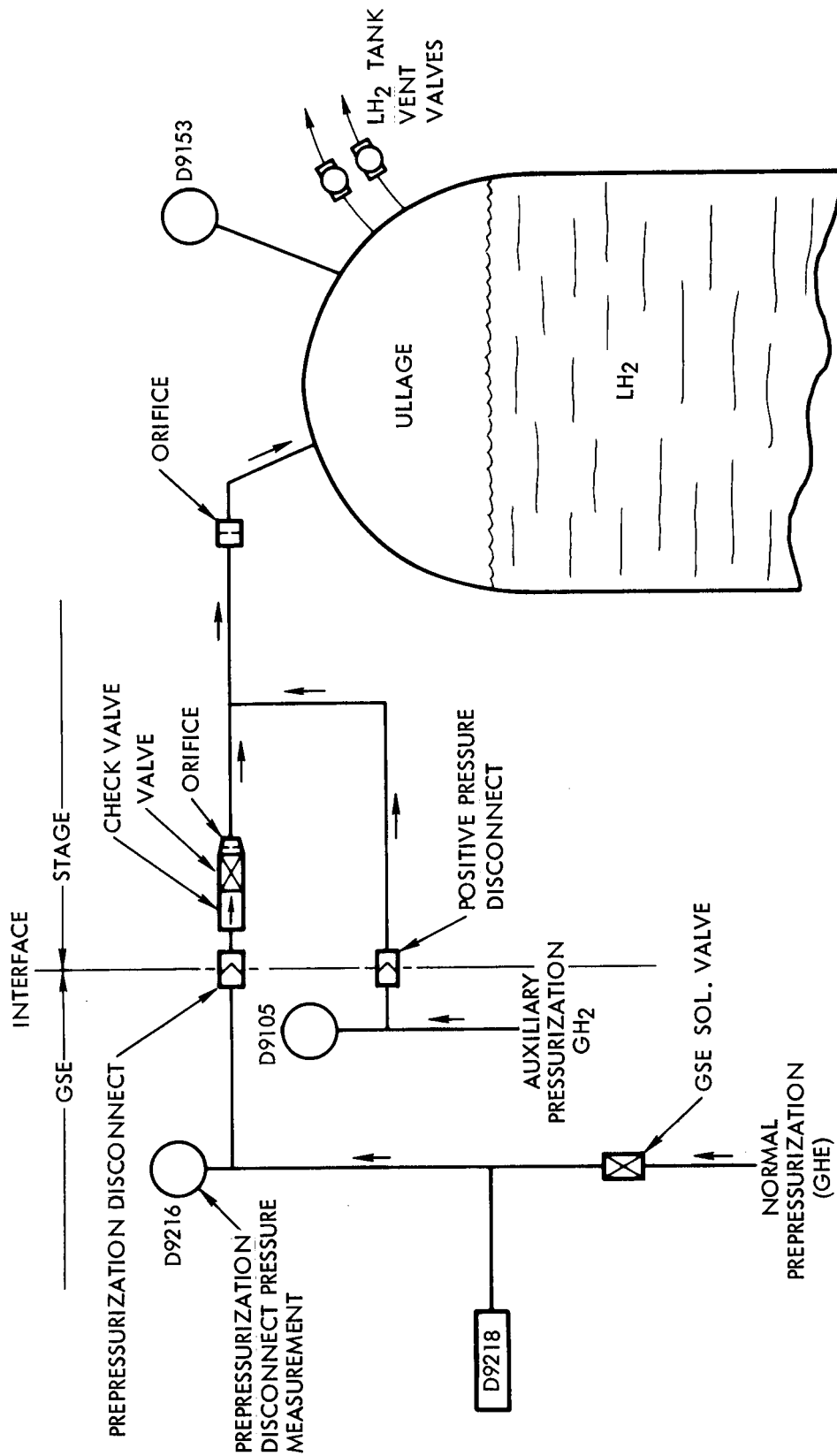
Figure 2.2-17. LH$_2$ Tank Prepressurization System Schematic

Figure 2.2-19. Engine LOX Pump Start Conditions

Figure 2.2-18. Vent Valve Operation During S-IC Boost (Simulated)

SD 69-329
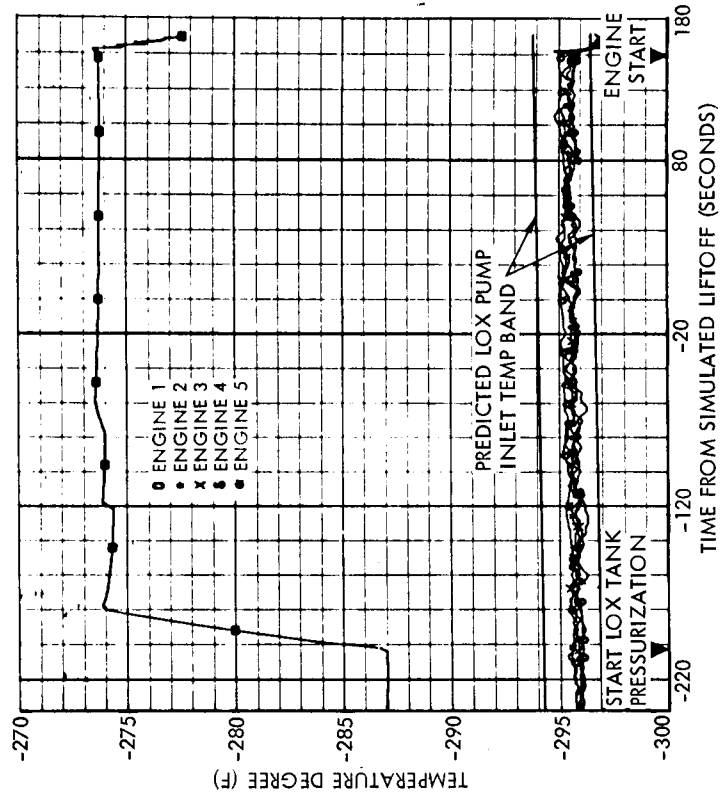
Figure 2.2-21. Engine 1 through 5 LOX Inlet Temperature
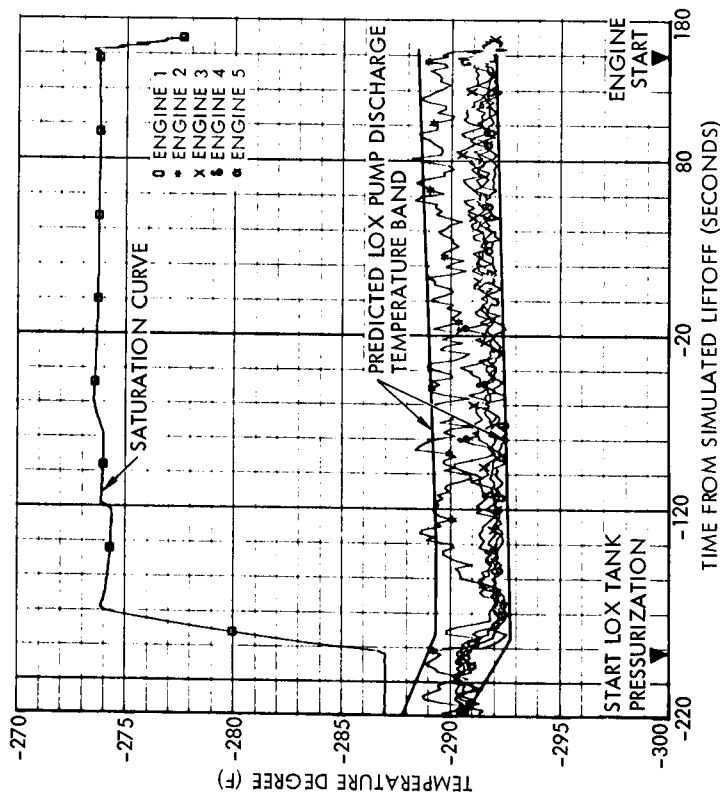
Figure 2.2-20. Engine 1 through 5 LOX Pump Discharge Temperature
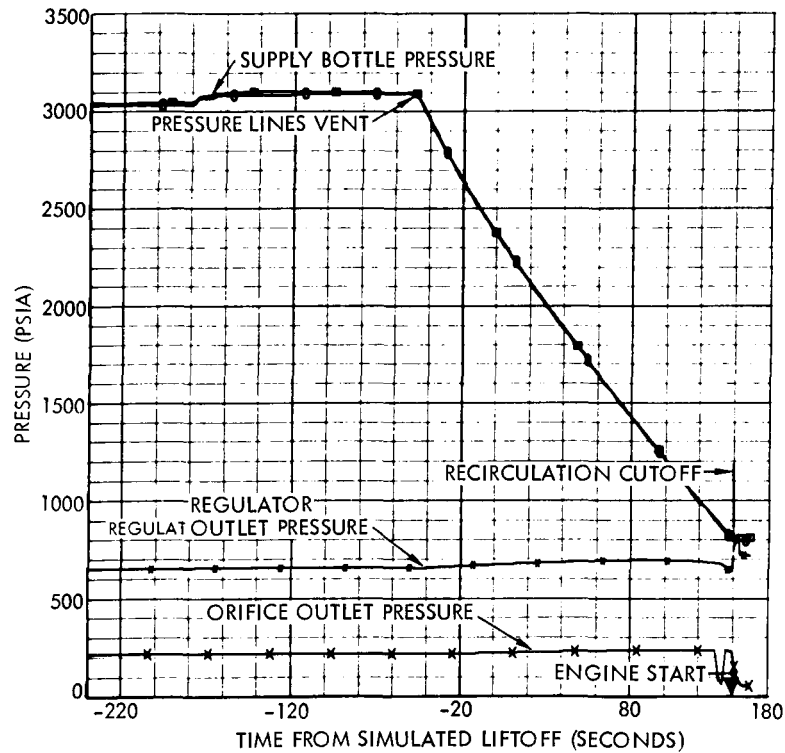
Figure 2.2-22. LOX Helium Injection System Performance
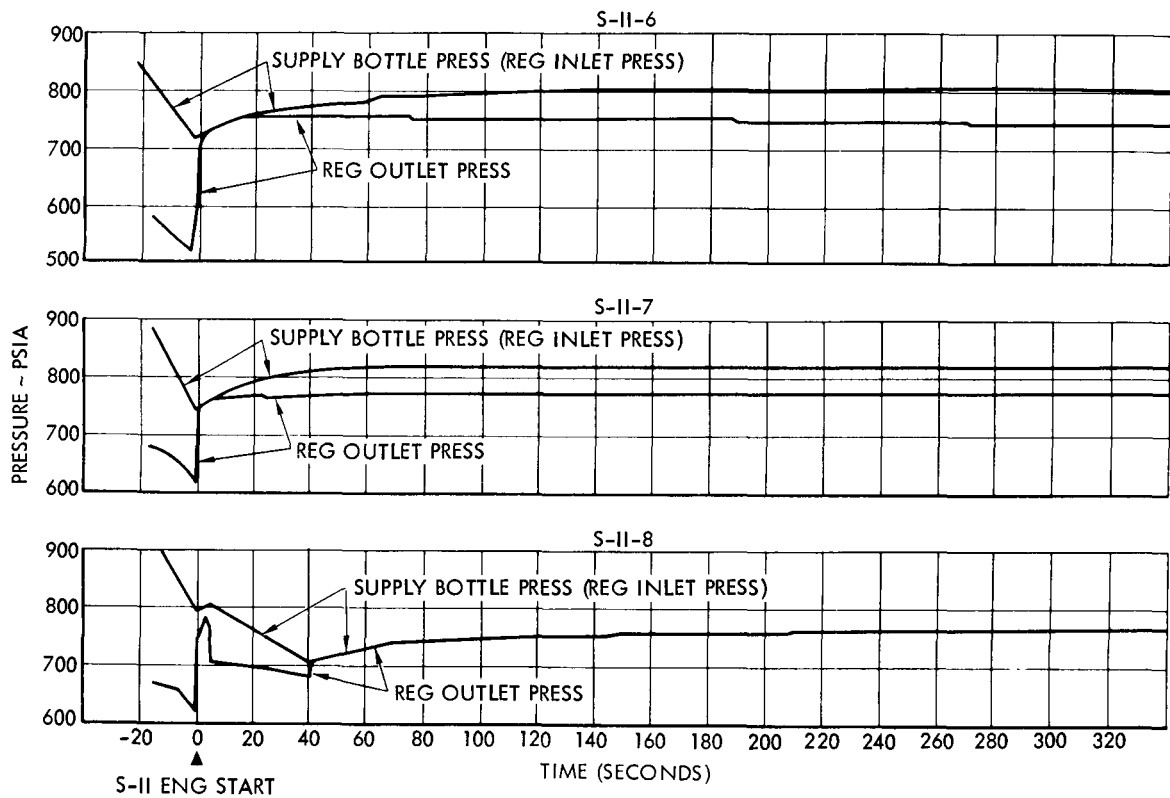
Figure 2.2-23. Helium Injection System Regulator Pressures
During Static Firing
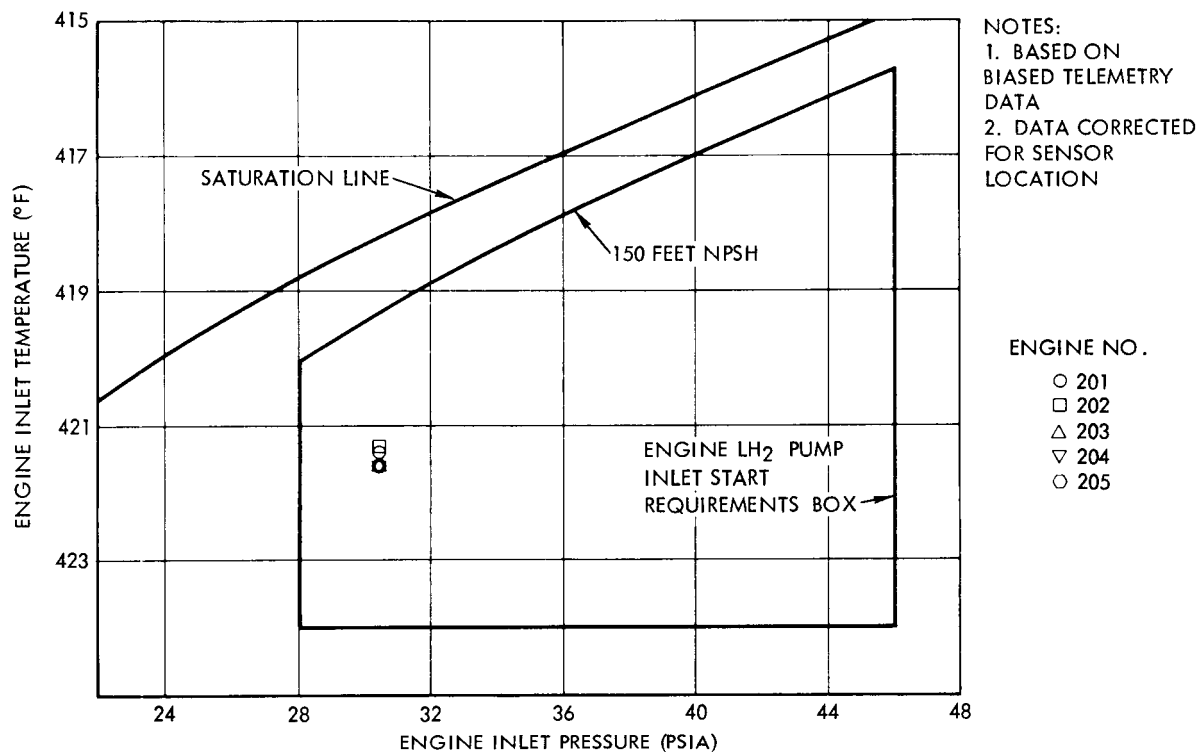
Figure 2.2-24. Engine Fuel Pump Start Conditions for Static Firing

Figure 2.2-25. Engine LH₂ Inlet Temperature

Figure 2.2-26. Feed Duct Vacuum vs Delta Temperature at Simulated Liftoff
Minus 22 Seconds

Figure 2.2-27. Feed Duct Vacuum vs Delta Temperature at Simulated
S-II Engine Start

2-43

2.3 PROPULSION SYSTEM START AND MAINSTAGE EVALUATION

This section contains an evaluation of all S-II-8 propulsion system performance during static firing test 546 from engine start through engine cutoff. All acceptance requirements imposed upon the propulsion system during start and mainstage were satisfied. Evaluation and supporting data for the acceptance requirements are presented in Volume 1 of this report.

START TRANSIENTS

All engine start conditions were satisfied at the initiation of engine start command, simulated liftoff (T_O) plus 159.803 seconds. A detailed discussion of the engine servicing and prestart conditioning is presented in subsection 2.2. During engine ignition, the PU system maintained the PU valves in the null position at -2 degrees. This provided a nominal engine mixture ratio (EMR) of 4.9 to 1 during engine buildup transients.

Individual engine thrust buildup was satisfactory on all engines. The thrust buildup profiles are presented in Figure 2.3-1 with the envelope requirement. Ninety percent thrust (184,500 pounds) at the null PU valve position was achieved between 3.8 and 4.6 seconds from engine start command. Engine 5 exhibited the fastest buildup rate and engine 1 the slowest. The mainstage OK pressure switch pickup times were in the band of 2.9 to 3.1 seconds, well within the 4.75 second allowable period.

Propellant flowrate and pump speed buildups during the engine start transients were normal. These data are presented in Figures 2.3-2 through 2.3-5. Flowrates were plotted from hardwire data, and the pump speeds were plotted from telemetry data. Differences in the propellant flowrate buildup data as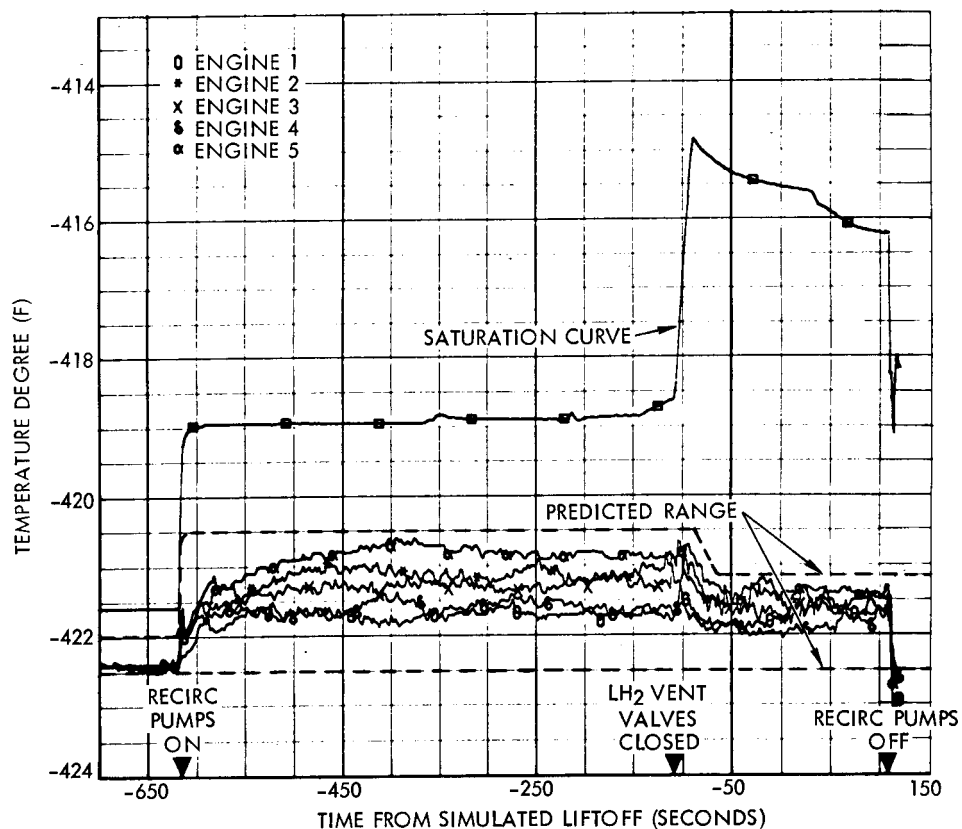 acquired by hardwire and telemetry instrumentation systems were discussed in the S-II-5 report (SD 68-377). Use of hardwire data was necessary to provide accurate propellant usage figures during the engine start transient.

The minimum fuel flowrate during transition was 39 pounds per second for Engine 4. Generally, during the 2.0 to 4.0 second time period, Engine 4 fuel flow was slightly lower than normal; however, no fuel pump stall situation was indicated. This was determined through the use of the fuel pump head versus flow curve. At 5700 gpm (approximately 58 pounds/second) the indicated stall margin was down to 200 gpm.

MAINSTAGE OPERATION

Mainstage Performance

Open-loop PU system operation commenced when high EMR was commanded at engine start (T_S) + 5.62 seconds as planned. An average stage thrust level of 1,164,000 pounds was produced throughout the high EMR (5.5) portion of the

static firing. The stage thrust profile was smooth throughout this period as shown in Figure 2.3-6. Small perturbations occurring between 65 and 100 seconds after engine start were the effects of the engine actuation system gimbal program. The slight decrease in stage specific impulse and the increase in stage mixture ratio at engine start plus 103.15 seconds was the effect of LOX tank step pressurization. The shift at 298.78 seconds was the effect of fuel tank step pressurization. These effects can be observed in Figures 2.3-7 and 2.3-8.

Following center engine cutoff (CECO) at engine start plus 297.78 seconds, the stage thrust was reduced to 928,000 pounds. At engine start plus 325.18 seconds, the low EMR command was initiated, driving the PU valves against the low EMR stop and providing an average engine mixture ratio of 4.39 to 1 for the low mixture ratio portion of the static firing. A minimum value of stage thrust at minimum PU was 690,000 pounds. Mainstage performance was satisfactory during the entire mainstage period.

Performance Analysis Summary Tape (PAST) 641 Analysis

Preliminary engine performance was presented for the Rocketdyne standard altitude conditions in Table B3-1 of Volume 1 of this report based on data from the hardwire instrumentation. Subsequent analysis has not produced any adjustments to these values. The engine acceptance log book values of specific impulse and mixture ratio have been adjusted in accordance with currently accepted values of LOX density.

Results of PAST 641 reductions using telemetry data are presented herein in Table 2.3-1. It is concluded that engine performance was satisfactory at the 60-second time slice. These figures will be used as a basis for S-II-8 flight performance comparisons.

With the advent of the open-loop PU operation, the accurate prediction of engine performance at low mixture ratio is of increased importance in minimizing the propellant residual. A section of data taken at the low engine mixture ratio level has been included in Table 2.3-2.

6N-011 Analysis

The results of the 6N011 engine performance calculation program are presented in Tables 2.3-3 and 2.3-4. Data are presented at both the high and low engine mixture ratio levels. These data differ from the PAST 641 values given earlier in Table 2.3-1 in that they represent the engine performance at actual test conditions (except for altitude ambient pressure) rather than at a predetermined set of standard conditions at the engine/stage interface. Therefore, these values more closely reflect the expected flight performance of the S-II-8 stage. Identical data bias and corrective techniques were applied to the 6N-011 program as were used in the PAST 641. Performance was computed from data averaged over each 1-second interval of the test period. Telemetry data were used wherever possible, and from these data it is concluded that engine performance was satisfactory during high mixture ratio.

General Engine Data

Traces of thrust, specific impulse, and engine mixture ratio, are presented in Figures 2.3-9 through 2.3-14 for the entire test duration. These data are taken from the 6N-011 propulsion performance program.

Engine altitude thrusts are presented individually in Figures 2.3-9 and 2.3-10. As mentioned previously, the effect of the engine gimbal function and the fuel tank step pressurization are evident in the data from the four outboard engines. The center engine neither gimbals nor provides fuel tank pressurant gas. LOX tank step pressurization is not evident in the individual engine performance.

During the high EMR portion, individual engine thrusts ranged from 234,713 pounds for Engine 1 down to 230,147 pounds for Engine 4. Following the PU step, thrust levels were reduced to a range of 176,513 to 173,201 pounds.

Individual engine specific impulse data are shown in Figure 2.3-11. Engine 2 has the highest performance level of 426.5 seconds, while Engine 4 has the lowest at 424.2 seconds. On the average, an increase in specific impulse of 5.8 seconds results from the PU step to low EMR operation.

Engine propellant mixture ratios are illustrated in Figure 2.3-12 in composite form. The overshoot exhibited during the first 100 seconds is similar to that experienced previously and is consistent with the engine manufacturer's prediction. The average engine mixture ratio at low EMR operation is 4.39 with a bandspread of less than 2 percent about the mean.

Main propellant flowrates for the engines are presented in Figure 2.3-13. LOX flowrates are in the band of 461.0 to 468.0 pounds per second, while fuel stabilized flowrates are between 82.7 to 84.6 pounds per second. At low EMR operation, the average LOX flowrate is 331.1 pounds per second, and the fuel flowrate is 75.3 pounds per second. Propellant pump speeds for the engines are presented in Figure 2.3-14.

ENGINE OPERATIONAL PROBLEM

Fuel Turbine Seal

During static firing operations, fire was observed at the exit of the fuel turbine seal drain line of Engine 1. Post-firing leak checks indicated that a blowing leak existed and that 8 psig was the maximum pressure that the drain system would contain.

The affected seal in Engine 1 (J2082) has been replaced and replacement subjected to leak checks. Maximum leakage rate measured was 550 scim. For subsequent leak check operations a maximum increase of 6000 scim will be allowable. Data presented in Figures 2.3-13 and 2.3-14 of fuel flowrate and fuel turbine speed illustrate the effects of this failure. The increase in flow and speed are the result of increases in fuel turbine pressure ratio related to the leak downstream of the turbine nozzles.

Engine Pneumatic Regulator Pressure

The erratic indications of regulator outlet pressure observed during the test were traced to faulty drag-in instrumentation cable equipment. This parameter was monitored extensively during all post-firing operations and no difficulties were observed.

EARLY CENTER ENGINE CUTOFF

Center engine cutoff occurred at Engine Start plus 297.777 seconds. The center engine was shut down early to verify that the low frequency oscillation buildup noted on previous static firings and AS-503 and AS-504 flights could be eliminated. A cutoff time prior to the oscillation buildup time of 321 seconds was required to demonstrate that termination of center engine operation would substantially reduce or eliminate the problem. The evaluation of pressure and vibration data verified that CECO eliminated the sustained oscillations (see Low Frequency Oscillation in this subsection).

The center engine LOX prevalve was replaced with a Parker-type prevalve incorporating a pressure relief valve. This was required to provide propellant feed duct pressure relief capability since the prevalves and engine bleed valves were closed at center engine cutoff, trapping a volume of fluid. The relief valves functioned as required, maintaining the pump inlet pressures at 66 to 74 psig, which is below the maximum allowable pressure of 150 psig (see Volume 1 of this report for details).

For flight, the same problems will not exist since the engine bleed valves will remain open after engine cutoff thus allowing two relief paths to the tank; through the prevalve relief valves or return line valves.

The center engine electrical control assembly (ECA) package was insulated for static firing to provide thermal protection from radiant heating. A temperature measurement (BC005-205) installed on the package revealed the maximum temperature attained was 70 F.

The center engine thrust chamber diffuser was removed for static firing. This was done to insure that the diffuser water spray did not interfere with operation of the water spray heat shield and thus have a detrimental effect on center engine cooling. Removal of the diffuser could be accomplished since it is required primarily for engine operation at low EMR and the center engine was shut down prior to this event.

A water spray heat shield was added around the exit plane of the thrust chamber to provide thermal protection to the center engine subsequent to cutoff. Evaluation of center engine special temperature measurements revealed all temperatures were well below the allowable limits (see Volume 1 of this report for details). The other thermal areas reviewed included the base heating effects on base area structure temperatures due to an early shutdown of the center engine. Using the water spray heat shield resulted in no increase in base area structure temperatures from CECO to outboard engine cutoff.

Evaluation of data from special vibration and acoustic measurements installed center engine revealed levels well below limits specified by Rocketdyne (see Volume 1 of this report for details).

The center engine oxidizer dome and thrust chamber purges were initiated at center engine cutoff to prevent the accumulation of moisture on the thrust chamber injector. Evaluation of system data indicates the purges operated as required (see Engine Servicing section for details).

Special post-static firing leak and functional checks were conducted on the center engine to verify component integrity following early shutdown. The checkouts were conducted and proved satisfactory on the following components:

1. Fast shutdown valve
2. Purge control valve
3. Fuel pump seal drain and purge check valves
4. Gas generator fuel and oxidizer purge check valves
5. Fuel and LOX turbine seal purge check valves
6. Main oxidizer valve sequence control valve
7. Start tank discharge swing gate
8. Start tank discharge valve piston and piston lipseal
9. Oxidizer turbine bypass valve drive shaft
10. Main fuel and oxidizer valves driver and idler shafts
11. Gas generator and ASI spark igniters
12. Oxidizer pump intermediate seal

LOW FREQUENCY OSCILLATION, S-II-7 AND S-II-8

Static firing data for measurements showing significant low frequency oscillations from vehicles S-II-7 and S-II-8 have been compiled in order to:

1. Verify that the center engine oscillations noted during S-II-7 static firing have been substantially reduced or eliminated on S-II-8.

2. Verify that the outboard engines are not adversely affected by early center engine cutoff (CECO), and that there are no adverse structural responses due to CECO.

3. Investigate oscillatory buildup and decay on engine 5 LOX pump inlet and outlet pressures from CECO through PU step of outboard engines.

RMS time histories (oscillographs) of 28 static firing measurements were prepared using a 1/3 octave filter centered at 16 cps. This range of frequencies was chosen because the major static firing low frequency oscillations vary from 16 to 18 cps.

The data comparisons between S-II-7 and S-II-8, as illustrated in Figures 2.3-15 through 2.3-27, were made between 280 and 348 seconds after engine start. This was the time period the low frequency oscillations were noted on previous stages during static firings and flights. Figures 2.3-15 and 2.3-16 present engine thrust chamber pressures for engines 5 and 1, respectively. The S-II-8 oscillations were terminated on engine 5 with CECO and no amplitude buildup occurred on engine 1.

Figure 2.3-17 shows engine 5 thrust pad vibration data. The amplitude on S-II-8 prior to CECO was approximately 1/3 of S-II-7 values, while after CECO the oscillatory period was reduced to an insignificant level.

Figure 2.3-18 presents LOX tank sump vibration data. The amplitude buildup noted on S-II-7 during the peak oscillatory period was eliminated on S-II-8. Both vehicles exhibited the same basic trends from CECO through 324 seconds. The amplitude prior to CECO on both vehicles was about the same, with S-II-8 amplitude decaying to .04 GRMS subsequent to PU step. A buildup in amplitude was noted on S-II-8 starting at 205 seconds and reaching a peak of 0.13 GRMS at 255 seconds.

Figure 2.3-19 compares the S-II-7 LOX tank bulkhead with S-II-8 LOX tank sump vibrations. Since a LOX tank bulkhead measurement did not exist on S-II-8 the LOX bulkhead measurement on S-II-7 was compared with the LOX sump on S-II-8. The amplitudes on S-II-7 and S-II-8 prior to CECO were about the same. A slight buildup in amplitude of 0.14 GRMS at 326 seconds was noted on S-II-7 and a similar buildup to 0.1 GRMS at 328 seconds on S-II-8. After PU step on S-II-8 the amplitude decayed to an insignificant level (.02 GRMS at 340 seconds). A buildup in amplitude was noted on S-II-8 starting at 205 seconds reaching a peak of 0.13 GRMS at 255 seconds.

Figures 2.3-20 and 2.3-21 present engine 1 thrust pad vibration data. The amplitude buildup noted on S-II-7 during the peak oscillatory period was eliminated on S-II-8. Subsequent to PU step on S-II-8 the amplitude decayed to a lower level.

Figure 2.3-22 shows engine 5 LOX pump inlet pressure measurement WD091-205. The amplitudes on S-II-7 and -8 prior to CECO were about the same. The amplitude buildup noted on S-II-7 during the peak oscillatory period was eliminated on S-II-8 due to center center shutdown. However after CECO through PU step of other S-II-8 engines, the amplitude increased to 0.7 psi RMS and oscillated between 0.5 and 0.7 psi RMS. The signature of this trace and the LOX tank sump vibration (WA020-206) showed equivalent signatures throughout the time period indicating the trapped fluid was reacting to sump motion. At CECO the prevalve and engine main LOX valve were closed, trapping a volume of fluid. The change in amplitude (cycling from 0.5 to 0.7 psi) may be the result of the integral relief valve in the prevalve cracking and reseating. Subsequent to PU step of the outboard engines, the amplitude decayed to 0.3 psi RMS. It should be noted that no amplitude buildup was noted on engine 1 LOX pump inlet pressure measurement WD091-201 for either S-II-7 or S-II-8 as shown in Figure 2.3-23.

Figure 2.3-24 presents engine 5 LOX pump inlet data (close coupled) (WD261-205). The amplitude buildup noted on S-II-7 during the peak oscillatory period was eliminated on S-II-8 due to center engine shutdown. However after CECO through P.U. step of outboard engines, the S-II-8 amplitude increased to 2 psi RMS and oscillated between 1 and 2 psi RMS. The signature of this trace and LOX tank sump (WA020-206) are nearly identical throughout the time period indicating the trapped fluid was reacting to sump or bulkhead motion. Subsequent to P.U. of outboard engines, the amplitude decayed to an insignificant level.

2-50

Figure 2.3-25 shows engine 1 LOX pump inlet pressure data (WD261-201). The amplitude buildup noted on S-II-7 during the peak oscillatory period was eliminated on S-II-8. Prior to CECO the amplitude on both vehicles was about the same. Subsequent to P.U. step on S-II-8 the amplitude decayed to an insignificant level. This measurement showed a buildup on S-II-7 whereas the redundant measurement WD091-201 (Figure 2.3-23) showed no buildup.

Figure 2.3-26 presents engine 5 LOX pump discharge pressure data. No amplitude buildup was noted on either S-II-7 or S-II-8 during the peak oscillatory period. As experienced in the S-II-8 pump inlet pressures on engine 5, the amplitude increased after CECO to 3.2 psi RMS maximum and decayed to an insignificant level after outboard engine PU step. Prior to CECO the amplitudes on S-II-7 and S-II-8 were about the same.

Figures 2.3-27 presents engine 1 LOX pump discharge pressure data. The small amplitude buildup noted on S-II-7 during the peak oscillatory period was eliminated on S-II-8. Prior to CECO the amplitude on S-II-7 and S-II-8 was similar. Subsequent to PU step the amplitude on S-II-8 decayed to less than 1 psi RMS. A buildup to 2.6 psi RMS was noted at 225 seconds, on S-II-8.

Analysis of all data gathered during both S-II-7 and S-II-8 acceptance static firing tests has resulted in the following set of conclusions relevant to the results of center engine cutoff.

1. Center engine oscillation buildup encountered during S-II-7 static firing at 324 to 348 seconds was eliminated during S-II-8 static firing by shutdown of the center engine at 298 seconds.

2. Center engine vibration measurements (thrust pad and LOX sump) indicated a substantial decrease in oscillation amplitude subsequent to CECO.

3. Outboard engine (Engine 1) measurements (chamber pressure, LOX pump pressures, and thrust pad) indicated a decrease in oscillation amplitude subsequent to CECO.

4. All S-II-8 measurements indicated a further decay in oscillation amplitude starting at PU step at 325 seconds and reaching an insignificant level at 340 seconds.

5. The LOX sump and engine 5 LOX pump inlet pressure traces subsequent to CECO through outboard engine PU step were nearly identical in wave form, indicating the trapped fluid was reacting to sump motion.

ENGINE CUTOFF TRANSIENTS

Outboard engine thrust decays following cutoff were normal. Decay to five percent of rated thrust took place within 0.37 seconds after engine cutoff signal. Center engine cutoff from the high EMR (5.5) level did not

result in any abnormal transients. However, the decay profile did not lie fully within the envelope predicted for cutoff from the null (5.0) EMR thrust level. Main LOX valve closing time for the center engine was 0.082 second delay and 0.182 second travel as contrasted with a nominal 0.073/0.150 for the outboard engines. The slower valve operation is consistent with the higher LOX flowrate associated with 5.5 EMR operation and explains the actual thrust decay profile and the nominal envelope. During the post-static firing dry engine sequence tests, center engine valve times were well within specification limits. Normalized thrust decay rate for the center engine is given in Figure 2.3-28.

PROPELLANT MANAGEMENT SYSTEM

General

Nominal open-loop PU system operation was observed throughout the static firing. See Tables 2.3-5 and 2.3-6 for system performance summaries. All acceptance test requirements were satisfied. Test results presented in Volume 1 of this report have been refined and are presented within this subsection. No propellant management system anomalies resulted from the planned early center engine shutdown.

At ESC + 325.18 seconds, the low EMR command was initiated driving the PU valves against the low EMR stop. This control provided an average EMR of 4.39 (predicted 4.36) for the remaining low mixture ratio portion of the static firing.

Predicted propellant depletion curves are compared with actual values in Figure 2.3-29 and indicate good correlation. The PU error at ECO signal was + 2350 pounds of LH_2 compared to an allowable 3-signma open-loop tolerance of ±4500 pounds. The actual tank depletion ratio just prior to flow decay was 4.35 versus a predicted tank depletion ratio of 4.32 at engine cutoff. Tank mixture ratios computed from PU system data and from engine flowmeter data, and actual and predicted PU valve position are plotted versus engine burn time in Figure 2.3-30. Close agreement can be observed between the two methods of computing tank mixture ratio. The response of the PU valve position to the predicted PU valve slew command indicates expected valve operation. Results of a PU valve response comparison with simulation data showed average valve travel times within 0.1 second of simulation values.

Propellant Depletion Engine Cutoff System Operation

A nominal 1.0 second time delay (actual delay was 0.85 seconds) was used for the first time on a static firing of a flight vehicle. Performance characteristics were similar to Battleship static firings that incorporated ECO time delays. Virtually no engine LOX flow decay characteristics or evidence of propellant vortexing were observed before ECO.

Automatic engine shutdown sequence was initiated by the LOX propellant depletion ECO point sensors at ESC plus 384.74 seconds which was 3.46 seconds shorter than expected. This was attributed to a slightly higher engine and pressurization flowrate than predicted and a slight underload of LOX.

Propellant residuals (mass in tanks and sump at ECO as determined from extrapolation of data from the 10, 5, 3, and 2-percent point level sensors to ECO) were 2300 pounds of LOX and 6881 pounds of LH$_2$ (see Figure 2.3-31). A predicted LOX residual of 2690 pounds was higher than the actual amount because a less accurate method, using only the two percent point sensor, was employed in determining the prediction. Higher LH$_2$ residual than the 4527 pounds predicted was due to an overload of LH$_2$ combined with reduced burn time. These residual and burn time variations from predicted are considered normal for open-loop operations.

Mass Probe to Tank Calibration

Table 2.3-7 presents a comparison of propellant masses as measured by the PU probes, flowmeters and point level sensors. The best estimate propellant mass is based on flowmeter integration data.

The point sensor masses are based on theoretical height-volume tables and actual bulk densities. The flowmeter integrated masses are based on flowmeter data from static firing referenced to the theoretical point sensor masses for LOX and LH$_2$ at ECO. The PU probe masses are calculated from the calibation data of Table 2.1-1. A comparison between the masses determined by the above three methods was made to determine the cryogenic calibration of the propellant tanks and PU probes for the AS-508 flight and the S-II-8 static firing. These comparisons are presented in Figures 2.3-32 through 2.3-37. It can be noted that close agreement between the three methods of measurement exists and that the general trends of the curves repeat between tests.

PU Valve Slew Tests

PU valve slew tests were performed after completing propellant loading on Tests 545 and 546 to verify performance under cryogenic conditions. PU valve fixed and control phase voltages and fixed phase currents were nominal with good correlation to actual static firing performance.

PRESSURIZATION SYSTEM

LOX Tank Mainstage Pressurization

A trace of LOX tank ullage pressure during mainstage operation is presented in Figure 2.3-38. The LOX tank pressure regulator maintained the ullage pressure within allowable limits of 36 to 38.5 psia until LOX tank step pressurization opened the regulator to its maximum position at T$_3$ + 104.4 seconds. Step pressurization is normally programmed for S-IC outboard engine cutoff (T$_3$) + 100 seconds. For this test it was inadvertently initiated a few seconds late. After the characteristic pressure surge following the initiation of step pressurization, the ullage pressure gradually increased to the vent range. However, no venting occurred. The rapid ullage pressure decay after EMR shift at T$_s$ + 325 seconds is the result of the marginal performance of the LOX heat exchangers at low EMR.

GOX pressurization flowrate presented in Figure 2.3-39 follows the regulator demands to support ullage pressure requirements. When the regulator

went to the maximum open position, the GOX pressurization flowrate reached a maximum as indicated, which included the five-engine total flow. The flowrate dropped abruptly to about 80 percent of maximum as anticipated after center engine cutoff. The characteristic drop in flowrate at EMR shift occurred, as anticipated.

GOX pressurization manifold pressure is presented in Figure 2.3-40. Ullage gas mass is presented in Figure 2.3-41. These data appear to be normal.

Engine Inlet LOX NPSH

The calculated engine inlet LOX NPSH is presented in Figure 2.3-42. The data indicated a substantial margin above the minimum requirements except at outboard engines cutoff, which was deliberately delayed past the normal LOX depletion level as a special test. The pressurization system was not designed to meet NPSH requirements beyond the normal LOX cutoff level.

The two parameters used in calculating LOX NPSH are engine LOX inlet temperature and calculated engine LOX inlet total pressure. These data are presented in Figures 2.3-43 and 2.3-44, respectively. The increase in LOX temperature was very abrupt near outboard engine cutoff because of the programmed delay after the LOX depletion sensor. The Δ T of 6.6 F as indicated was much higher than normal, however this is expected in a delayed cutoff.

The total heat load of 157,000 Btu (Figure 2.3-45) represents the total heat obsorbed by the LOX between the time of ullage prepressurization and engine cutoff at the end of static firing. The heat load was obtained by integrating with respect to time the engine inlet parameters; namely, volumetric flow, density, and temperature.

LH$_2$ Tank Mainstage Pressurization

The LH$_2$ tank ullage pressure was maintained within the allowable regulator range of 28.5 to 31 psia until the regulator was stepped open at T_s + 298.7 seconds. The LH$_2$ tank ullage pressure is presented in Figure 2.3-46. Venting occurred as expected with both vent valves cracking at a pressure of 32.4 psid. Both vent valves were in the high mode.

The GH$_2$ pressurization flowrate is presented in Figure 2.3-47. Unlike LOX pressurization flowrate, the GH$_2$ pressurization flowrate is obtained from the four outboard engines. Consequently, center engine early cutoff has no effect on the GH$_2$ pressurization supply. GH$_2$ regulator inlet pressure is presented in Figure 2.3-48. The GH$_2$ flowrate and regulator inlet pressure appear to be normal and promptly responded to step pressurization and EMR shift as expected. LH$_2$ tank ullage mass presented in Figure 2.3-49 appears to be normal.

Engine LH$_2$ NPSH

The actual engine inlet LH$_2$ NPSH, which was calculated from LH2 temperature and pressure data, is presented in Figure 2.3-50. The minimum required NPSH is also presented. This figure represents LH$_2$ NPSH for all engines during this test. The NPSH requirements for all engines were satisfied throughout the test, and the actual NPSH is well above the allowable lower limit.

The two measurements upon which the LH_2 NPSH is based are engine inlet total pressure and engine inlet LH_2 temperature. Traces of these data are presented in Figures 2.3-51 and 2.3-52, respectively. The 0.6 F increase in LH_2 temperature shown in Figure 2.3-52 is the result of normal liquid stratification in the LH_2 tank.

The actual total heat load of 72,500 Btu, (Figure 2.3-53), represents the total heat obsorbed by the LH_2 during the period from ullage prepressurization to outboard engine cutoff. The heat load was obtained by integrating a heat capacity function with respect to time. The function contains the engine inlet parameters: LH_2 volumetric flow, density, and temperature. All five engines are included in the total heat loads shown in the figure.

Composite Pressurization System Performance

Figure 2.2-54 is a composite presentation of the pressurization system performance including ullage pressures during prepressurization and mainstage with pertinent events and times noted. It is concluded that the pressurization system performed satisfactorily throughout the S-II-8 acceptance static firing test.

VALVE ACTUATION SYSTEM

At T_0-30 seconds the receiver pressure (see Figure 2.3-55) in the valve actuation system was approximately 3090 psia the minimum acceptable pressure for flight at T_0-19 seconds is 2800 psia. However, for static firing, due to the GSE capability for make-up gas, the minimum pressure is specified as 1500 psia. At S-II engine start, prior to actuating closed the eleven recirculation valves, the receiver pressure had decayed to approximately 3075 psia. This minimal decay was due to the improved leakage capability of the new prevalves. The receiver pressure dropped 150 psi when the eleven recirculation valves were actuated closed at S-II engine start; the predicted pressure drop was 140 psi.

Due to early center engine cutoff at T_S + 297.6 seconds, the center engine prevalves were closed at approximately T_S + 300 seconds. This is shown by the 50 psi drop in receiver pressure at this time. Final stage ECO occurred at T_S + 384.7 seconds, resulting in a total pressure drop in the receiver of 200 psi. Predicted pressure drop for five engines is 250 psi.

The regulator outlet pressure (Reference Figure 2.3-55) remained at a constant 715 psia except for momentary pressure drops when the recirculation valves were actuated closed at engine start, when the center engine LOX return line valve was opened at approximately T_S + 260 seconds, when the center engine prevalves were closed at approximately T_S + 300 seconds, and when the outboard engine prevalves were actuated closed after the engines were cut off at T_S + 384.7 seconds. Recovery period for the regulator outlet pressure did not exceed 20 seconds for any of the events listed above. The regulator band is 690 to 765 psia.

PROPELLANT FEED SYSTEM

The propellant feed system evaluation and supporting data for the acceptance test requirements are presented in Volume 1 of this report. All propellant feed system acceptance requirements were satisfied.

Table 2.3-8 presents the average valve actuation times. The LH_2 prevalve opening times at the end of recirculation were within the specified requirement of 1.0 second or less. The average opening time was 490 milliseconds. At engine cutoff, the LH_2 prevalves closed in an average time of 263 milliseconds.

The center engine LOX prevalve was replaced with a ME284-0358 (Parker) prevalve, the outboard engine LOX prevalves were V7-480700 (LAD) prevalves and are scheduled to be replaced prior to CDDT. Therefore the performance of the LOX prevalves cannot be considered applicable to the flight stage.

Table 2.3-1. Maximum P.U. Engine Performance Standard Altitude Conditions – Past 641 Using Telemetry Data

Engine Serial Number Engine Vehicle Position		J-2082 201	J-2099 202	J-2102 203	J-2098 204	J-2100 205
Engine Thrust (lb)	Rocketdyne Acceptance	230,798	229,804	231,272	229,070	228,464
	Stage Acceptance	231,845	231,187	231,734	227,434	227,836
	Percent Change	+0.45	+0.60	+0.20	-0.71	-0.27
Engine Mixture Ratio	Rocketdyne Acceptance	5.51	5.53	5.53	5.54	5.54
	Stage Acceptance	5.49	5.58	5.53	5.51	5.52
	Percent Change	-0.36	+0.90	0	-0.54	-0.36
Engine Specific Impulse (sec)	Rocketdyne Acceptance	425.0	426.5	424.6	423.7	424.3
	Stage Acceptance	425.1	426.6	425.0	423.4	423.5
	Percent Change	+0.02	+0.02	+0.09	-0.07	-0.19

2-57

Table 2.3-2.   Minimum PU Engine Performance Standard Altitude Conditions - Past 641

Engine Serial Number Engine Vehicle Position	J-2082 201	J-2099 202	J-2102 203	J-2098 204	J-2100 205
Thrust (lb)	171,950	171,338	173,660	172,529	-
Engine Mixture Ratio	4.20	4.32	4.32	4.34	-
Specific Impulse Seconds	431.5	431.6	431.3	431.3	-
LOX Flowrate (lb/sec)	321.9	322.3	327.0	325.1	-
LH_2 Flowrate (lb/sec)	76.6	74.6	75.7	75.0	-
Chamber Pressure (psia)	595.0	590.0	598.0	589.0	-

Table 2.3-3. Engine Maximum PU Performance Analysis - 6N011 (Test 546)

Item	Engine 1 (J-2082)	Engine 2 (J-2099)	Engine 3 (J-2102)	Engine 4 (J-2098)	Engine 5 (J-2100)
ENGINE PERFORMANCE					
Thrust, lb (site)	166,615.7	165,911.5	166,110.8	162,097.3	163,964.9
Thrust, lb (altitude)	234,713.4	233,986.2	234,213.3	230,147.0	231,979.7
Specific impulse, sec (site)	301.5	302.4	301.0	298.1	300.0
Specific impulse, sec (altitude)	424.7	426.5	424.4	423.2	424.4
Mixture ratio	5.53	5.64	5.57	5.57	5.52
Oxidizer weight flow, lb/sec	467.99	465.93	467.82	461.05	462.85
Fuel weight flow, lb/sec	84.6	82.7	84.0	82.8	83.8
Total weight flow, lb/sec	552.59	548.59	551.86	543.83	546.64
Ambient pressure, psia	14.70	14.70	14.70	14.70	14.70
GAS GENERATOR PERFORMANCE					
Oxidizer weight flow, lb/sec	3.77	3.55	3.56	3.40	3.37
Fuel weight flow, lb/sec	3.96	3.69	3.68	3.55	3.50
Total weight flow, lb/sec	7.72	7.24	7.25	6.94	6.87
Mixture ratio	0.952	0.963	0.967	0.958	0.963
Chamber pressure, (injection), psia	738.0	704.4	706.3	675.2	668.4
Fuel turbine inlet pressure, psia (calculated)	705.2	674.1	675.9	646.1	639.6
PRESSURIZATION INFORMATION					
Oxidizer flowrate, lb/sec	1.55	1.51	1.61	1.47	1.48
Fuel flowrate, lb/sec	0.77	0.74	0.80	0.91	0.00
	FUEL			OXIDIZER	
Ullage pressure, psia	30.0			37.7	
Pressurization flow, lb/sec	3.23			7.6	

Note: Data time slice taken at engine start plus 60.38 seconds.

Table 2.3-3. Engine Maximum PU Performance Analysis - 6N011 (Test 546) (Cont)

Item	Stage
	STAGE PERFORMANCE
Thrust, lb (altitude)	1,165,039.5
Thrust, lb (site)	824,700.1
Specific impulse, sec (altitude)	423.0
Specific impulse, sec (site)	299.4
Mixture ratio	5.54
Oxidizer weight flow, lb/sec	2,333.3
Fuel weight flow, lb/sec	421.1
Total weight flow, lb/sec	2,754.4

Item	FUEL	OXIDIZER
Propellant consumed, lb (engine)	24,151.0	131,402.5
Propellant consumed, lb (pressurization)	160.1	453.1
Propellant remaining, lb (liquid)	137,183.2	686,959.3
Propellant remaining, lb (ullage)	322.9	798.2
Bulk density, lb/ cu ft	4.40	71.2

Note: Data time slice taken at engine start plus 60.38 seconds.

2-60

Table 2.3-4. Engine Minimum PU Performance Analysis - 6N011 (Test 546)

Item	Engine 1 (J-2082)	Engine 2 (J-2099)	Engine 3 (J-2102)	Engine 4 (J-2098)	Engine 5 (J-2100)
ENGINE PERFORMANCE					
Thrust, lb (site)	107,279.3	105,126.8	108,411.1	106,610.3	0.0
Thrust, lb (altitude)	175,377.1	173,201.4	176,513.5	174,659.9	0.0
Specific impulse, sec (site)	263.2	261.1	264.2	263.0	0.0
Specific impulse, sec (altitude)	430.3	430.2	430.2	430.8	0.0
Mixture ratio	4.31	4.41	4.44	4.44	0.00
Oxidizer weight flow, lb/sec	330.74	328.20	334.81	330.86	0.00
Fuel weight flow, lb/sec	76.8	74.4	75.5	74.6	0.0
Total weight flow, lb/sec	407.53	402.57	410.26	405.42	0.00
Ambient pressure, psia	14.70	14.70	14.70	14.70	14.70
GAS GENERATOR PERFORMANCE					
Oxidizer weight flow, lb/sec	2.77	2.58	2.61	2.50	0.04
Fuel weight flow, lb/sec	3.52	3.29	3.24	3.18	0.05
Total weight flow, lb/sec	6.28	5.88	5.85	5.68	0.08
Mixture ratio	0.787	0.785	0.807	0.785	0.785
Chamber pressure, (injection)	571.4	542.5	544.6	524.9	7.7
Fuel turbine inlet pressure, psia (calculated)	545.8	519.0	521.1	502.1	7.4
PRESSURIZATION INFORMATION					
Oxidizer pressure, psia	2.94	2.90	2.97	2.92	0.00
Fuel flowrate, lb/sec	1.37	1.29	1.46	1.43	0.00
	FUEL			OXIDIZER	
Ullage pressure, psia	32.1			39.8	
Pressurization flow, lb/sec	5.54			11.7	

Note: Data time slice taken at engine start plus 340.38 seconds.

2-61

Table 2.3-4. Engine Minimum PU Performance Analysis -
6N011 (Test 546) (Cont)

Item	Stage
	STAGE PERFORMANCE
Thrust, lb (altitude)	699,751.9
Thrust, lb (site)	427,427.4
Specific impulse, sec (altitude)	425.9
Specific impulse, sec (site)	260.1
Mixture ratio	4.36
Oxidizer weight flow, lb/sec	1,336.3
Fuel weight flow, lb/sec	306.7
Total weight flow, lb/sec	1,643.1
	FUEL / OXIDIZER
Propellant consumed, lb (engine)	137,857.1 / 753,390.8
Propellant consumed, lb (pressurization)	1,201.9 / 4,351.3
Propellant remaining, lb (liquid)	22,375.4 / 61,024.7
Propellant remaining, lb (ullage)	1,376.2 / 4,744.5
Bulk density, lb/cu ft	4.39 / 70.8

Note: Data time slice taken at engine start plus 340.38 seconds.

SPACE DIVISION OF NORTH AMERICAN ROCKWELL CORPORATION

Table 2.3-5. Propellant Loading Summary, Test 546

Item	LOX (Pounds)		LH$_2$ (Pounds)	
	Actual	Predicted	Actual	Predicted
Thrust buildup (ESC to ESC + 3 seconds)	838	595	408	401
Mainstage consumption (ESC + 3 seconds to ECO)	810,785	812,518	150,845	151,559
Pressurization (ESC to ECO)	4,877	4,659	1,487	1,427
Boiloff (ESC to ECO)	66	67	80	86
Residuals at ECO (includes thrust decay and PU bias)	2,300	2,690*	6,881	4,527*
Total loaded propellants (Includes tank and sump)	818,866	820,529	159,701	158,000
Reference Information				
Thrust decay (Consumption after cutoff signal)	247	247	91	109
Bias (ECO)		-0-		1,917
ECO system cutoff level, pounds		4,000		2,610
Propellant trapped external to tank and sump		1,563		244
Propellant management estimate total loaded (includes tank and sump, and trapped (external))	980,374 pounds			

*Predicted residual is based on a non-linear analysis with ECO occurring at the LOX ECO point sensor plus a 1.0 second time delay.

2-63

SD 69-329

Table 2.3-6. Propellant Mangement System Performance Summary

Item	LOX Actual	LOX Predicted	LH$_2$ Actual	LH$_2$ Predicted
Propellant loaded, (flowmeter pounds)	818,866	820,529	159,701	158,000
Propellant loaded, (point sensor, pounds)	821,970	820,529	160,614	158,000
Propellant loaded (PU fine mass pounds)	820,695	820,529	158,678	158,000
Fine mass potentiometer percent:				
@Liftoff minus 187 seconds	95.75	95.781*	95.87	95.614*
@Liftoff	95.92	95.901*	95.52	95.114*
@ESC	95.85	95.676**	95.63	94.836**
Ullage volume at ignition, cubic feet	1,239.5	1,220.1	1,425.9	1,753.2
Cutoff residuals, pounds	2,300	2,690	6,881	4,527
PU probe loading sensitivity (10^{-3} picofarads/pound)	0.326318	0.326318	2.25470	2.26160
PU probe static firing sensitivity (10^{-3} picofarads/pound)	0.325505	0.325511	2.22257	2.25498
PU probe equivalent flight sensitivity (10^{-3} picofarads/pound)	0.325268	0.325361	2.22060	2.24930

	Actual	Predicted
PU error at manual ECO signal	+2350 pounds LH$_2$	±4500 pounds LH$_2$
High EMR command signal	5.62 seconds	5.50 seconds
Low EMR command signal	325.18 seconds	325.0 seconds
Firing duration (ESC to ECO signal)	384.743 seconds	388.2 seconds
Average EMR after low EMR command	4.39 EMR	4.36 EMR
EMR at cutoff	4.32 EMR	4.36 EMR
LOX ECO time delay	0.853 seconds	1.0 seconds
Cutoff Mode	LOX Depletion ECO	LOX Depletion ECO

*based on probe loading gain
**based on probe static firing gain

Table 2.3-7. S-II-8 Propellant Mass History (Pounds)

Event, Time from ESC	Predicted		Point Sensor Analysis		PU System Analysis		Best estimate (Engine flow-meter integration)	
	LOX	LH_2	LOX	LH_2	LOX	LH_2	LOX	LH_2
Simulated Liftoff (-159.8 seconds)	820,529	158,000	821,970	160,614	820,695	158,678	818,866	159,701
S-II ESC 0.0 seconds	820,529	158,000	821,970	160,614	822,113	159,327	818,866	159,701
S-II PU valve step 325.18 seconds	87,268	23,964	84,379	25,695	80,299	25,015	83,528	25,222
S-II engine cutoff 384.743 seconds	2,690	4,527	2,300	6,881	4,006	6,682	2,300	6,881
S-II residual after thrust decay	2,443	4,418	2,053	6,790	3,759	6,591	2,053	6,790

NOTE: Table is based on mass in tanks and sump only. Propellant trapped external to tanks and LOX sump is not included.

Table 2.3-8. Valve Actuation Times (Average)
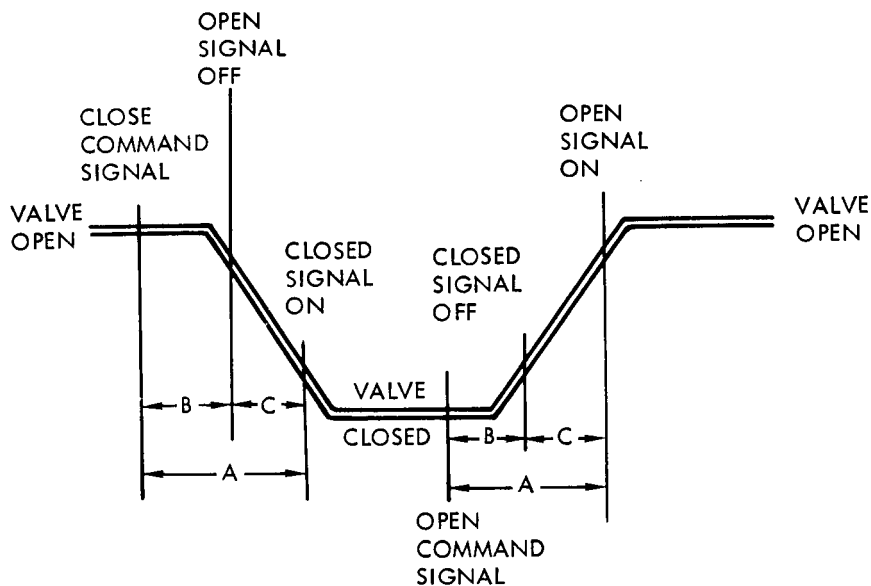
MEASUREMENT

A - COMMAND SIGNAL TO COMMANDED POSITION SIGNAL ON
B - COMMAND SIGNAL TO SIGNAL OFF (RESPONSE TIME)
C - SIGNAL OFF TO OPPOSITE SIGNAL ON

Actuation Mode	Measurement	Prevalves (milliseconds)		Fill Valves (seconds)		Recirculation Valves (seconds)	
		LH_2 (5)	LOX (5)	LH_2 (1)	LOX (1)	LH_2 (6)	LOX (5)
Open	A	263**	499**	16.18	8.42	2.14*	0.729*
to	B	127	181	8.67	3.94	0.95	0.326
close	C	136	318	7.51	4.48	1.19	0.403
Close	A	470*	498	14.92	7.70	23.90**	7.24**
to	B	185	181	6.24	4.14	15.49	5.16
open	C	305	317	8.68	3.56	8.41	2.08

Note: Number in parenthesis indicates number of valves on stage

*At recirculation stop
**After ECO
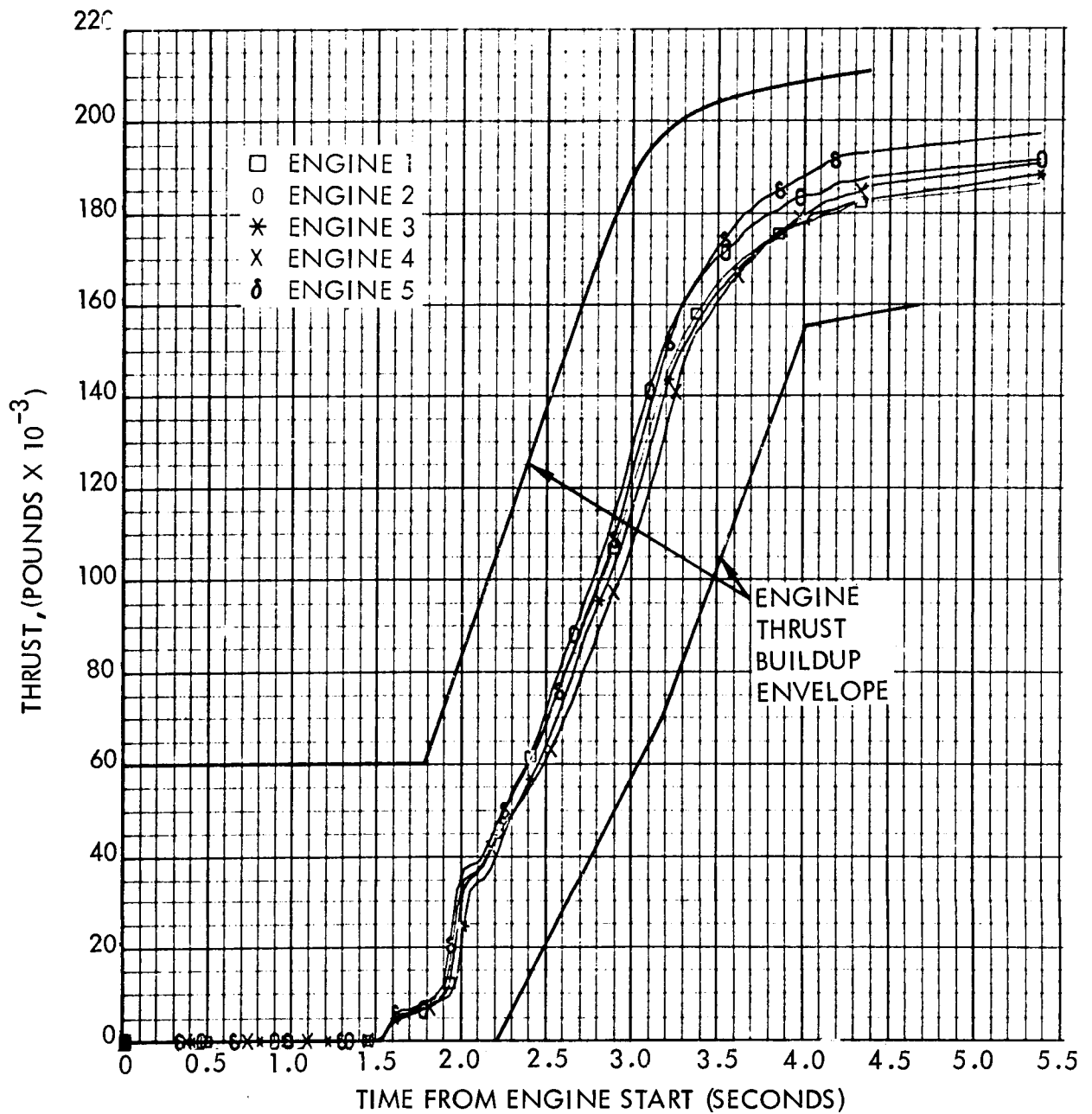
Figure 2.3-1. J-2 Engine Thrust Buildup
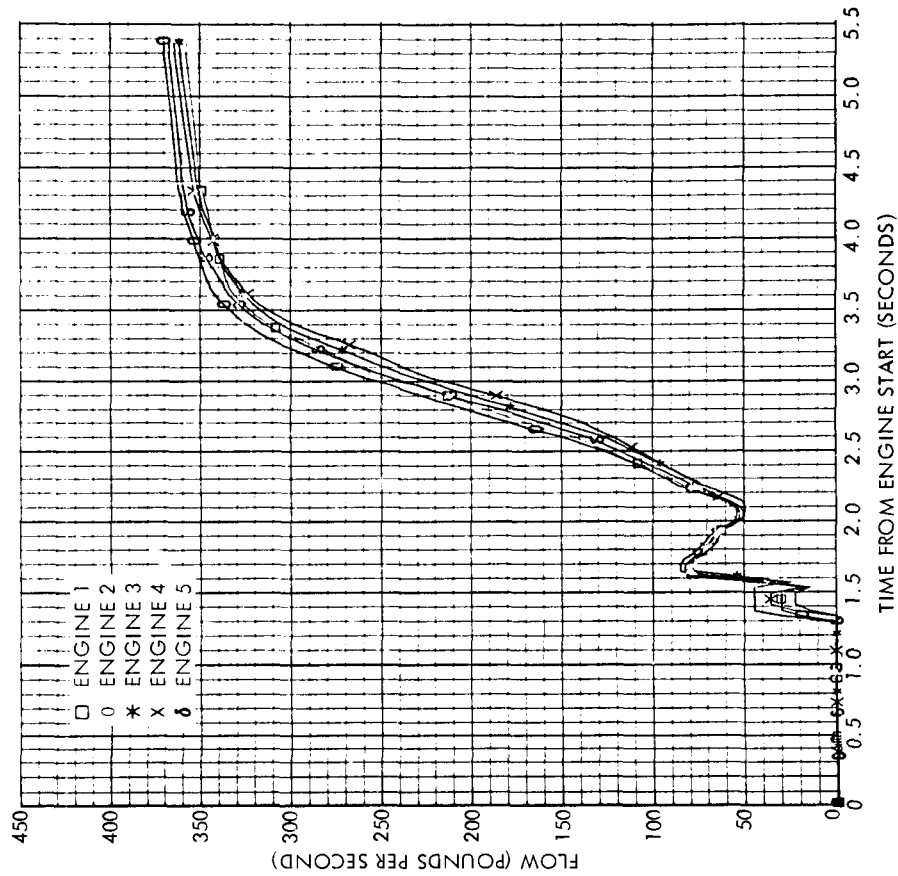
Figure 2.3-3. Engine LOX Flowrate - Start Transient
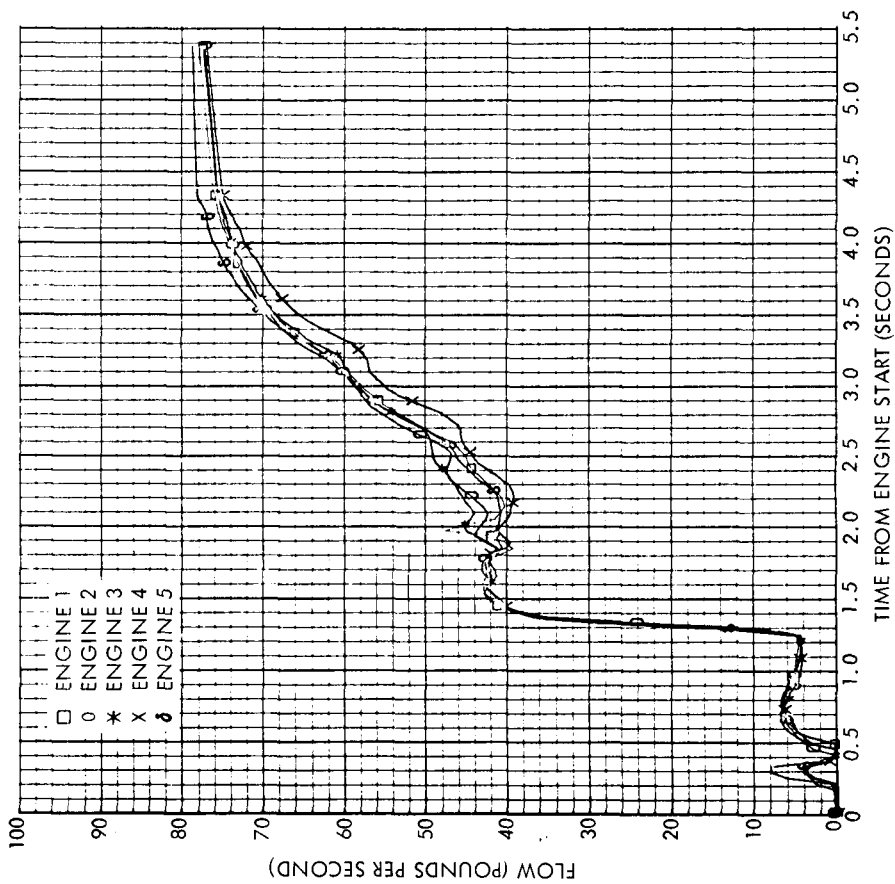
Figure 2.3-2. Engine Fuel Flowrate - Start Transient
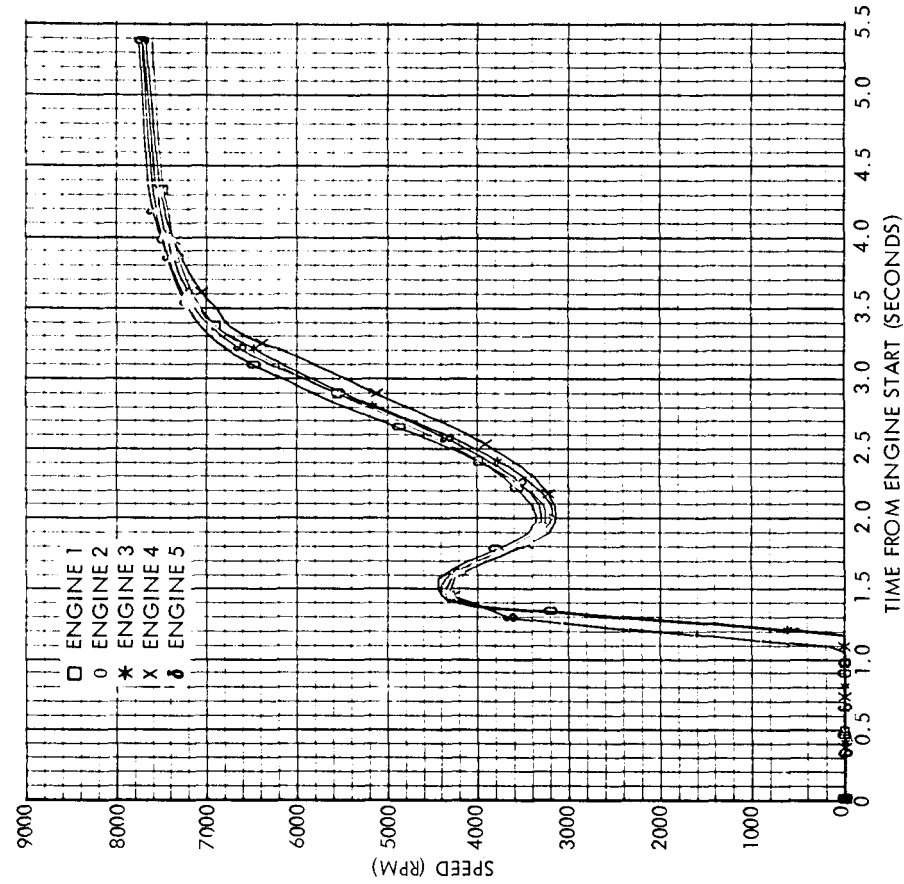
Figure 2.3-5. Engine LOX Pump Speed - Start
Transient
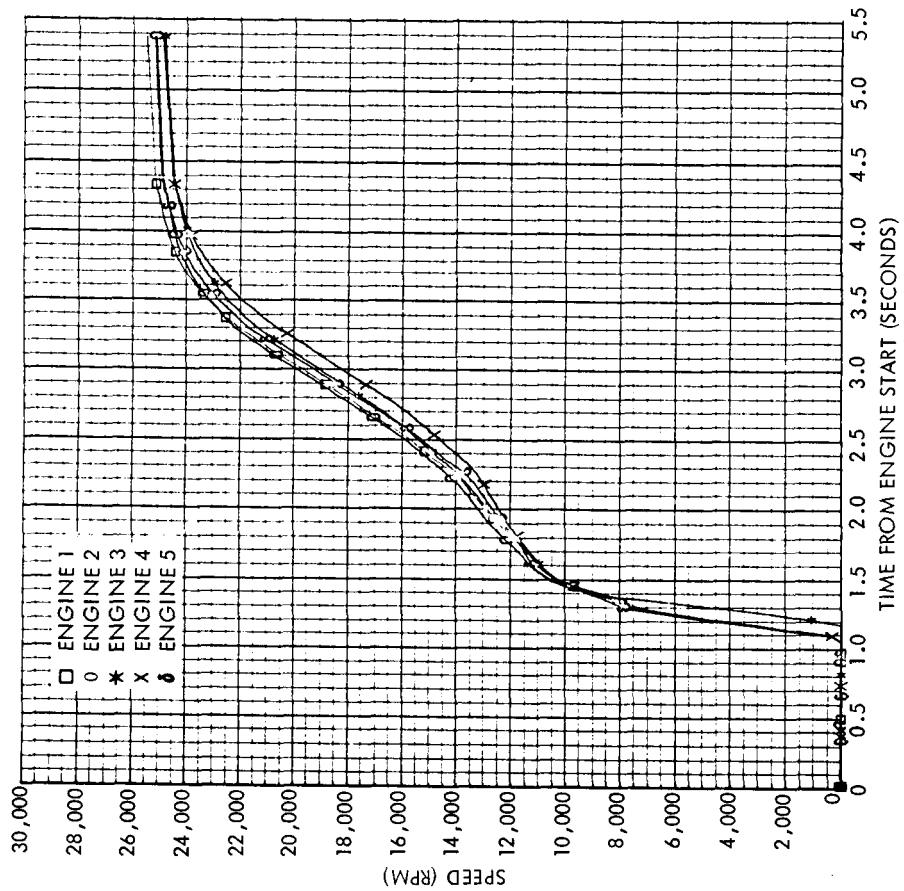
Figure 2.3-4. Engine Fuel Pump Speed - Start
Transient

2-69

SPACE DIVISION of NORTH AMERICAN ROCKWELL CORPORATION
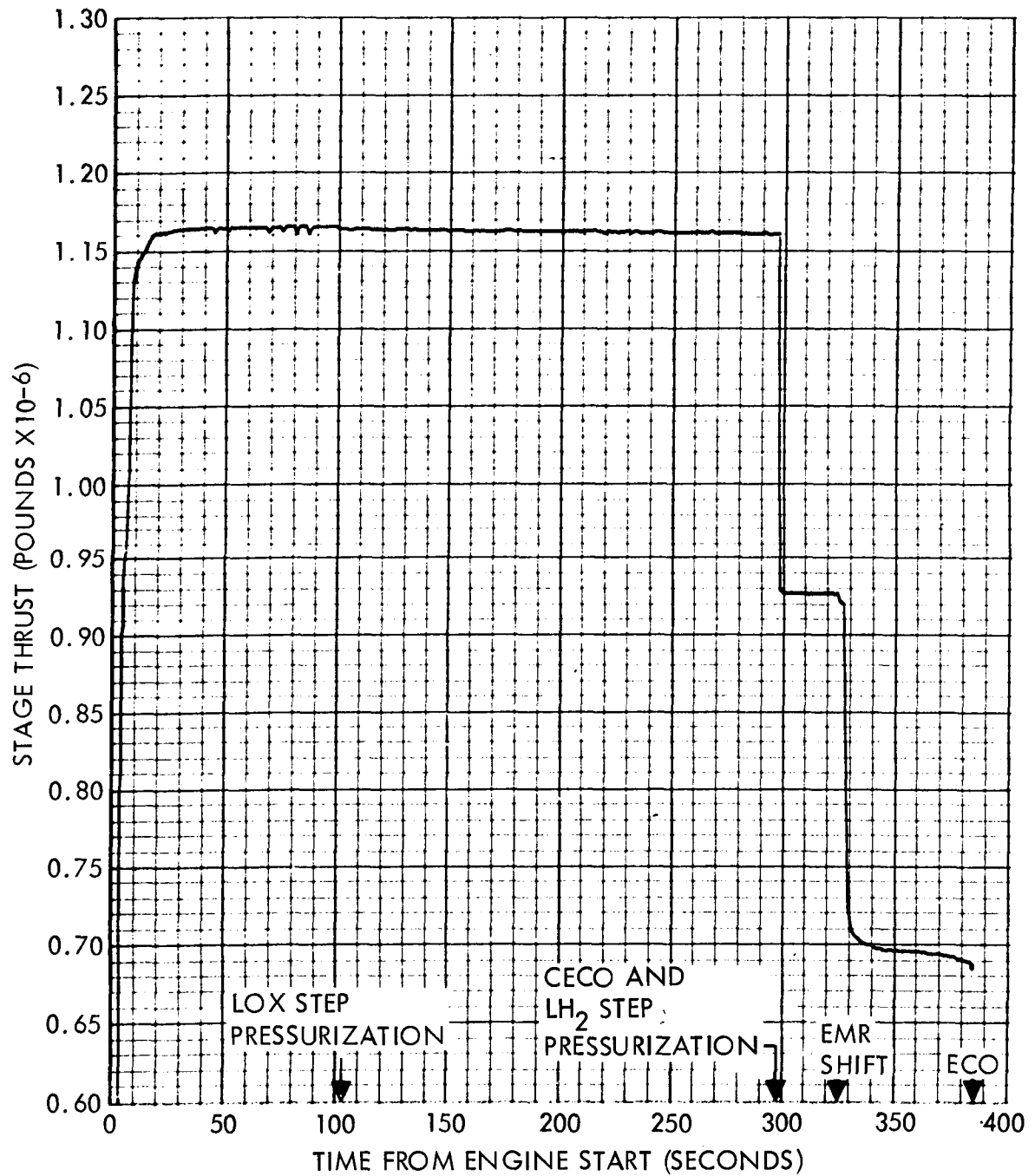
Figure 2.3-6.   Stage Altitude Thrust

2-70

SD 69-329
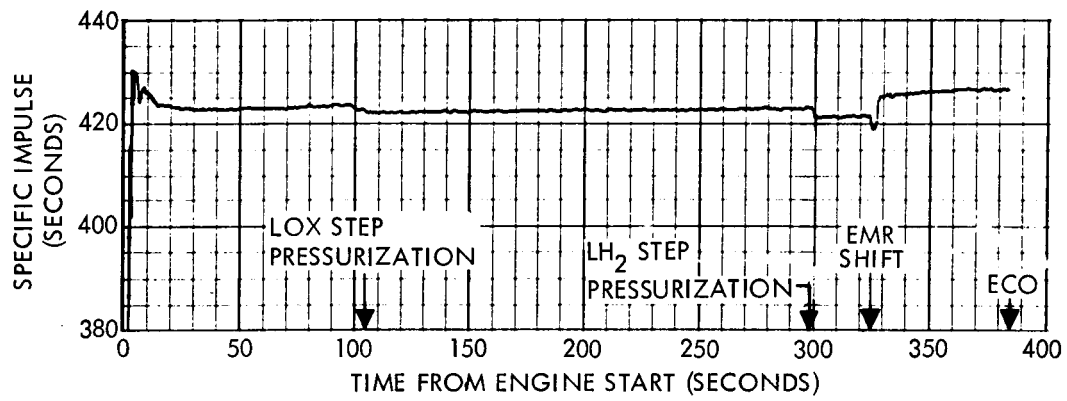
Figure 2.3-7. Stage Specific Impulse
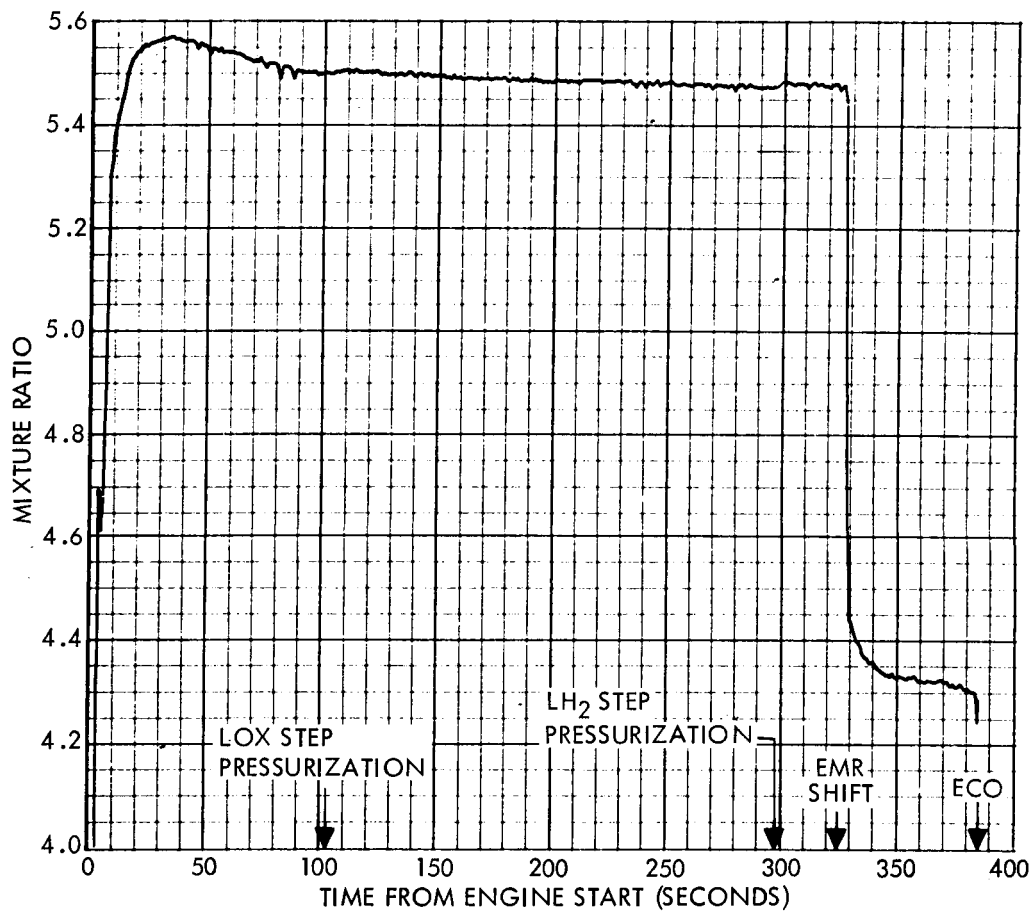
Figure 2.3-8. Stage Mixture Ratio
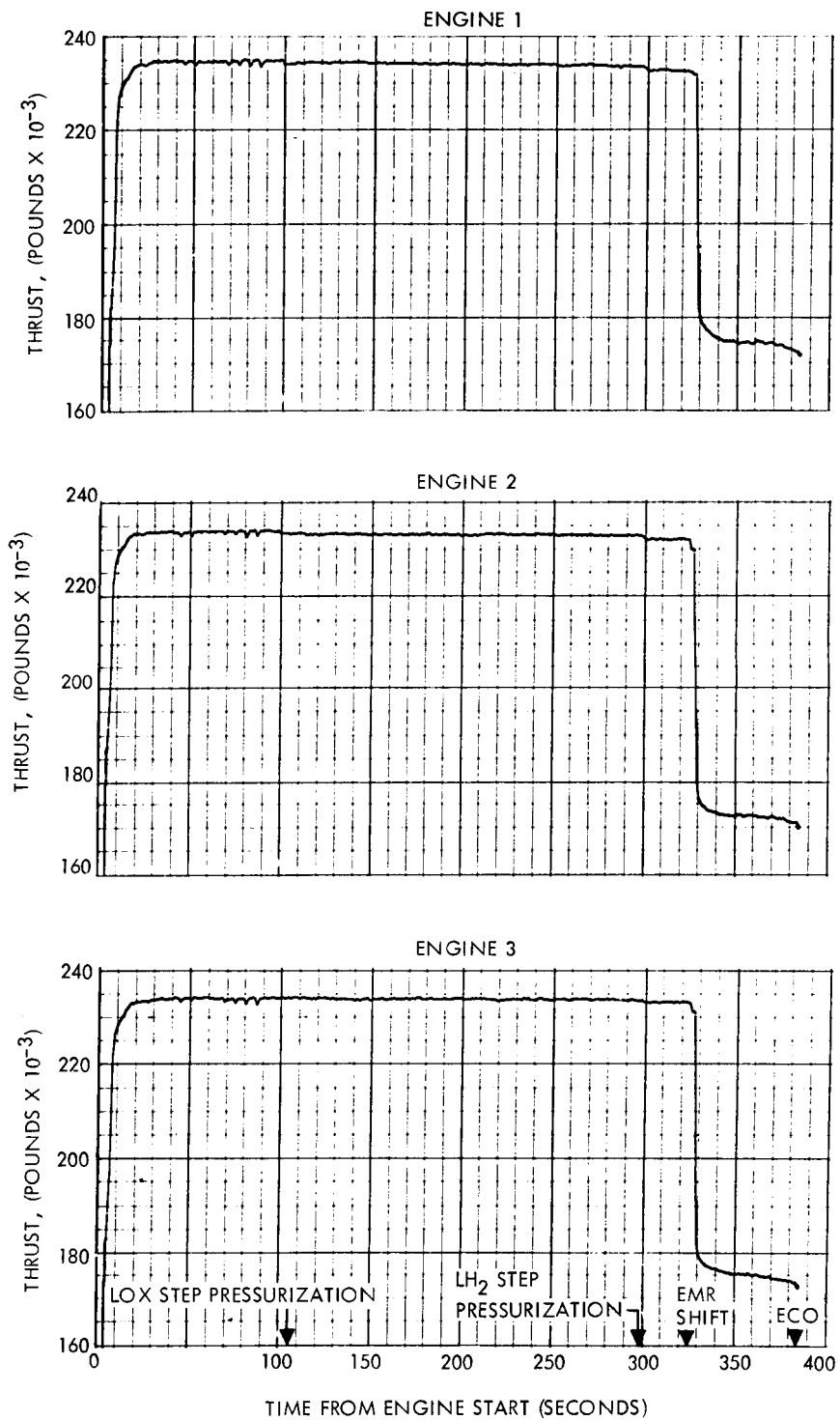
Figure 2.3-9. Engines 1, 2, and 3 Altitude Thrust
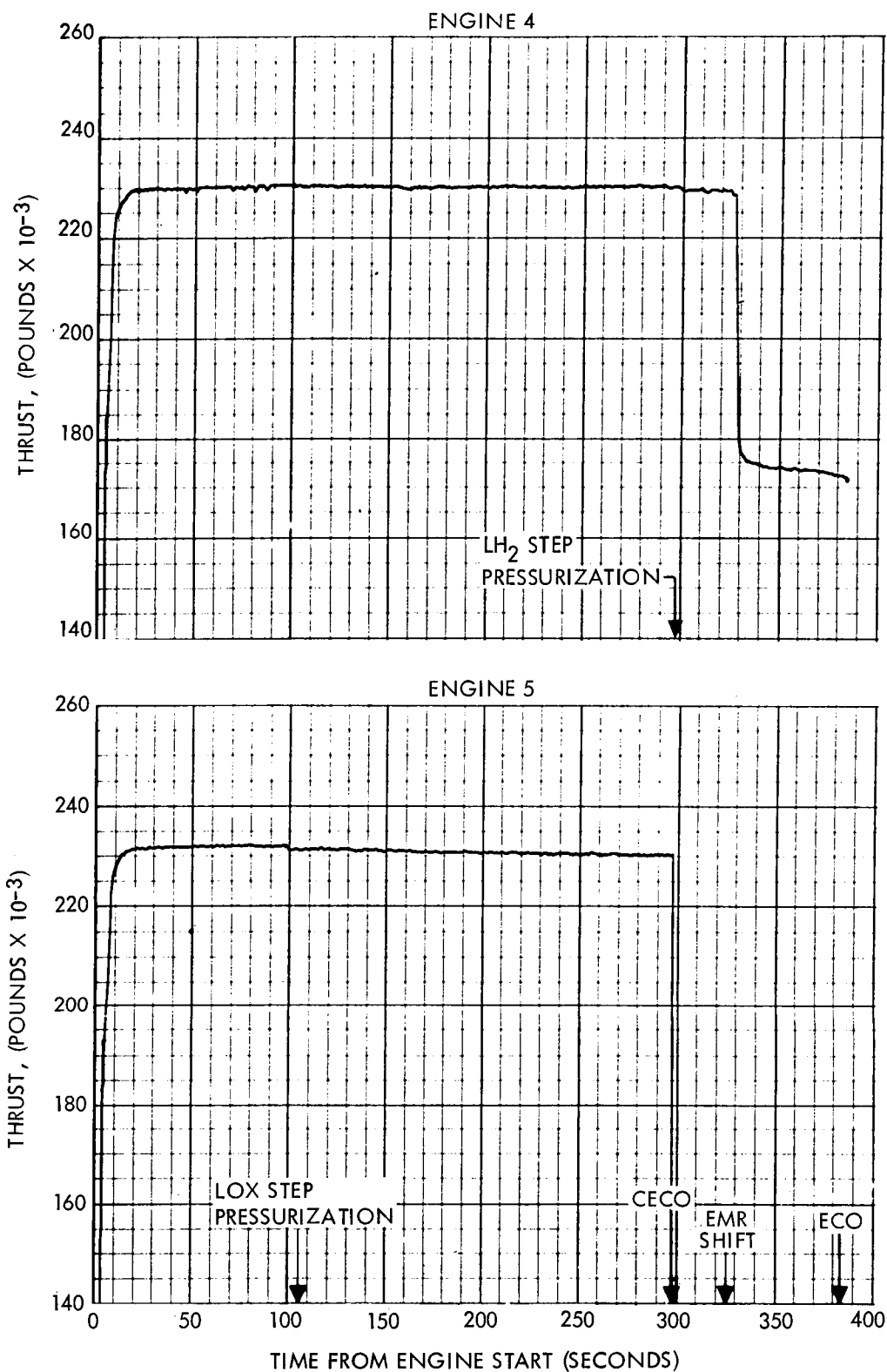
Figure 2.3-10.   Engines 4 and 5 Altitude Thrust
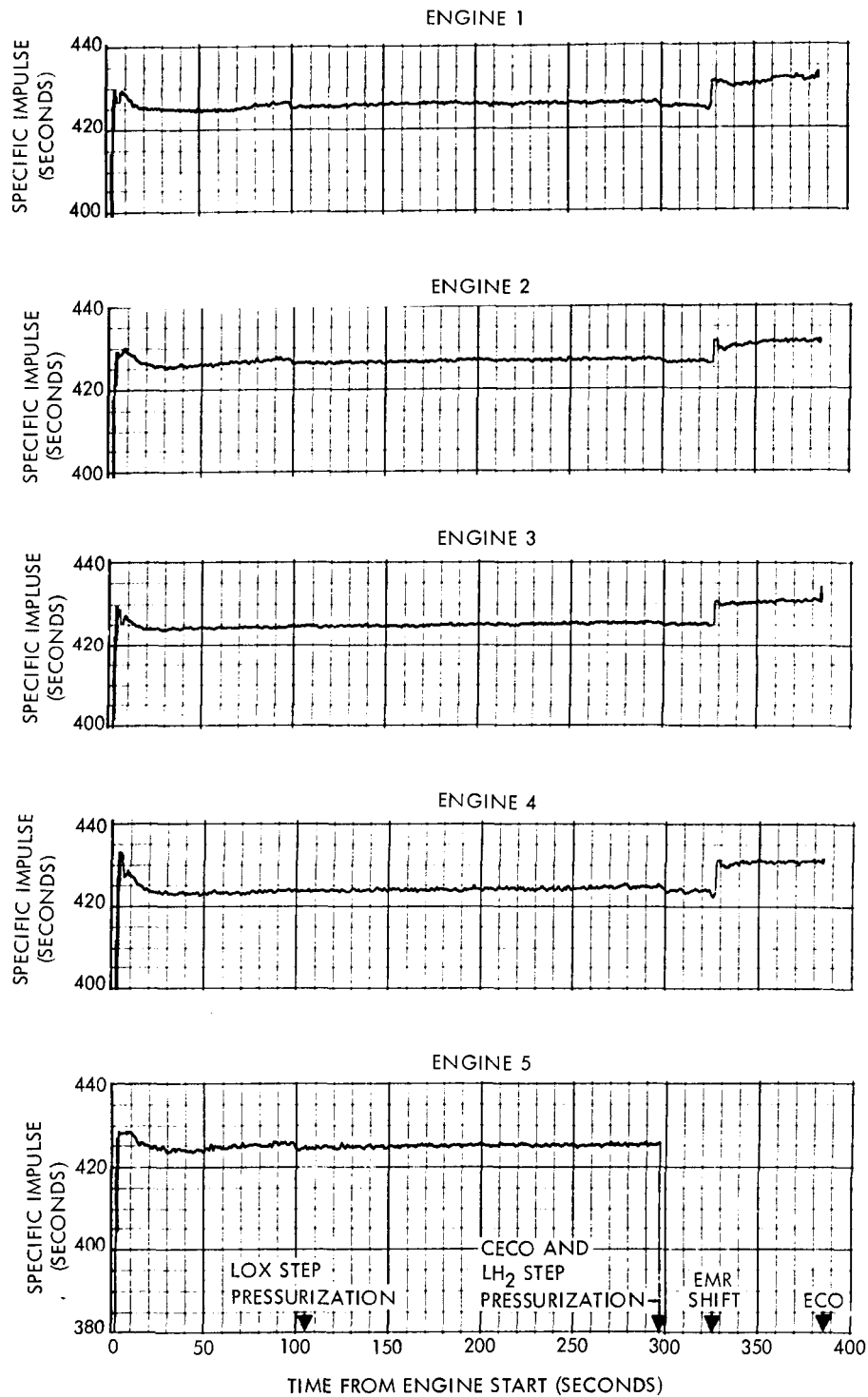
Figure 2.3-11.   Engine Altitude Specific Impulse
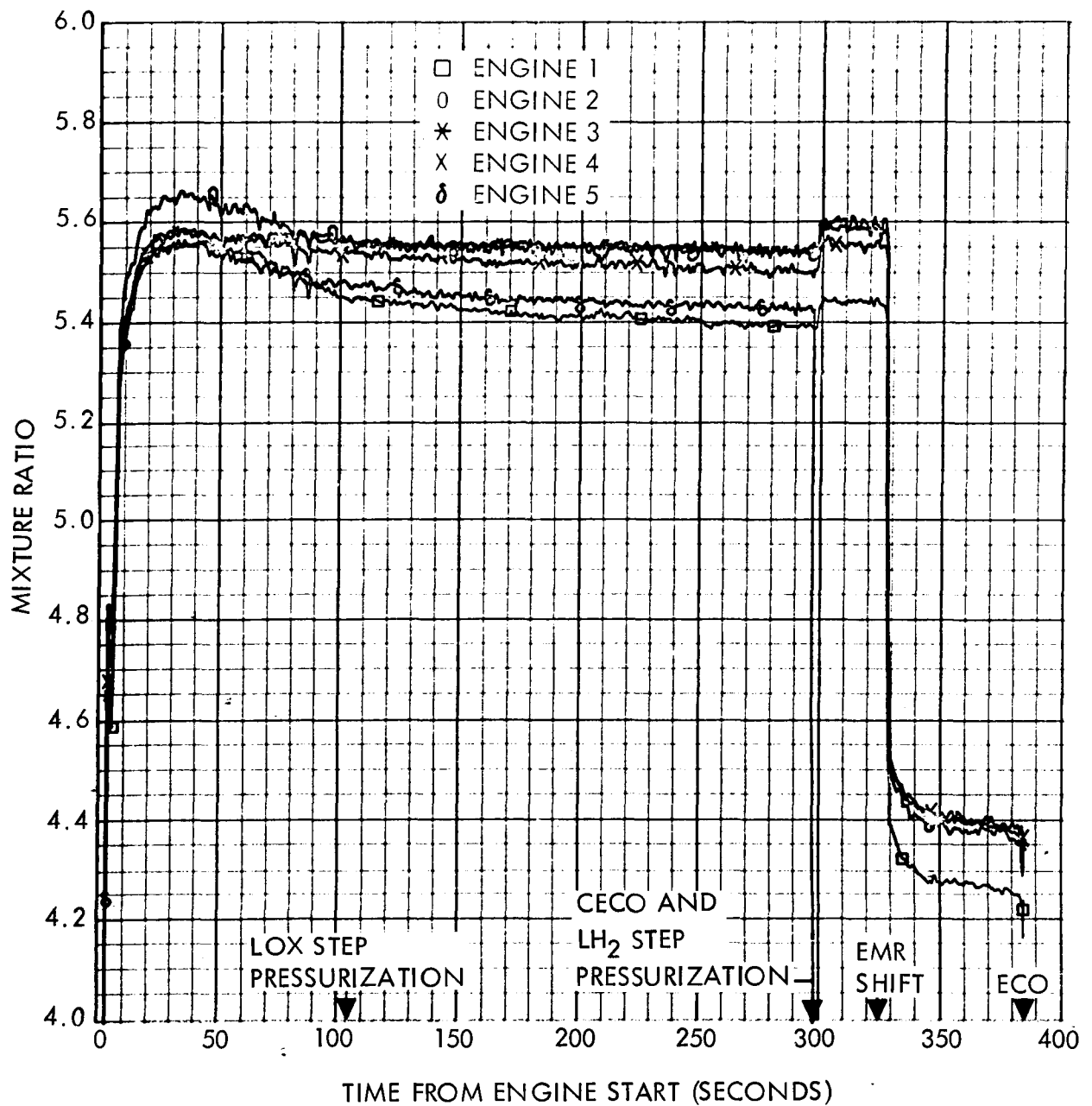
Figure 2.3-12.   Engine Mixture Ratio
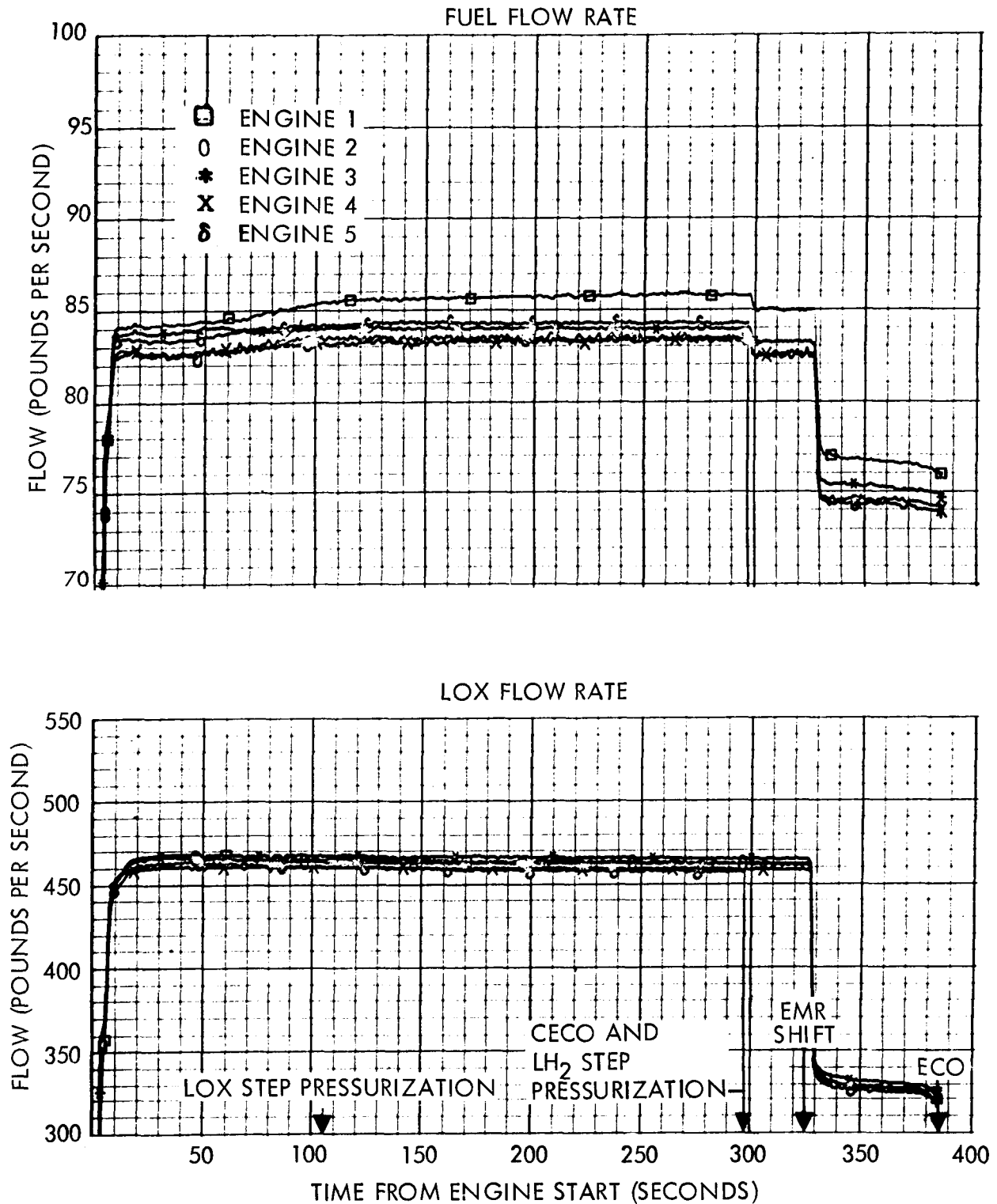
Figure 2.3-13. Engine Propellant Flowrates

2-76
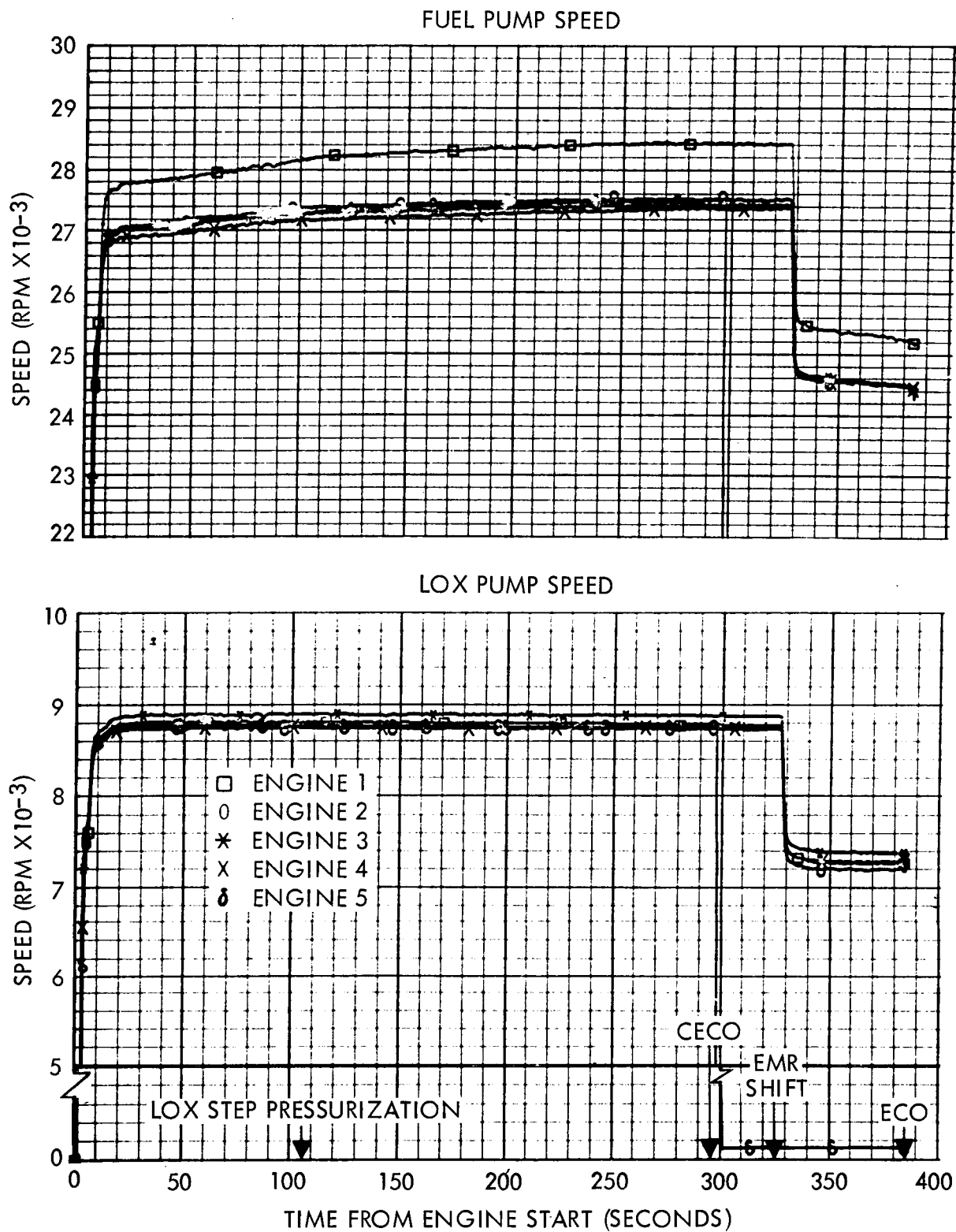
Figure 2.3-14.   Engine Propellant Pump Speed
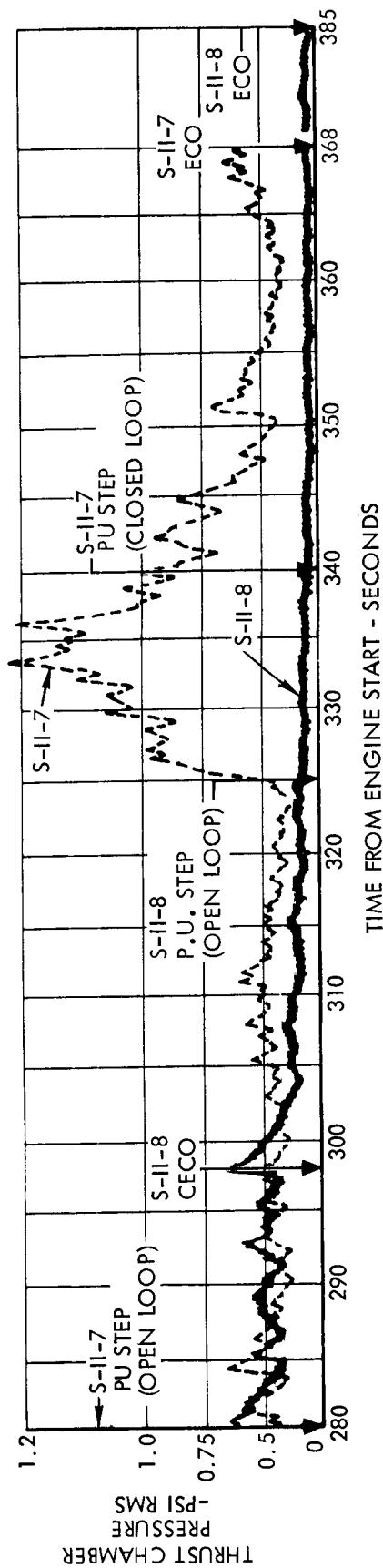
Figure 2.3-15.   Engine 5 Thrust Chamber Pressure History (D013-205)
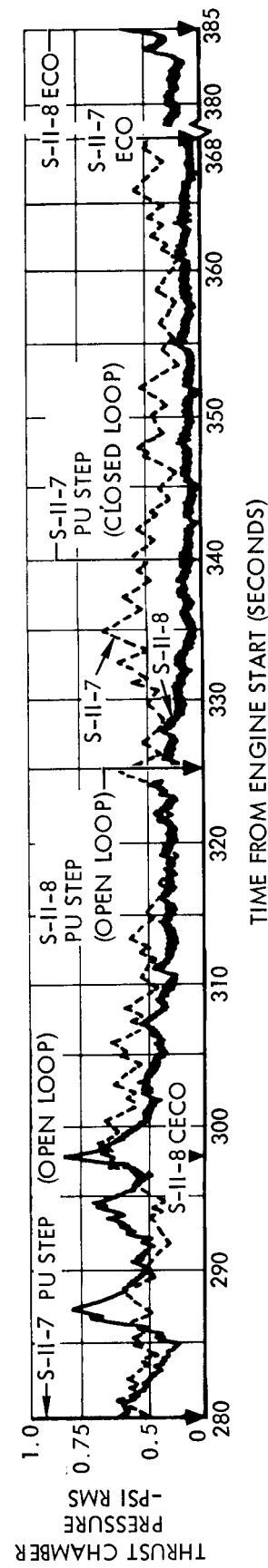
Figure 2.3-16.   Engine 1 Thrust Chamber Pressure History (D013-201)
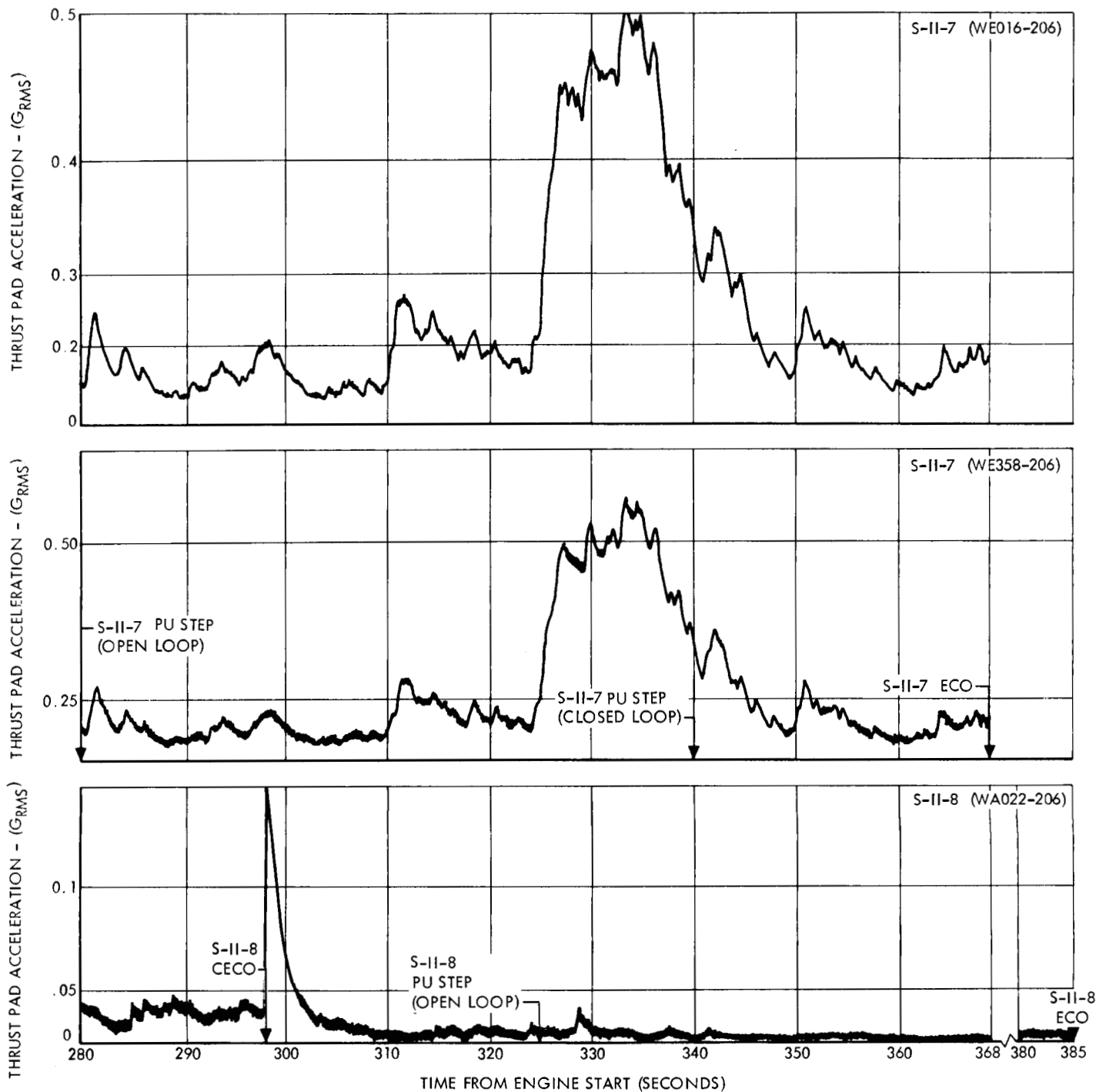
Figure 2.3-17. Engine 5 Thrust Pad Vibration History
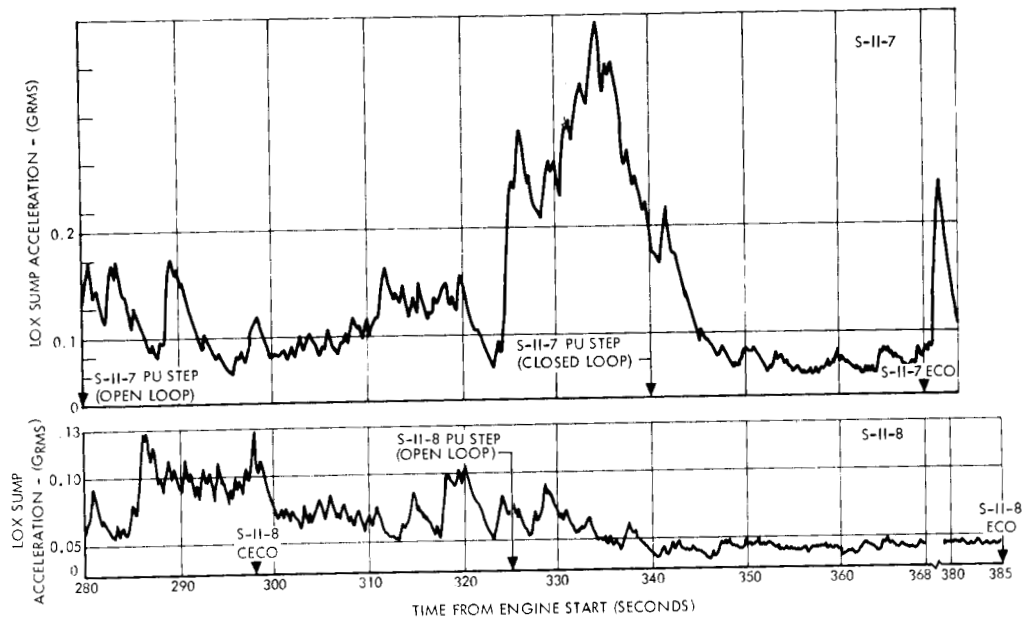
Figure 2.3-18. LOX Tank Sump Longitudinal Vibration History,
WE 246-206
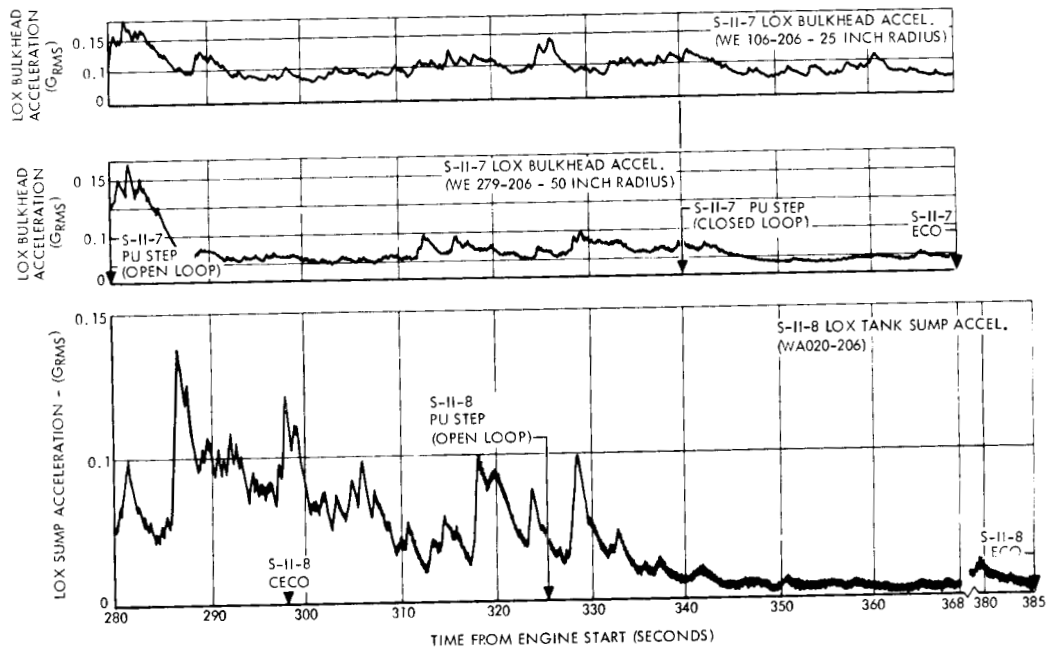
Figure 2.3-19. LOX Tank Bulkhead Vibration History
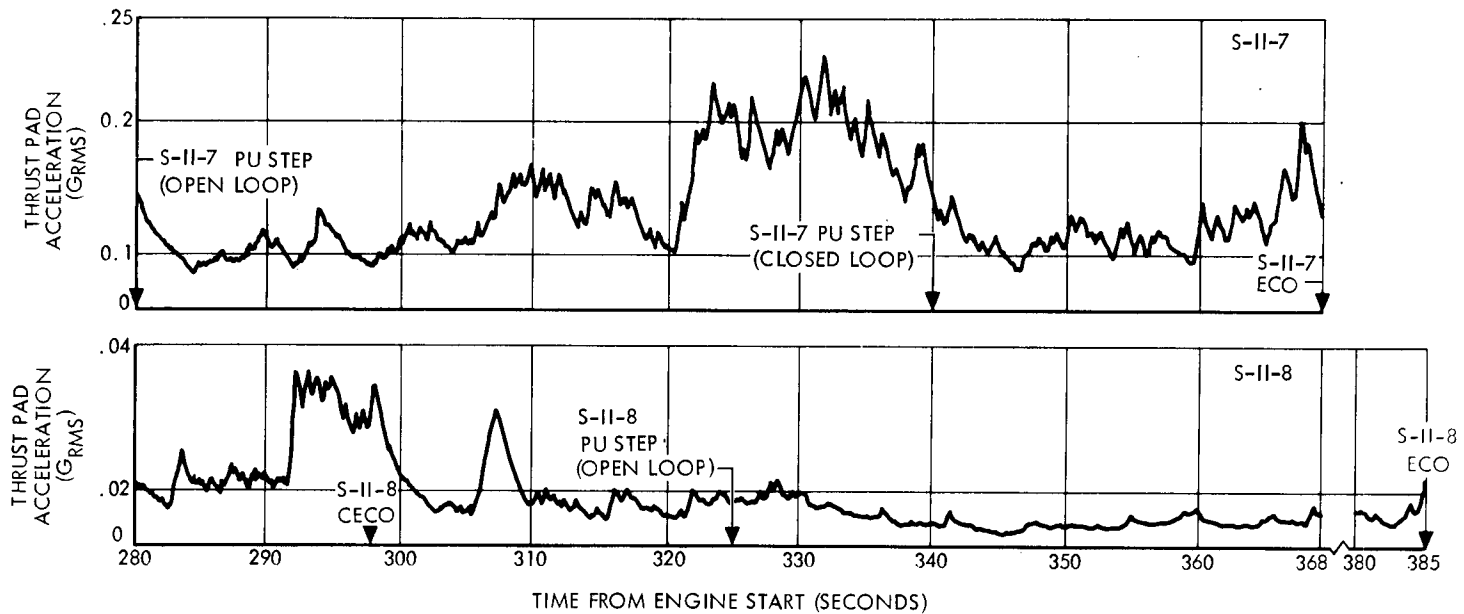
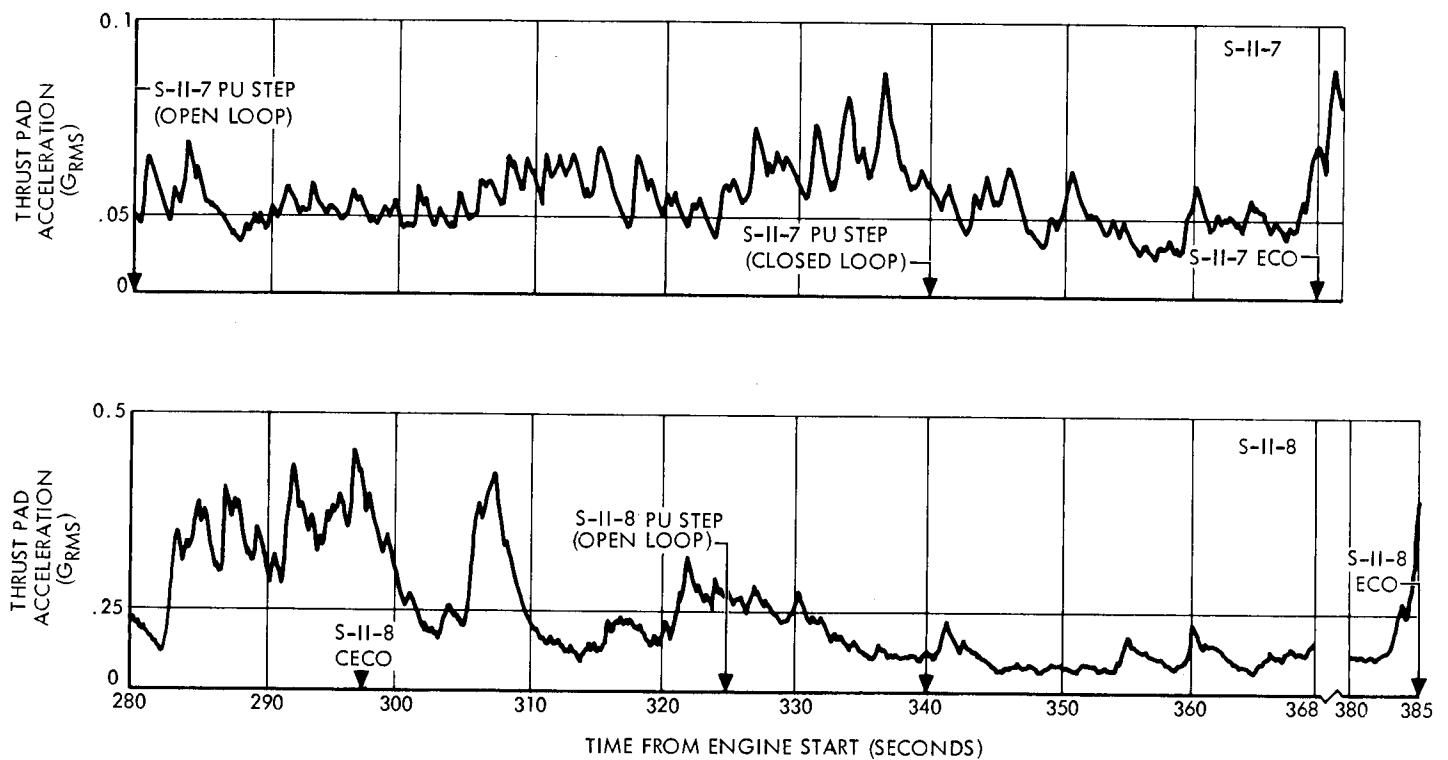Figure 2.3-20. Engine 1 Thrust Pad Vibration History,
WA 021-206

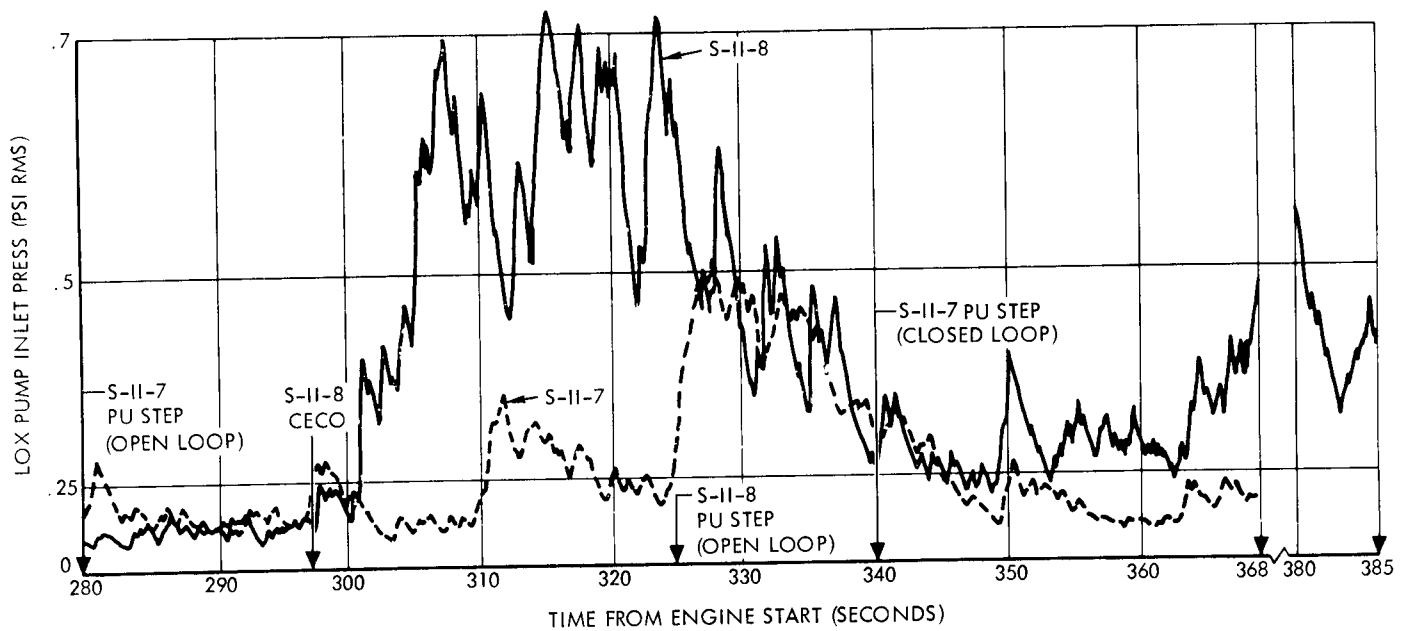Figure 2.3-21. Engine 1 Thrust Pad Vibration History,
WE 357-206

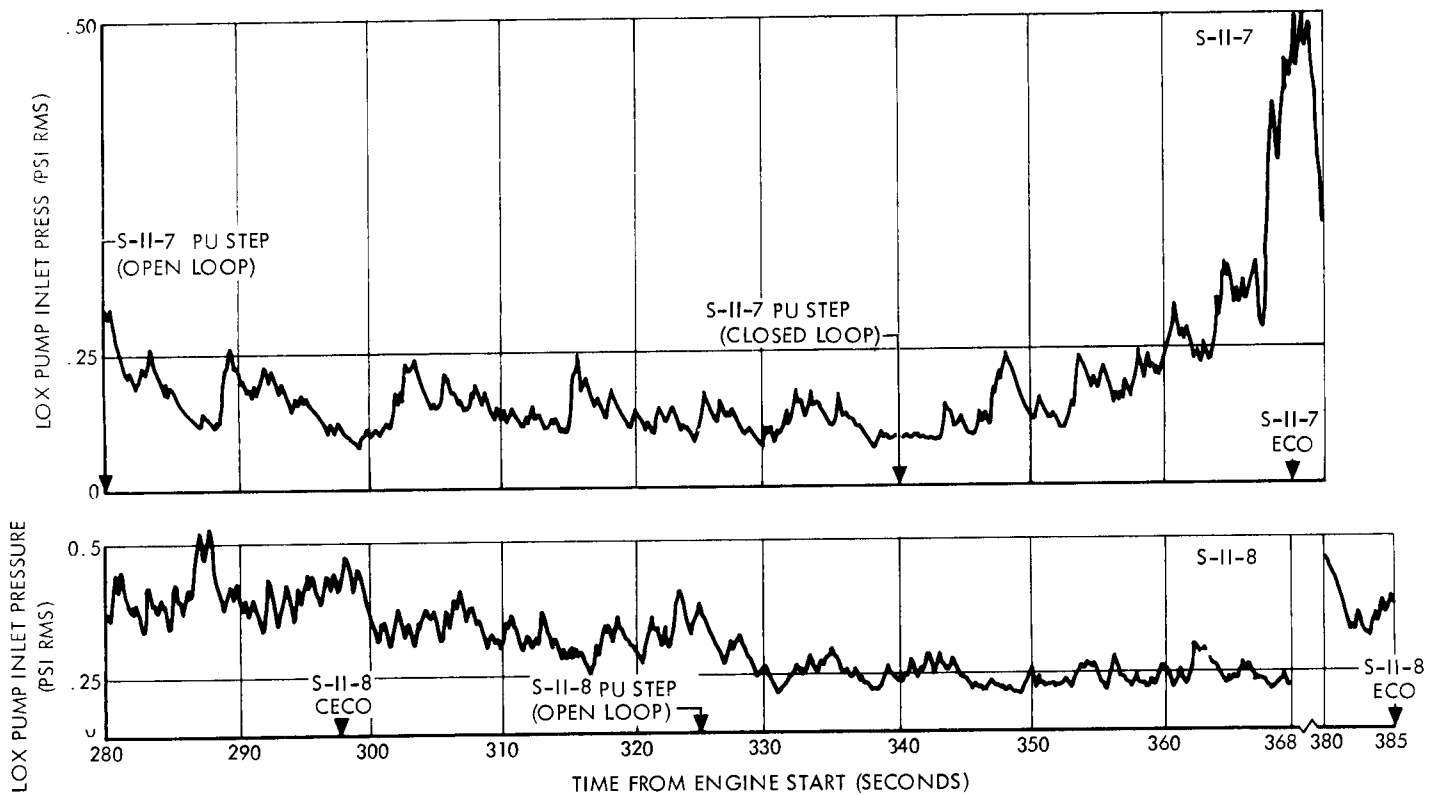Figure 2.3-22. Engine 5 LOX Pump Inlet Pressure History,
WD091-205

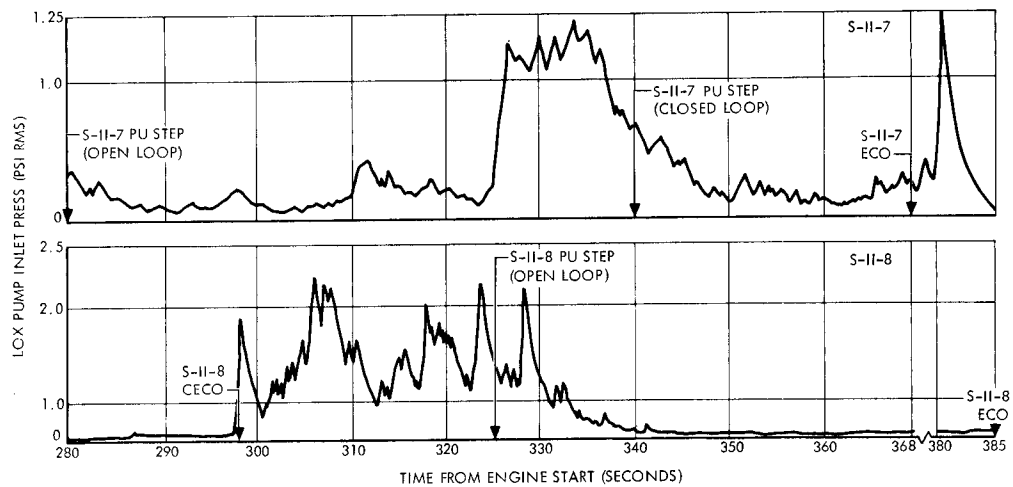Figure 2.3-23. Engine 1 LOX Pump Inlet Pressure History,
WD091-201

2-82

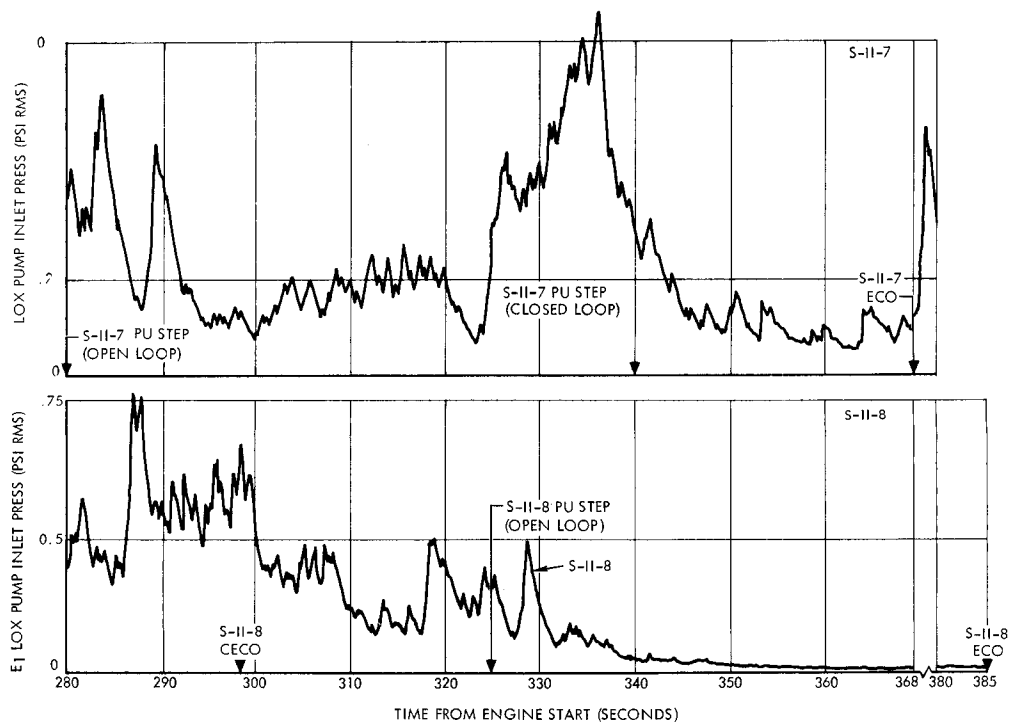Figure 2.3-24. Engine 5 LOX Pump Inlet Pressure History,
WD 261-205

Figure 2.3-25. Engine 1 LOX Pump Inlet Pressure History,
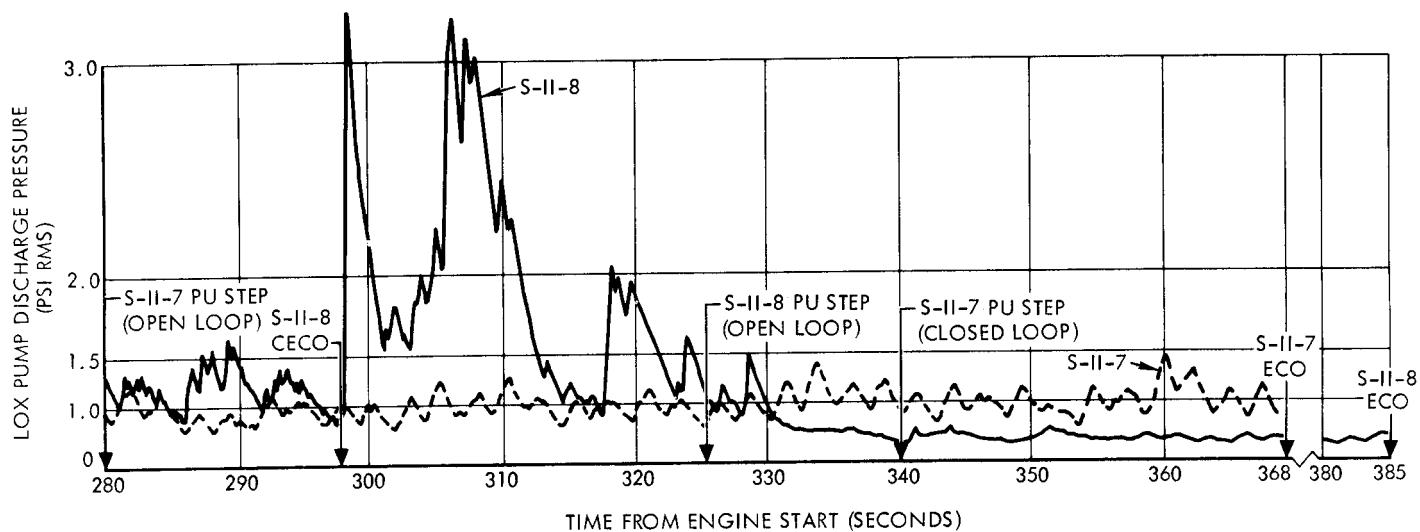WD 261-201

2-83

SD 69-329

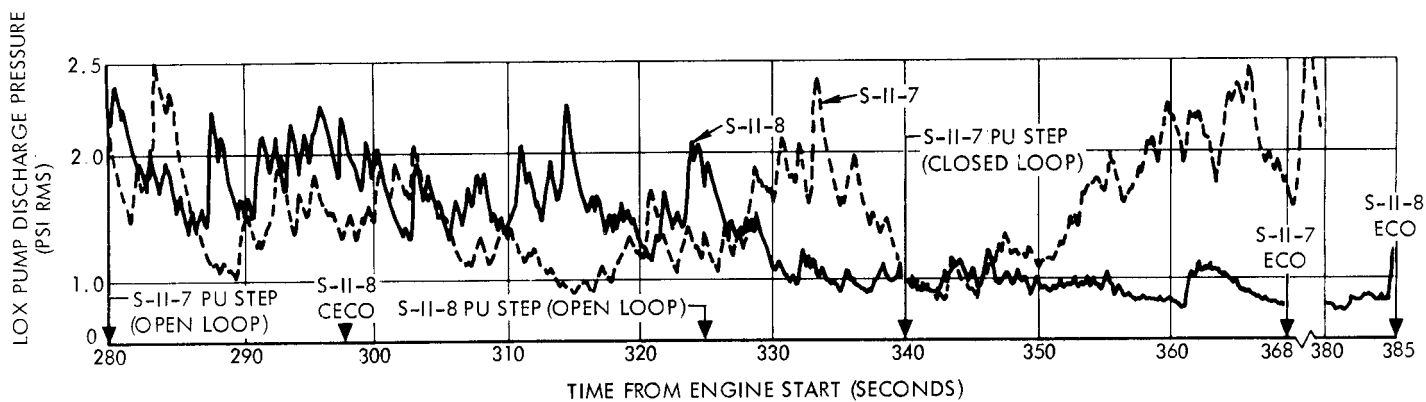Figure 2.3-26.   Engine 5 LOX Pump Discharge Pressure History

Figure 2.3-27.   Engine 1 LOX Pump Discharge Pressure History
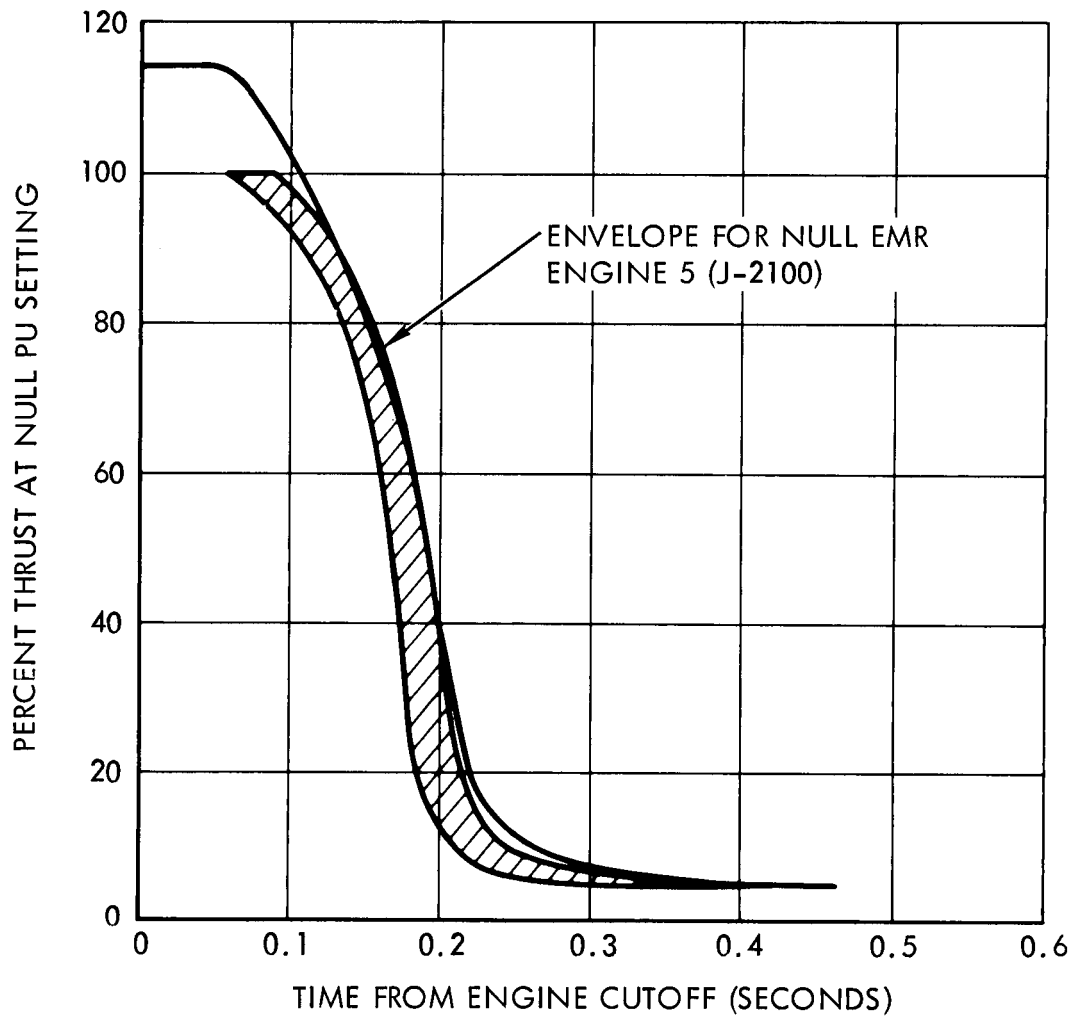
Figure 2.3-28. Center Engine Thrust Decay Transient
(Normalized to Null PU)
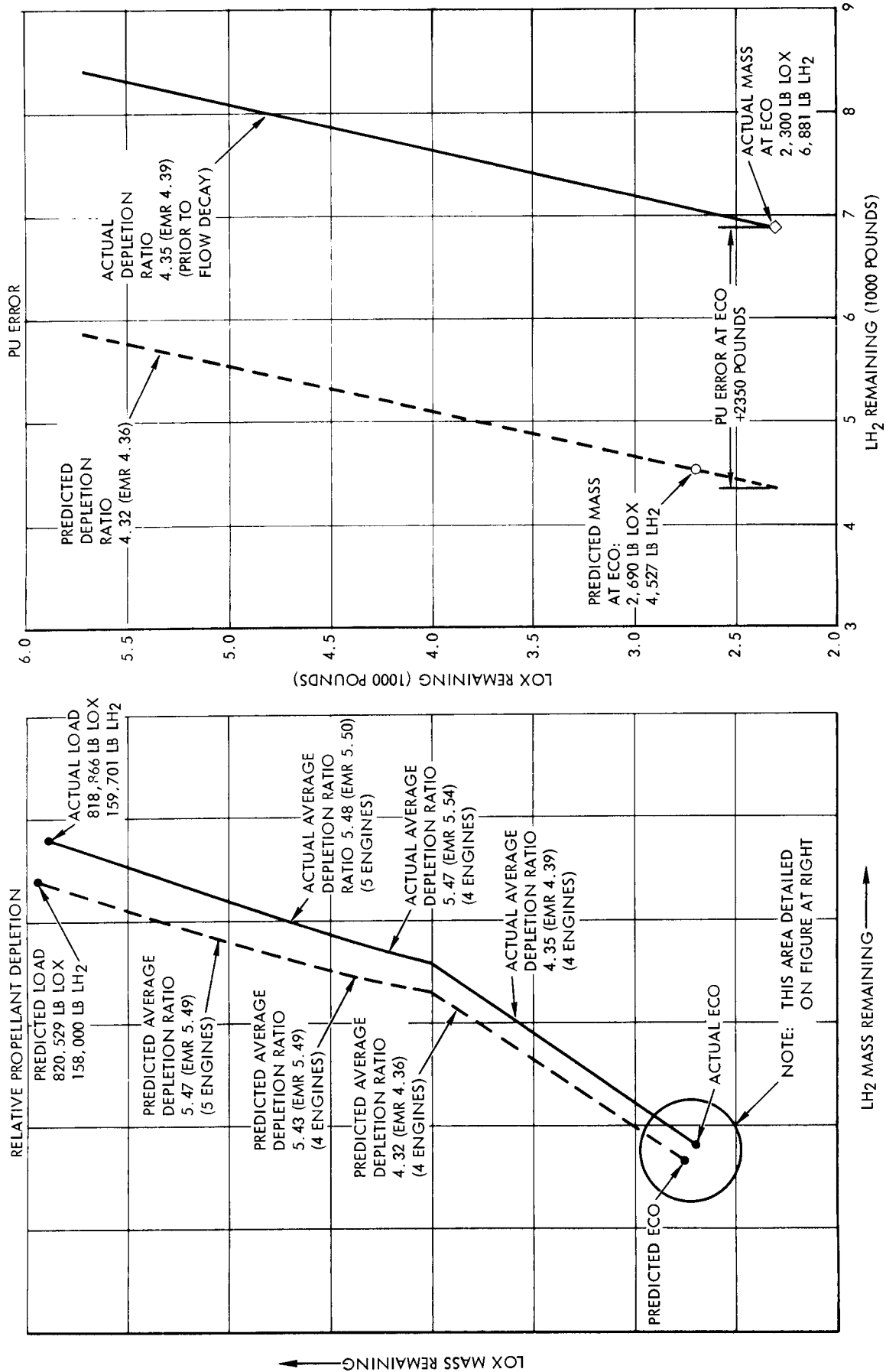
Figure 2.3-29.   Relative Propellant Depletion and PU Error

SD 69-329
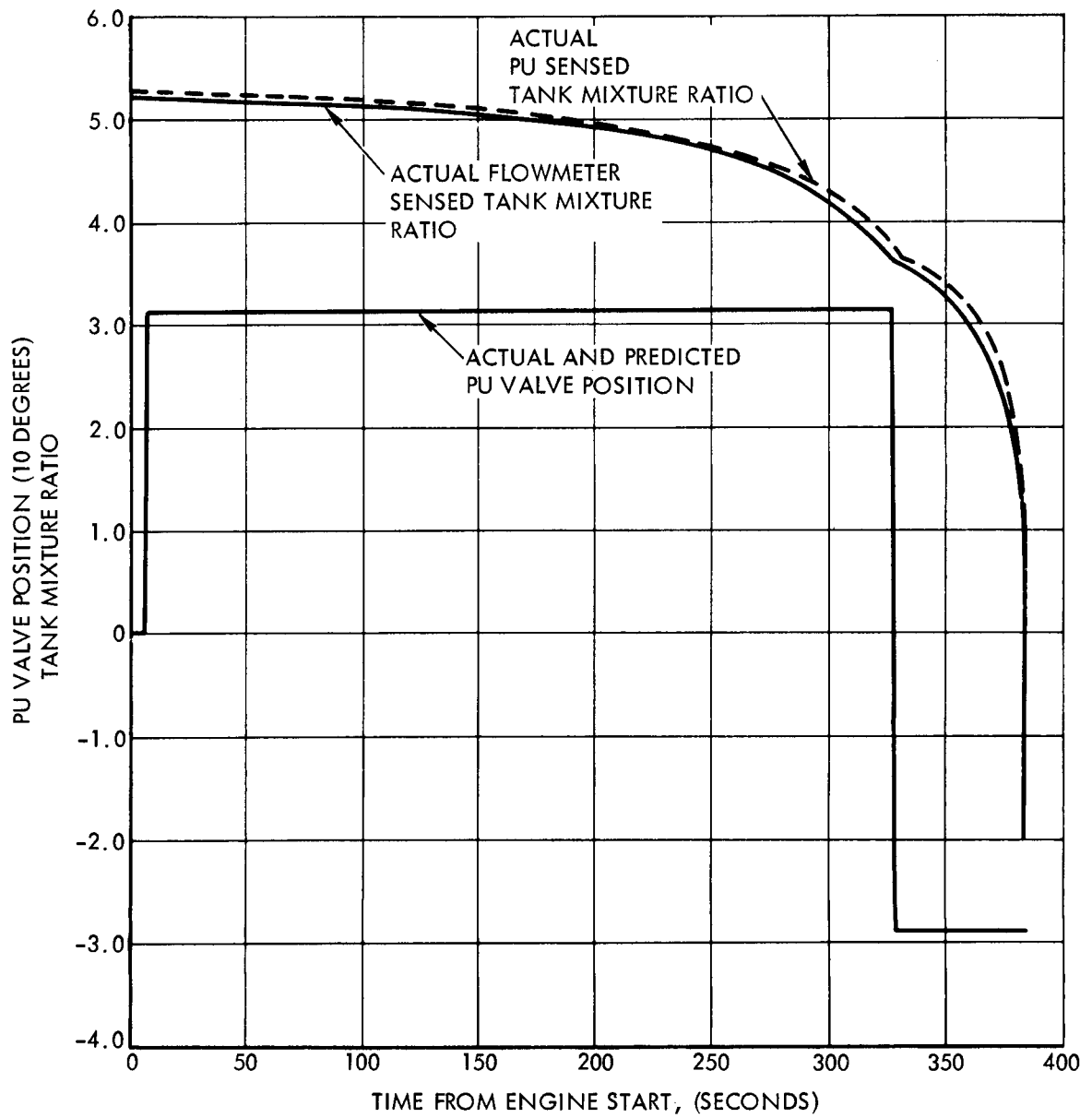
Figure 2.3-30. · PU System Performance
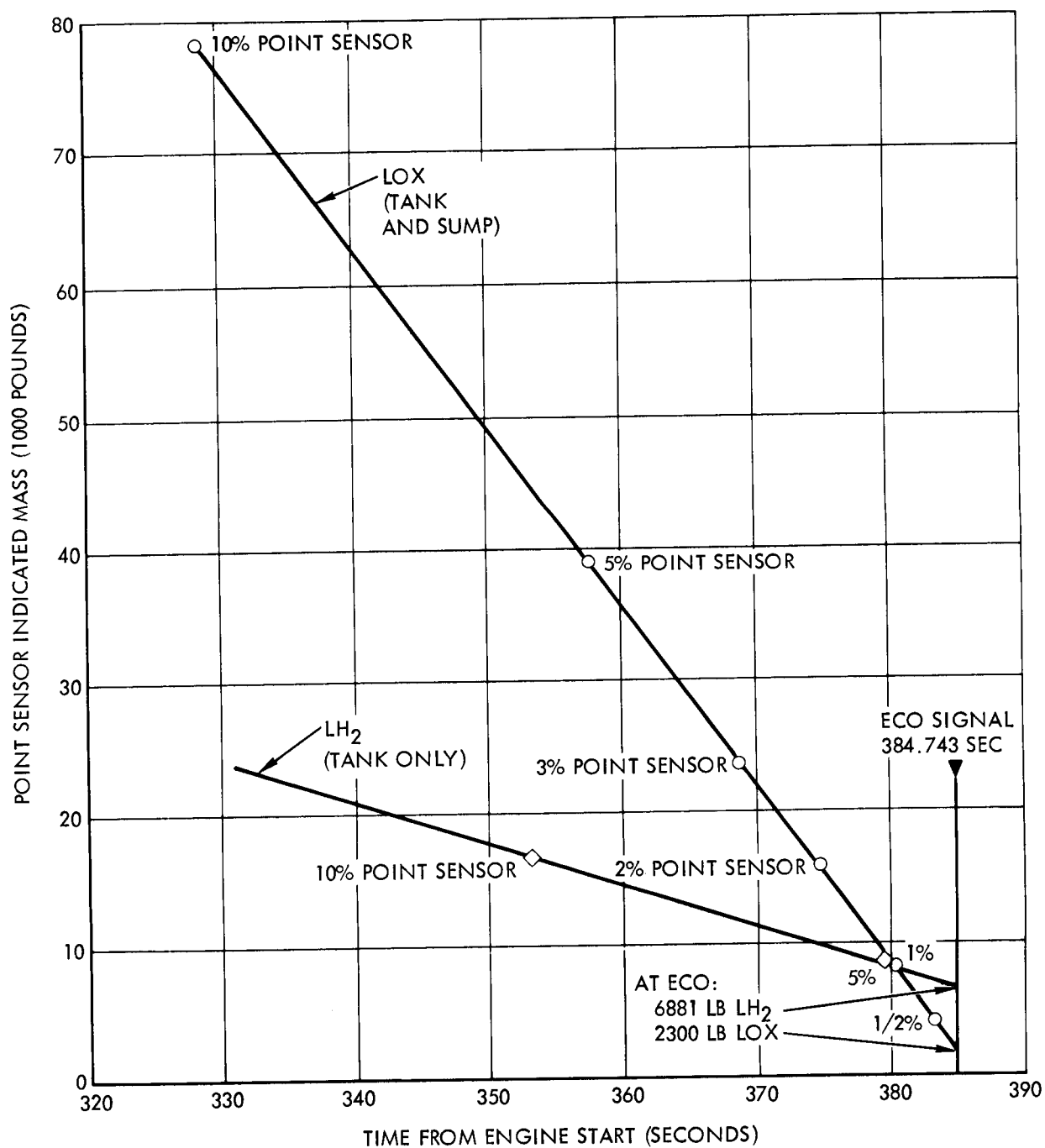
Figure 2.3-31. Engine Cutoff Propellant Residuals
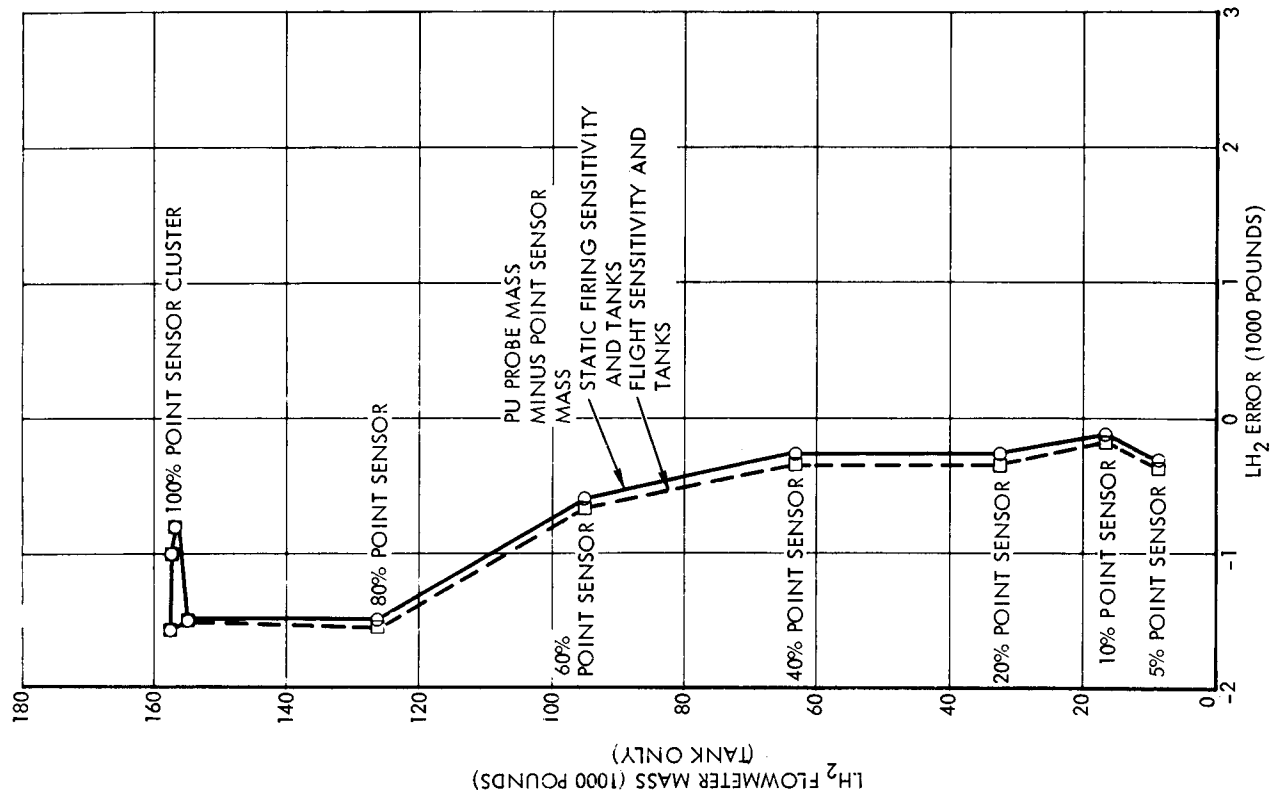
Figure 2.3-33. LH₂ PU Probe Mass Indication Error (Static Firing)
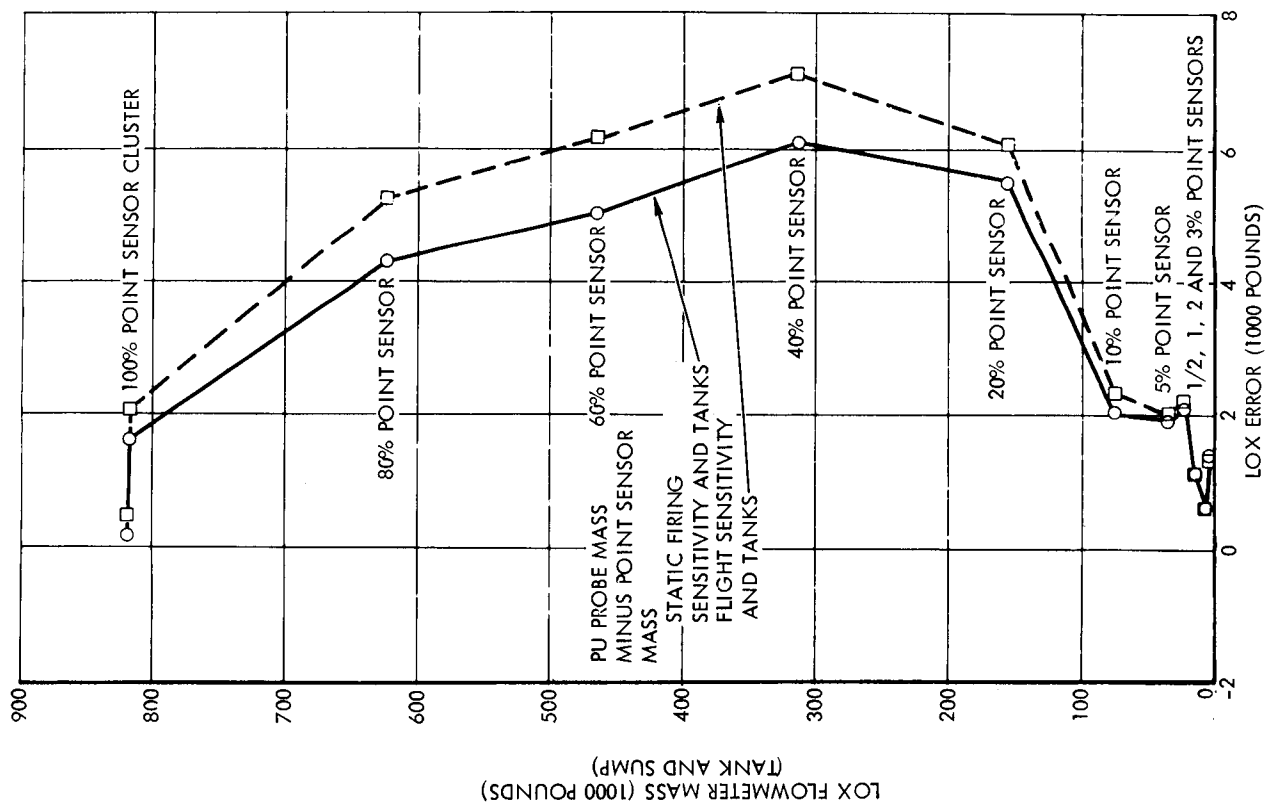
Figure 2.3-32. LOX PU Probe Mass Indication Error (Static Firing)
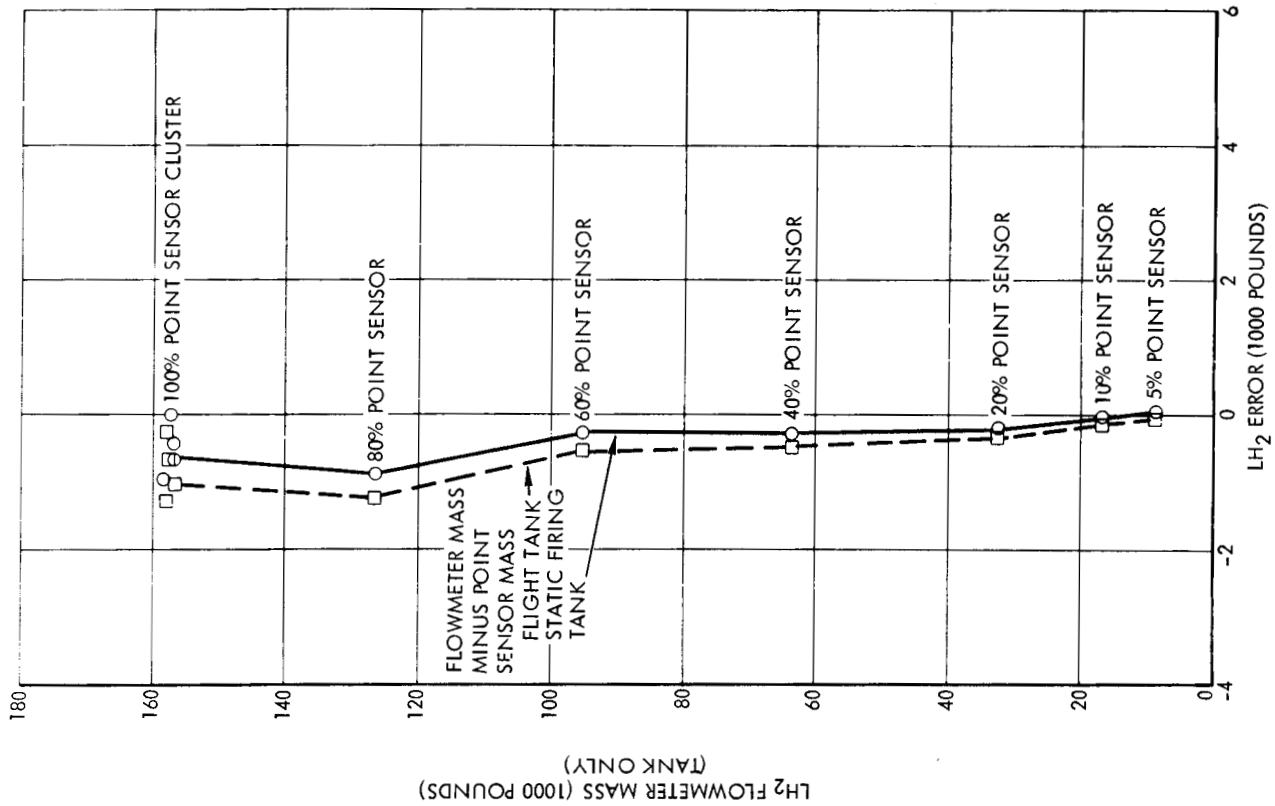
Figure 2.3-35. LH₂ Tank Error (Static Firing)
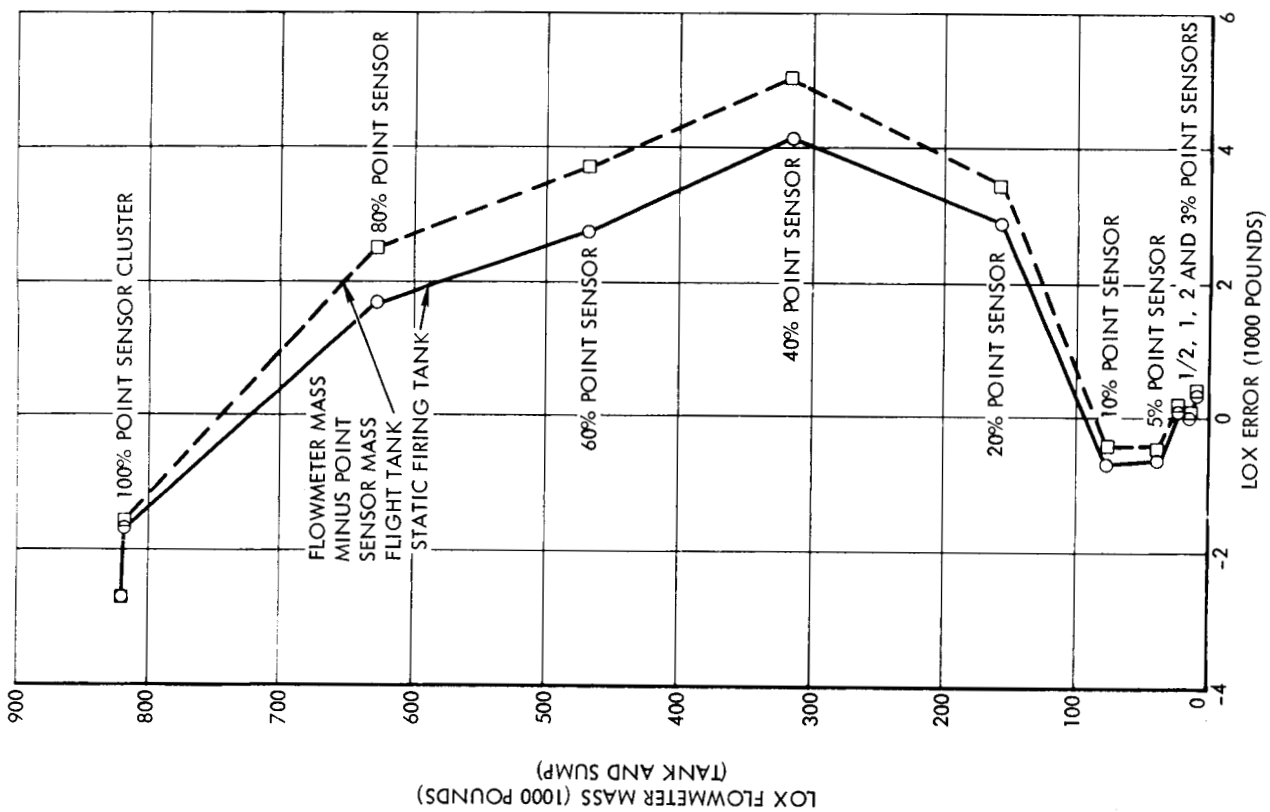
Figure 2.3-34. LOX Tank Error (Static Firing)
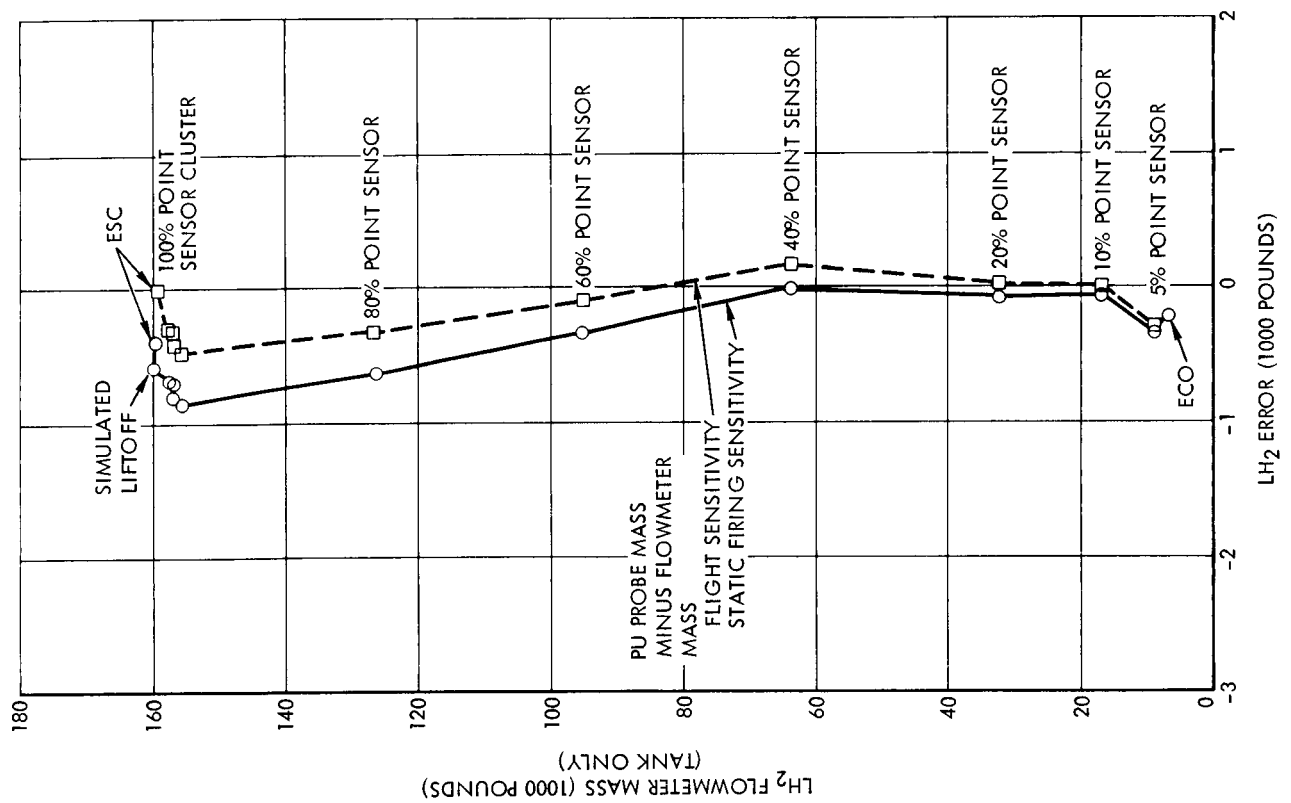
Figure 2.3-37. LH₂ PU Probe/Tank Mismatch (Static Firing)
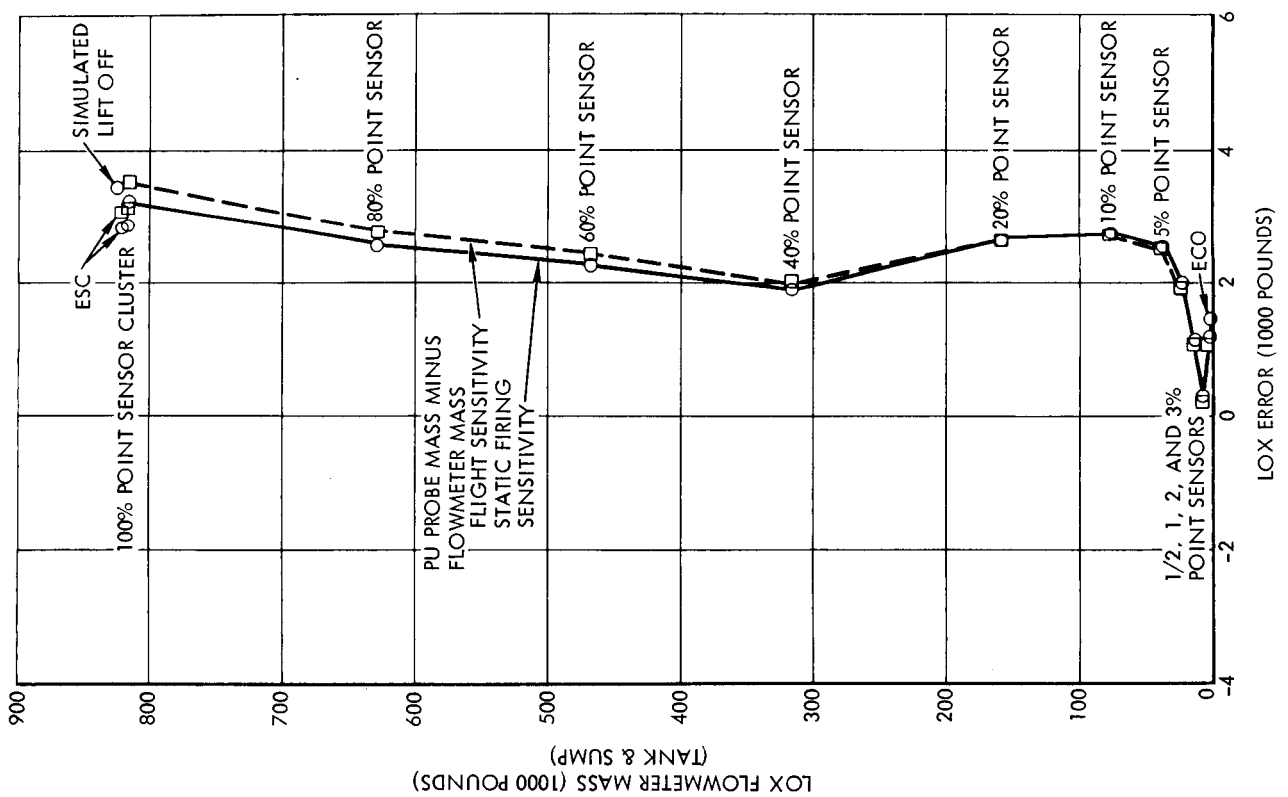
Figure 2.3-36. LOX PU Probe/Tank Mismatch (Static Firing)

Figure 2.3-39. GOX Pressurization Flowrate

Figure 2.3-38. LOX Tank Ullage Pressure, Mainstage
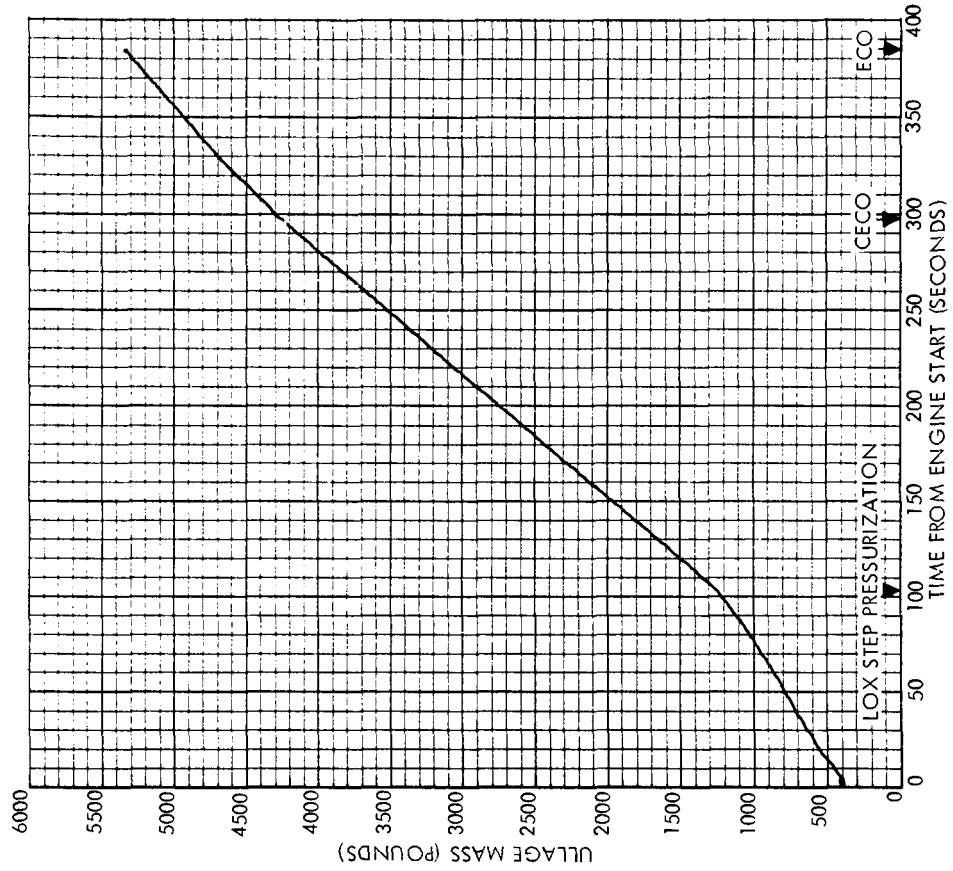
Figure 2.3-41. LOX Tank Ullage Mass
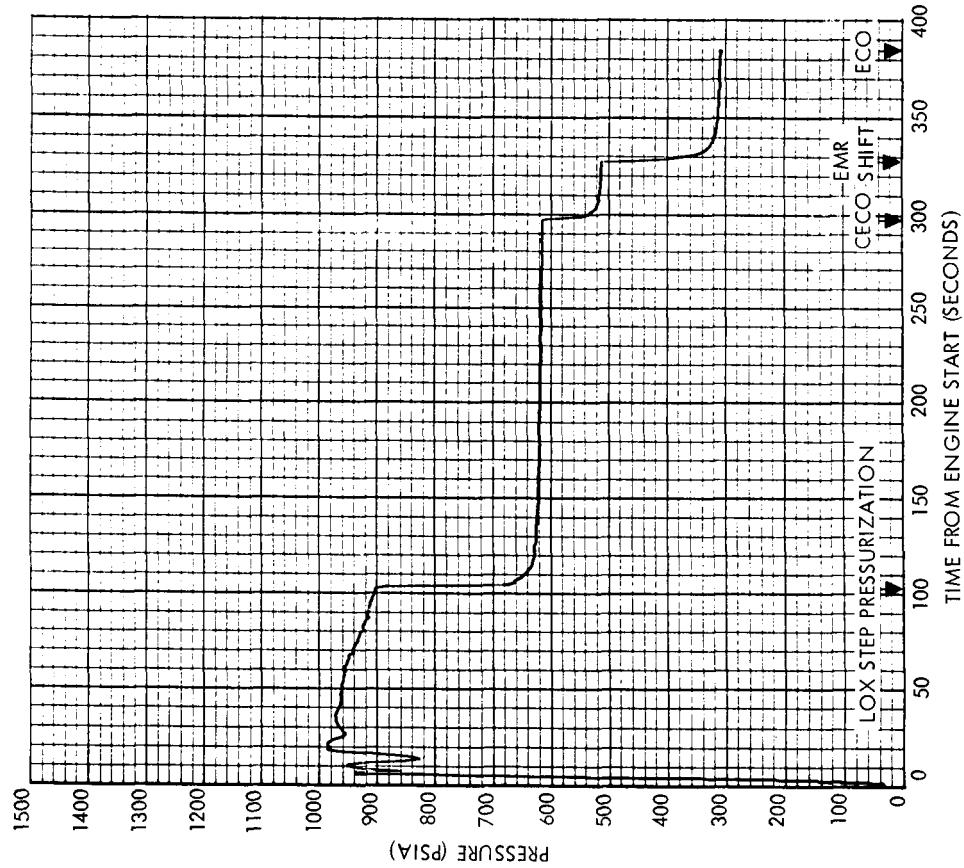
Figure 2.3-40. GOX Pressurization Manifold Pressure

Figure 2.3-43. Engine Inlet LOX Temperature

Figure 2.3-42. Calculated Engine Inlet LOX NPSH

SD 69-329
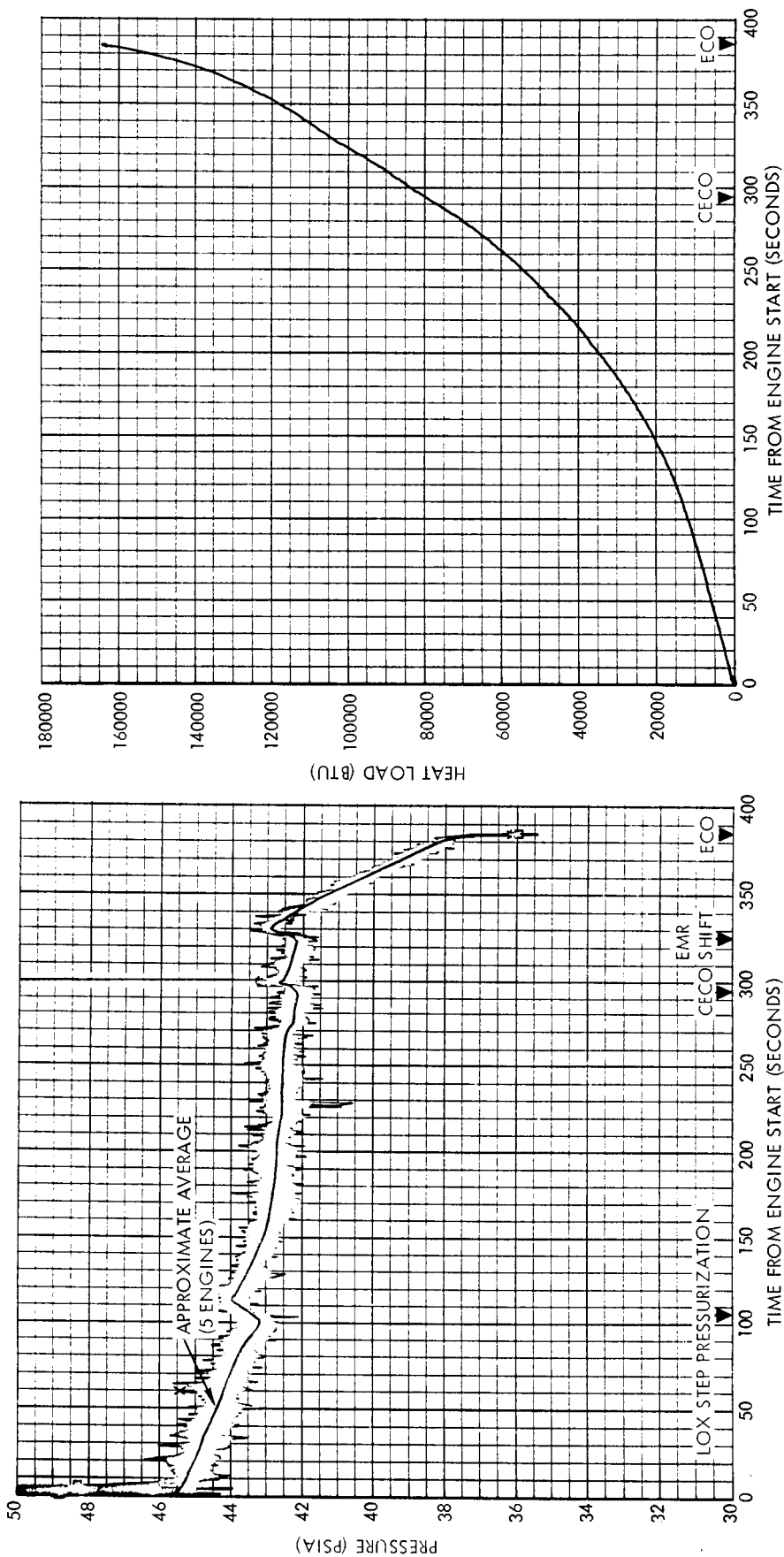
Figure 2.3-45. LOX Accumulated Heat Load

Figure 2.3-44. Engine Inlet LOX Total Pressure

ROCKWELL CORPORATION
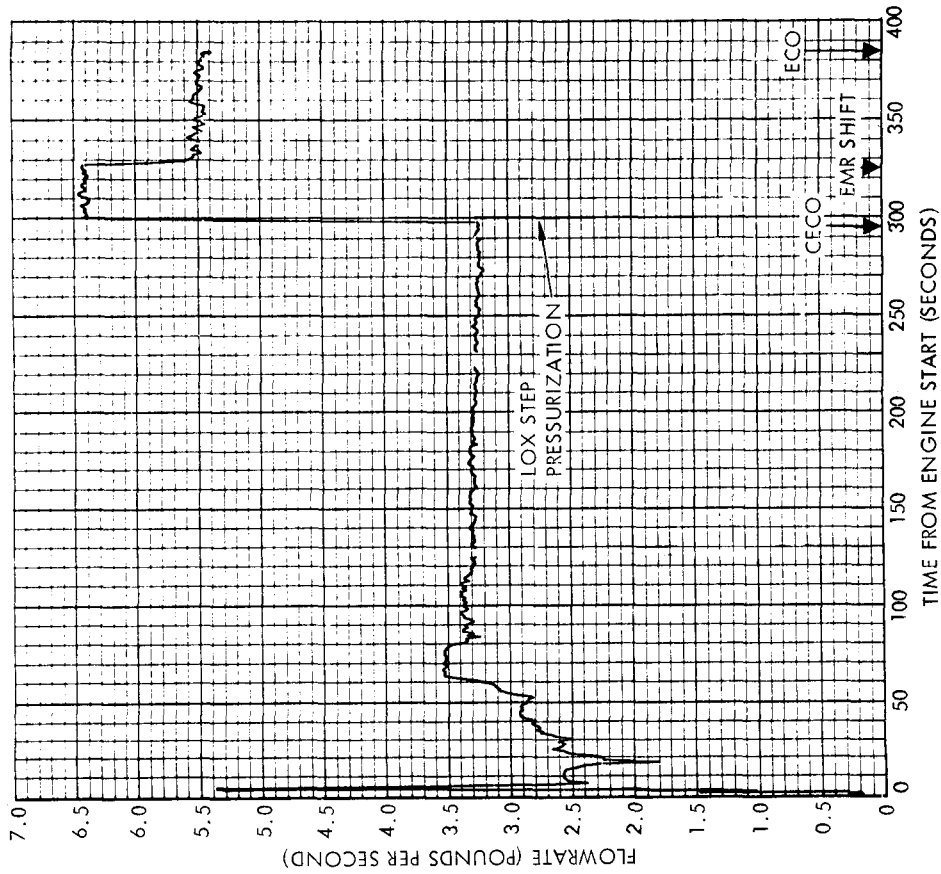
Figure 2.3-47. GH$_2$ Pressurization Flowrate
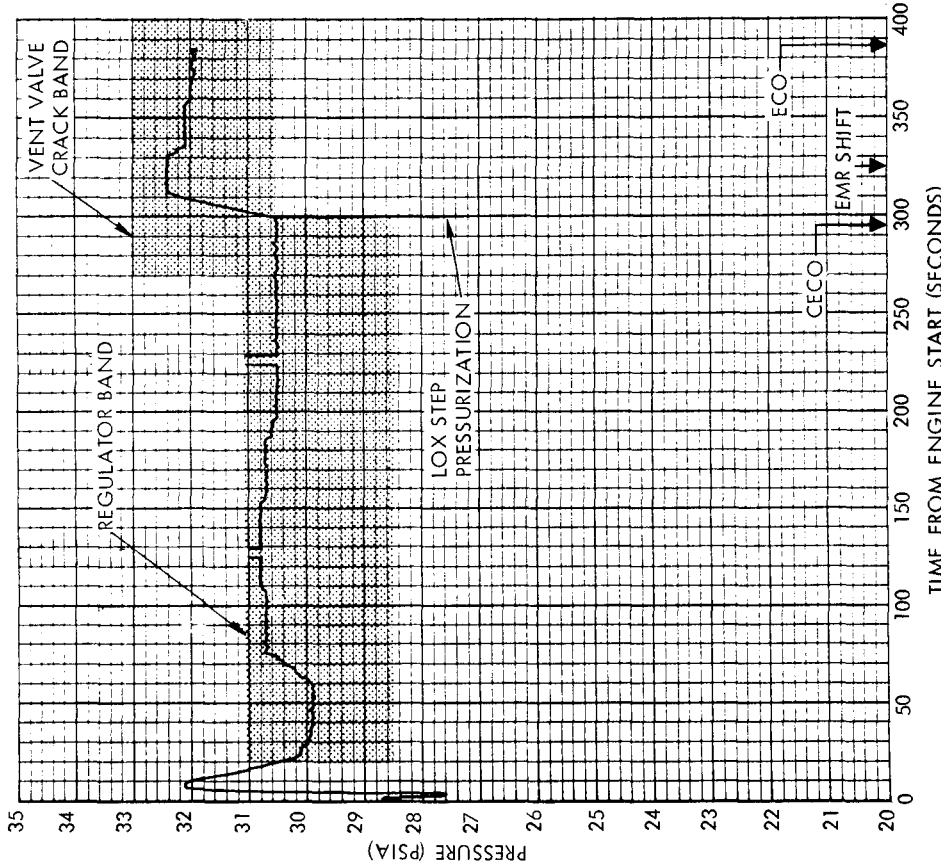
Figure 2.3-46. LH$_2$ Tank Ullage Pressure, Mainstage

2-96
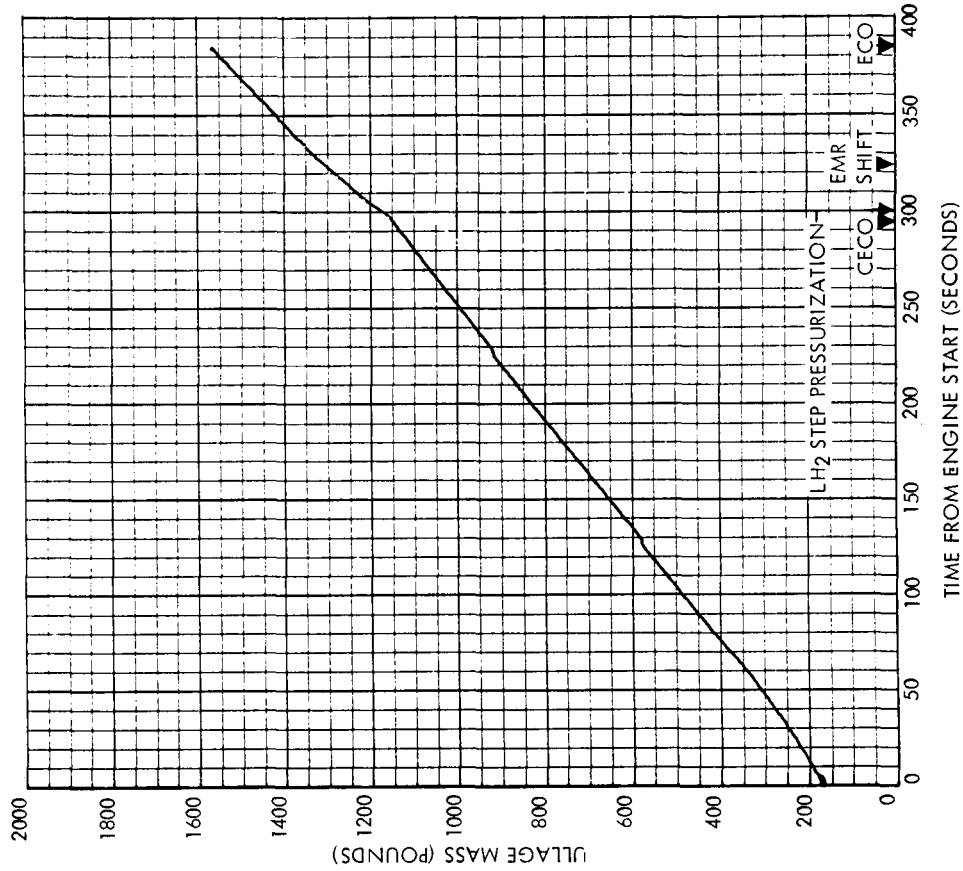
Figure 2.3-49. Total LH₂ Tank Ullage Mass

Figure 2.3-48. GH₂ Regulator Inlet Pressure
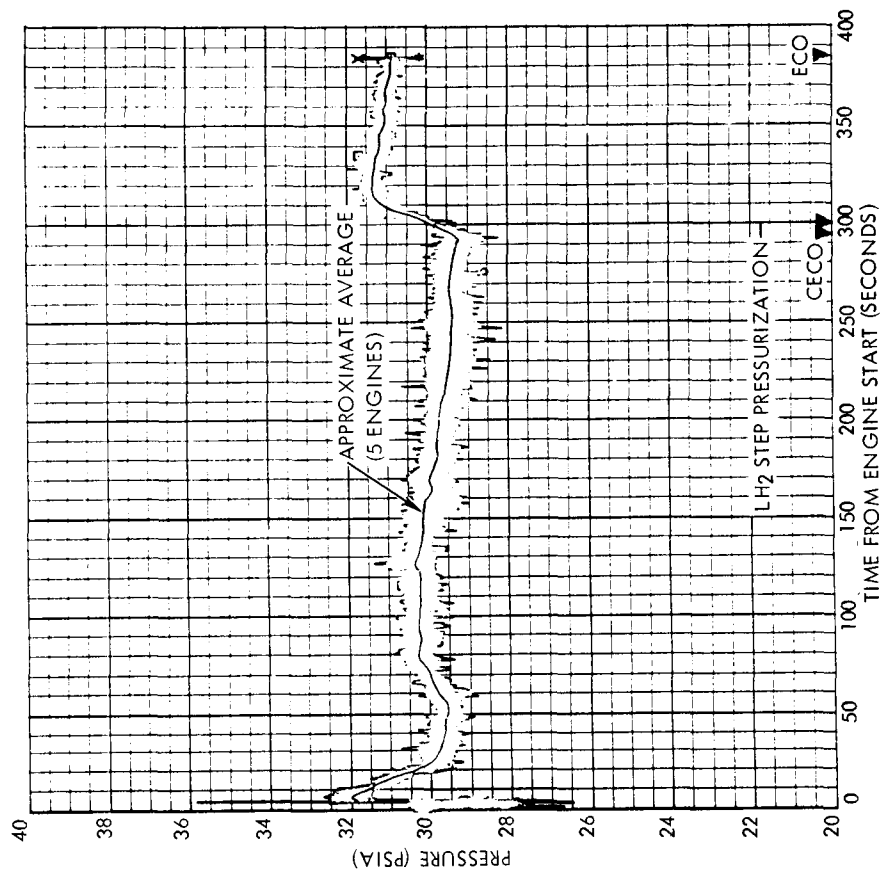
Figure 2.3-51. Engine Inlet LH$_2$ Total Pressure
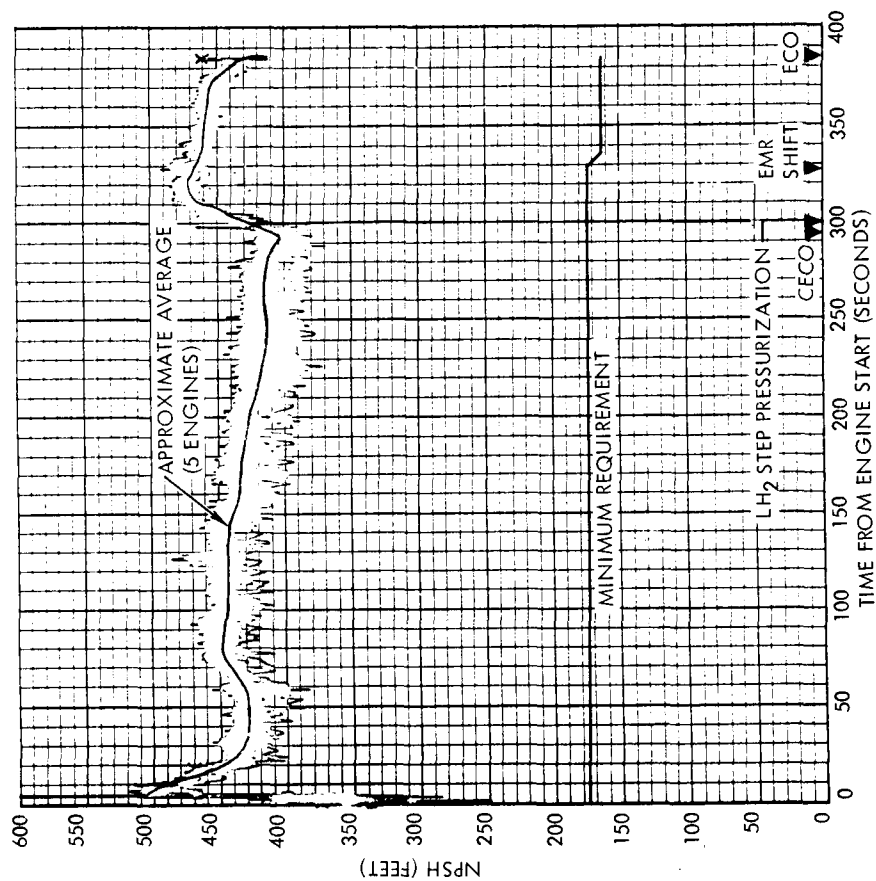
Figure 2.3-50. Engine Inlet LH$_2$ NPSH

SPACE DIVISION of NORTH AMERICAN ROCKWELL CORPORATION
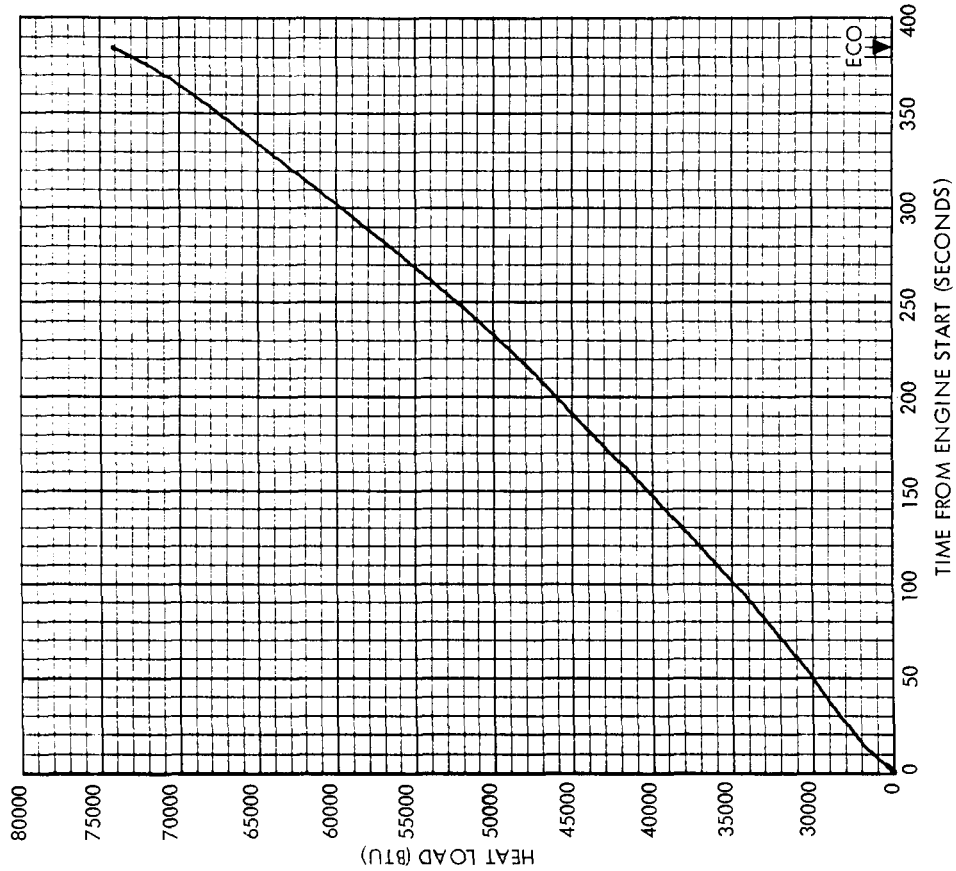
Figure 2.3-53. LH$_2$ Accumulated Heat Load
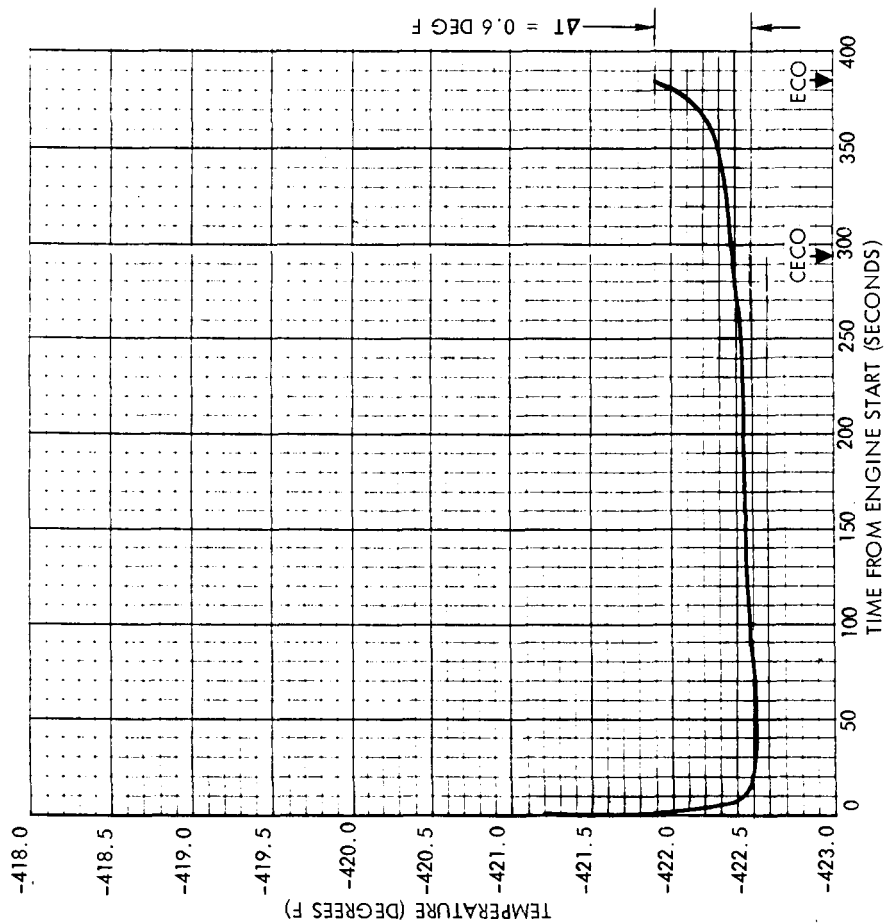
Figure 2.3-52. Engine Inlet LH$_2$ Temperature

2-99

SD 69-329
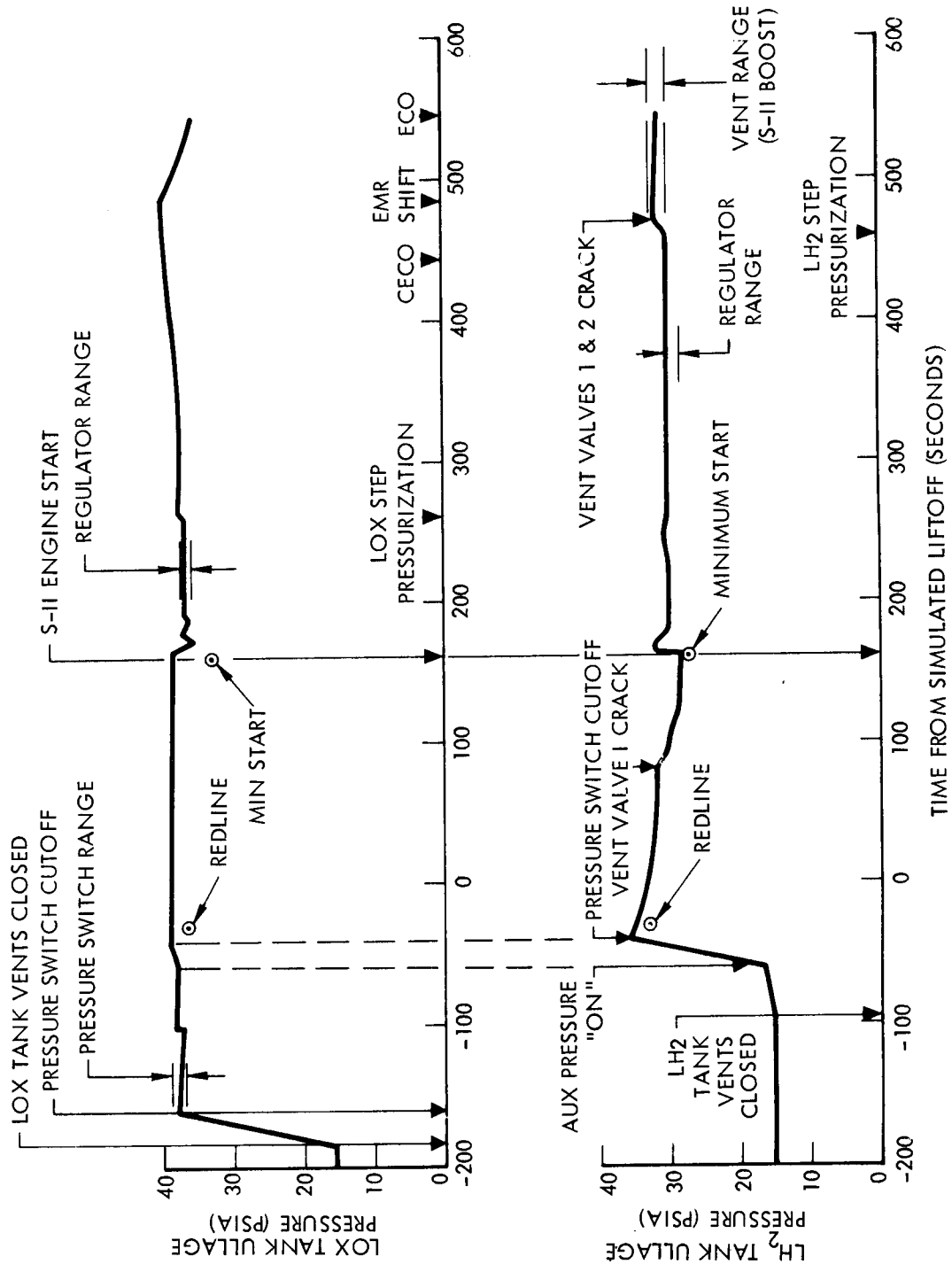
Figure 2.3-54. Pressurization System Ullage Pressure Composite
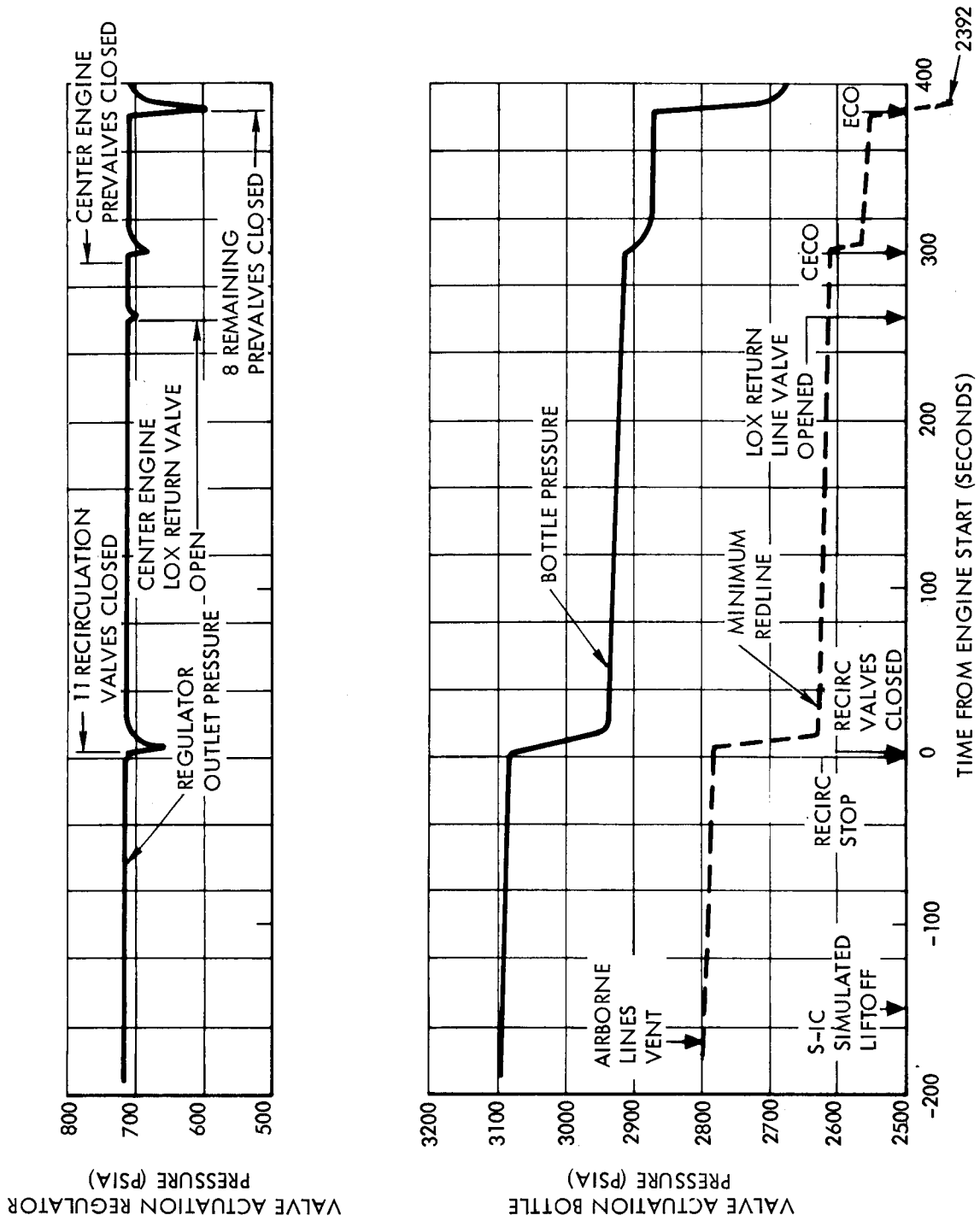
Figure 2.3-55. Valve Actuation System Pressures

3.0 ENGINE ACTUATION SYSTEM

SYSTEM DESCRIPTION

A complete, separate, and identical engine actuation system (EAS) is provided for each gimbaled J-2 engine. The closed hydraulic system provides power and forces to gimbal the engine. The engine position feedback control loop for each of the pitch and yaw axes is closed within the system by means of a mechanical feedback device located within each servoactuator. Major system components include an engine-driven main pump, an auxiliary electric motor-driven pump, two electrically-controlled hydraulically-powered servo-actuators, and an accumulator reservoir manifold assembly. Fluid is distributed throughout the system by means of flexible hose assemblies and rigid tubing. A detailed description of the system is contained in SID 63-895, Production Engine Actuation Subsystem for Saturn S-II, dated 1 February 1965.

TEST EVALUATION

The evaluation and supporting data for the acceptance test requirements are presented in Volume 1 of this report. All EAS acceptance requirements were satisfied.

During the test, Engines 1, 2, 3, and 4 were automatically gimbaled using computer-initiated servoanalyzer commands. Step gimbaling of plus and minus 3.5 degrees amplitude was accomplished simultaneously on the four engines in the pitch, yaw and roll modes. Duration of each step command was one-half second. Additional step gimbaling of plus and minus 0.5 degree was performed in the pitch and yaw modes. Sinusoidal gimbaling also was performed, on one engine at a time in the pitch and yaw modes. The command amplitudes in this case were 6 milliamperes (equivalent to 0.9 degree) peak-to-peak at frequencies of 1, 2, 3, 4, 5, 6 and 8 Hertz. Four to five cycles were performed at each frequency. Total gimbaling time was 210 seconds. Throughout step gimbaling, the actuator responses approached the command values with no detectable overshoot or tendency to diverge from the commands, indicating ample stability. Actuator response rates also were satisfactory and are listed in Volume 1 of this report. The rates ranged from 18 to 21 degrees per second. Representative plots of commands and responses are shown in Figure 3-1.

Frequency Response

Frequency response characteristics of the actuators were determined from the static firing data. A power spectral density analysis program was employed on a digital computer to obtain frequency response characteristics from the sinusoidal gimbaling portion of the 100 samples-per-second test data. These data were then run through a least-squares curve-fit routine that obtained the transfer function and Bode plots of the Fourier transformed test data.

Figures 3-2 and 3-3 show plots of amplitude ratio and phase lag for the four pitch and four yaw actuators, respectively. The actual data points obtained at each test frequency are plotted for each actuator. The curves represent averages of the data obtained from the least-squares fit program. The top curve, in each case, shows the ratio of actuator output to input command in decibels (20 log ratio) versus frequency in radians per second. The curves have been normalized to a gain of unity at zero frequency. The bottom curves show the corresponding phase angle differences between input and output.

Table 3-1 summarizes important data from the frequency response tests. The following definitions apply:

ω_s = engine/structure resonant frequency, radians/second

ζ_s = structural damping ratio (caused mainly by gimbal friction)

ω_T = actuator closed-loop resonant frequency, radians/second

ζ_T = actuator damping ratio

K_c = actuator closed-loop gain, 1/second

ϕ_{psd} = phase lag of output position to input command from power spectral density analysis at 1 Hertz, degrees

ϕ_{MTF} = phase lag at 1 Hertz from Volume 1 of this report, degrees

The last two columns of Table 3-1 lists phase lags obtained for each actuator at 1 Hertz. The first of these columns shows the values obtained from the power spectral density program, and the last column gives the values from Volume 1 of this report. Close agreement is indicated.

A transfer function of i_c (input current in milliamperes) to X_A (actuator position in inches), based upon the average values in Table 3-1, is as follows:

$$32.2 \frac{ma}{in.} \left(\frac{X_A}{i_c} \right) = \frac{\dfrac{s^2}{(34)^2} + \dfrac{2(0.10)}{34} s + 1}{\left(\dfrac{s}{13} + 1 \right) \left(\dfrac{s^2}{(29)^2} + \dfrac{2(0.26)}{29} s + 1 \right)}$$

3-2

SPACE DIVISION of NORTH AMERICAN ROCKWELL CORPORATION

Hydraulic Pressures and Temperatures

Figure 3-4 shows accumulator gas and oil pressures and reservoir volume and pressure, representative of the four systems, during a period of significant activity. The pressure and volume fluctuations seen during the early portion of the firing and periodically thereafter to a lesser degree reflect normal values and are the result of open actuator cylinder bypass valves during the engine start transient and of gimbaling transients.

Table 3-2 lists transient accumulator hydraulic and reservoir pressures recorded during the test. The accumulator pressures varied between 3120 and 3670 psia. The range for normal operation under this condition is 2700 to 3900 psia. The reservoir pressures varied between 94 and 160 psia and compared favorably to a normal range of 60 to 175 psia.

Table 3-3 lists actuator forces during gimbaling, prior to cutoff, and during the cutoff transient. The highest force of 28,000 pounds occurred during step gimbaling. This is well below the engine design gimbaling force limit of 46,000 pounds. A plot of one of the forces on Figure 3-1 illustrates the nature of actuator forces during step gimbaling.

Temperature histories of main pump case and reservoir fluids representative of the four systems are shown in Figure 3-5. The temperature ranges were well within design limits of -65 F to 275 F.

Table 3-1. Results of EAS Frequency Response Analysis

Actuator	ω_s rad/sec	ζ_s	ω_T rad/sec	ζ_T	K_C 1/sec	ϕ_{PSD} at 1 Hz degrees	ϕ_{MTF} at 1 Hz degrees
Pitch							
Engine 1	34	0.10	30	0.23	10	-34	-34
Engine 2	35	0.10	29	0.27	13	-31	-30
Engine 3	35	0.09	30	0.27	14	-31	-32
Engine 4	34	0.12	28	0.27	13	-30	-31
Average Pitch	34	0.10	29	0.26	13	-31	-32
Yaw							
Engine 1	34	0.11	29	0.24	13	-30	-29
Engine 2	34	0.09	30	0.23	16	-28	-26
Engine 3	34	0.12	29	0.29	12	-33	-31
Engine 4	35	0.10	29	0.27	14	-31	-29
Average Yaw	34	0.10	29	0.26	14	-30	-29
Average Stage	34	0.10	29	0.26	13	-31	-30

Table 3-2. EAS Accumulator Hydraulic and Reservoir Pressures

Mode of EAS Operation	Accumulator Pressure, BD103-201/4, (psia)				Reservoir Pressure, BD104-201/4, (psia)			
	Engine 1	Engine 2	Engine 3	Engine 4	Engine 1	Engine 2	Engine 3	Engine 4
Minimum transient (3.5 degrees roll step gimbaling)	3120	3140	3160	3150	94	97	98	95
Maximum transient (3.5 degrees roll step gimbaling)	3620	3630	3670	3640	160	156	152	160

3-5

Table 3-3. EAS Actuator Forces

Mode of EAS Operation	Force (Thousands of Pounds)							
	Engine 1		Engine 2		Engine 3		Engine 4	
	Pitch BD167-201	Yaw BD166-201	Pitch BD167-202	Yaw BD166-202	Pitch BD167-203	Yaw BD166-203	Pitch BD167-204	Yaw BD166-204
Step Gimbaling Transient	-27 to +21	-28 to +20	-21 to +26	-24 to +26	-22 to +26	-20 to +27	-24 to +24	-20 to +27
Sinusoidal Gimbaling Transient	-16 to +7	-17 to +4	-8 to +16	-12 to +16	-7 to +13	-6 to +15	-11 to +11	-7 to +15
Steady State Prior to Cutoff	-5	-4	0	0	0	+3	-3	0
Cutoff Transient	-7 to +1	-6 to 0	-7 to +4	-8 to +5	-7 to +2	-5 to +5	-5 to +4	-6 to +2

NOTE: Positive and negative values indicate compressive and tensile forces (respectively) at the actuator-to-engine and actuator-to-structure attach points.
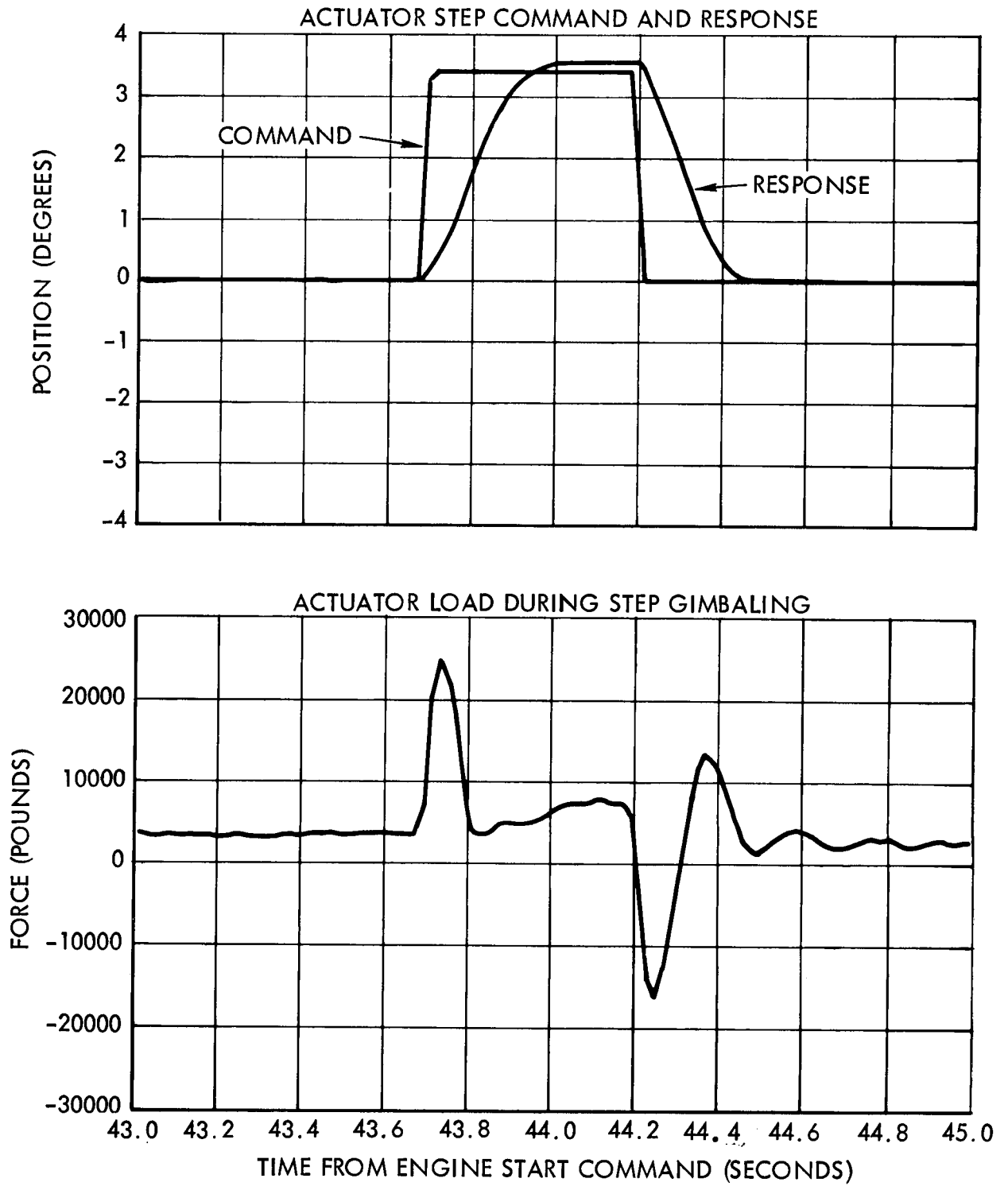
Figure 3-1. Representative Actuator Command, Response and Force
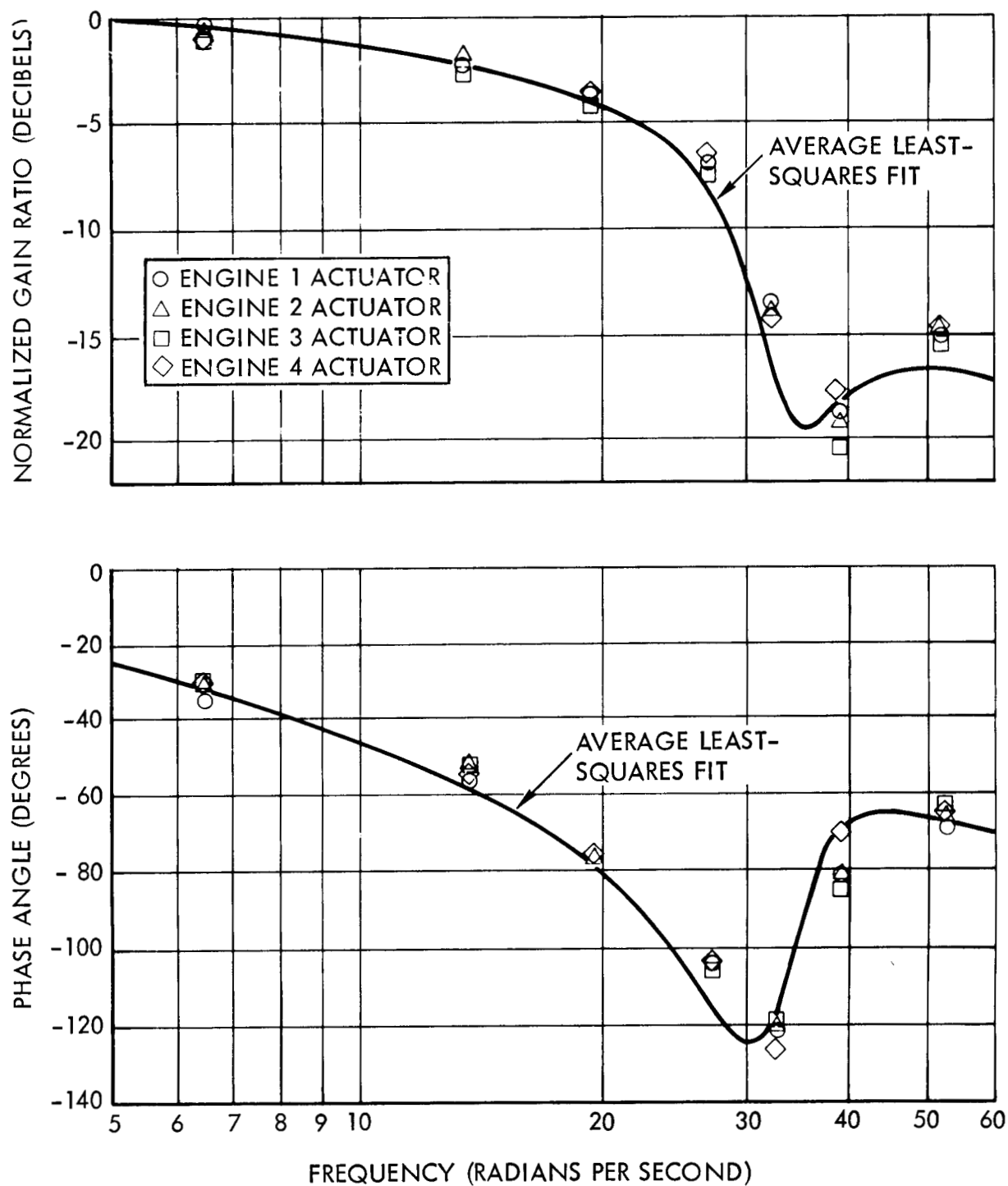
Figure 3-2.   Frequency Response Characteristics of Pitch Actuators
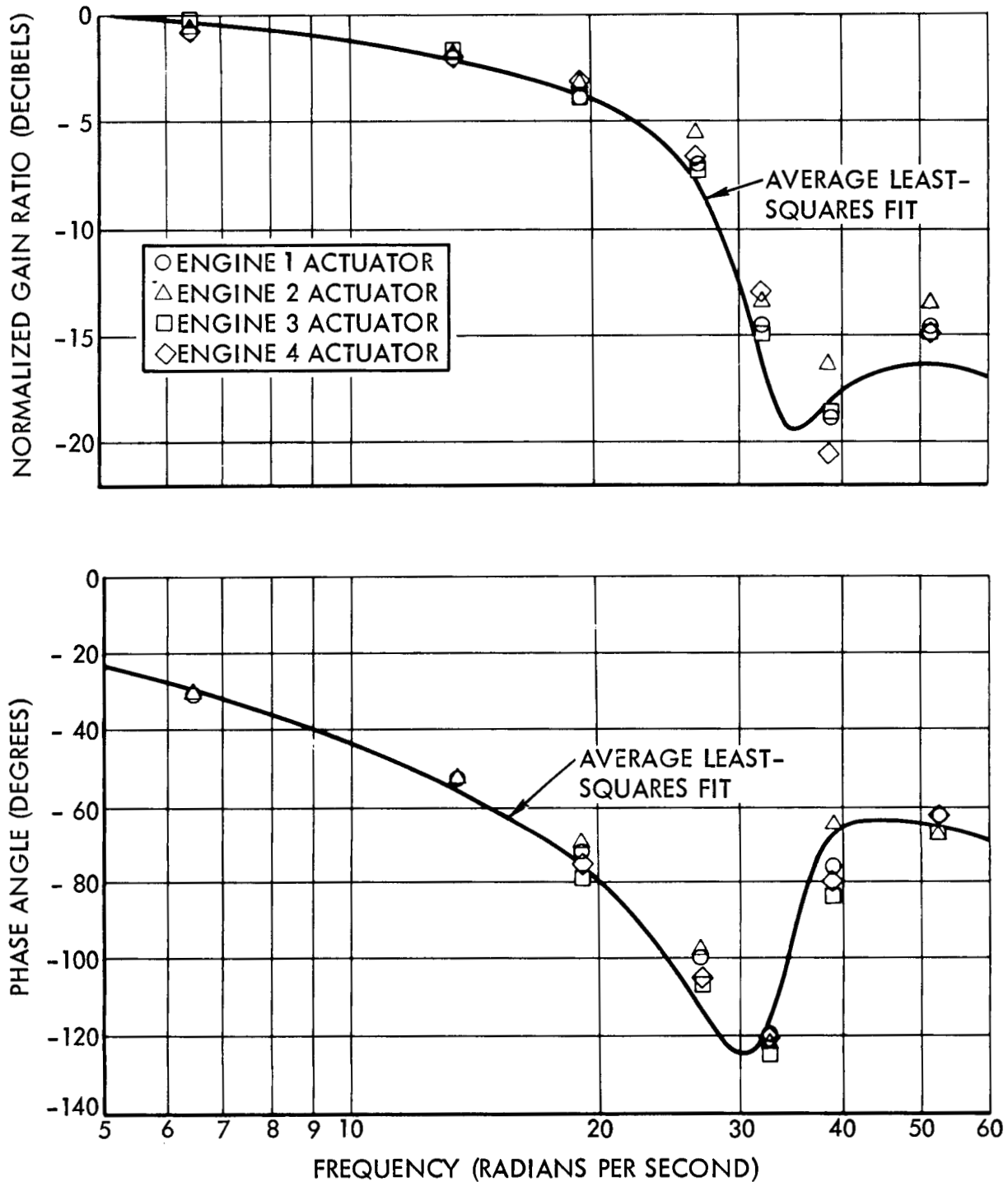
Figure 3-3. Frequency Response Characteristics of Yaw Actuators
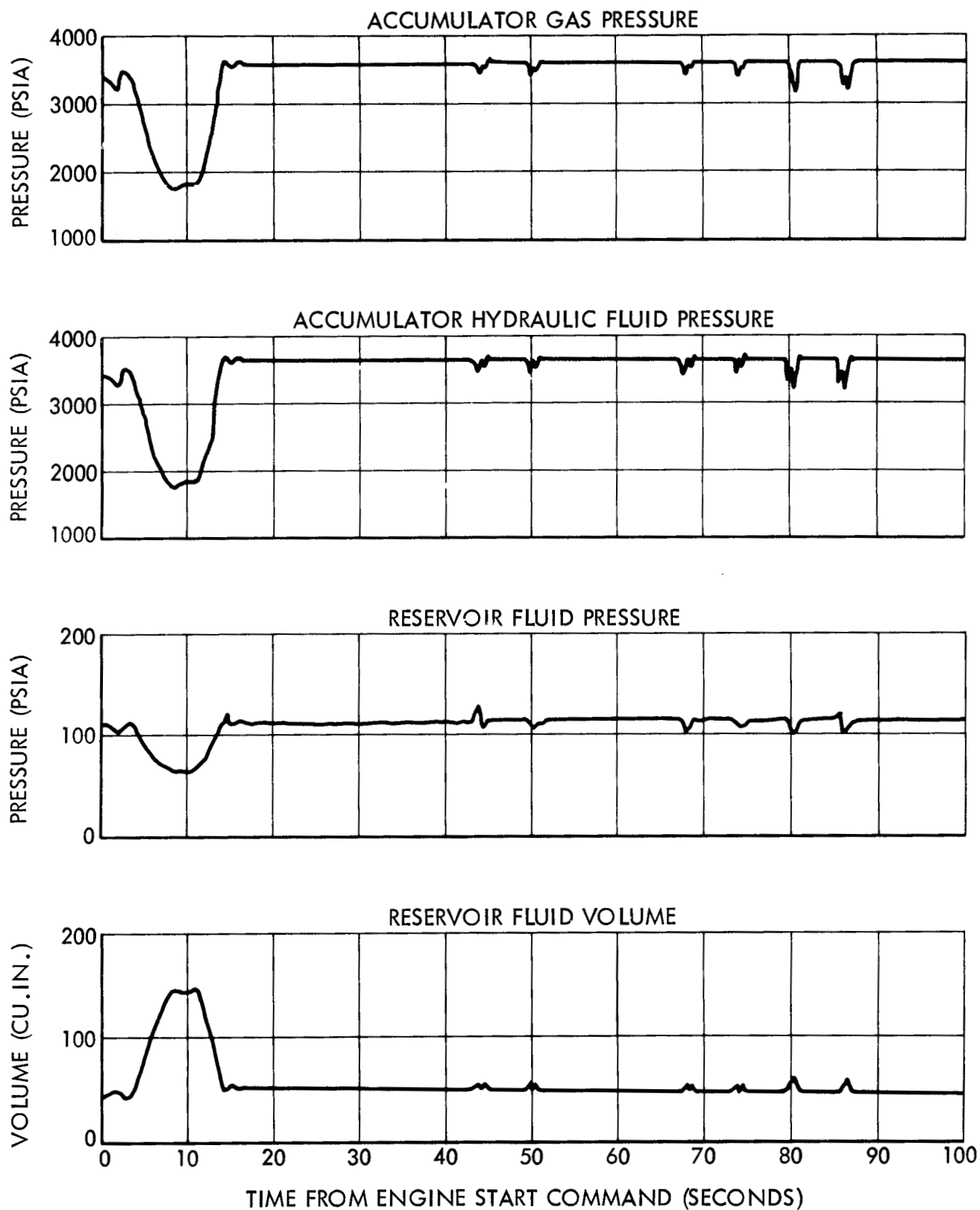
Figure 3-4. Representative EAS Pressures and Reservoir Volume
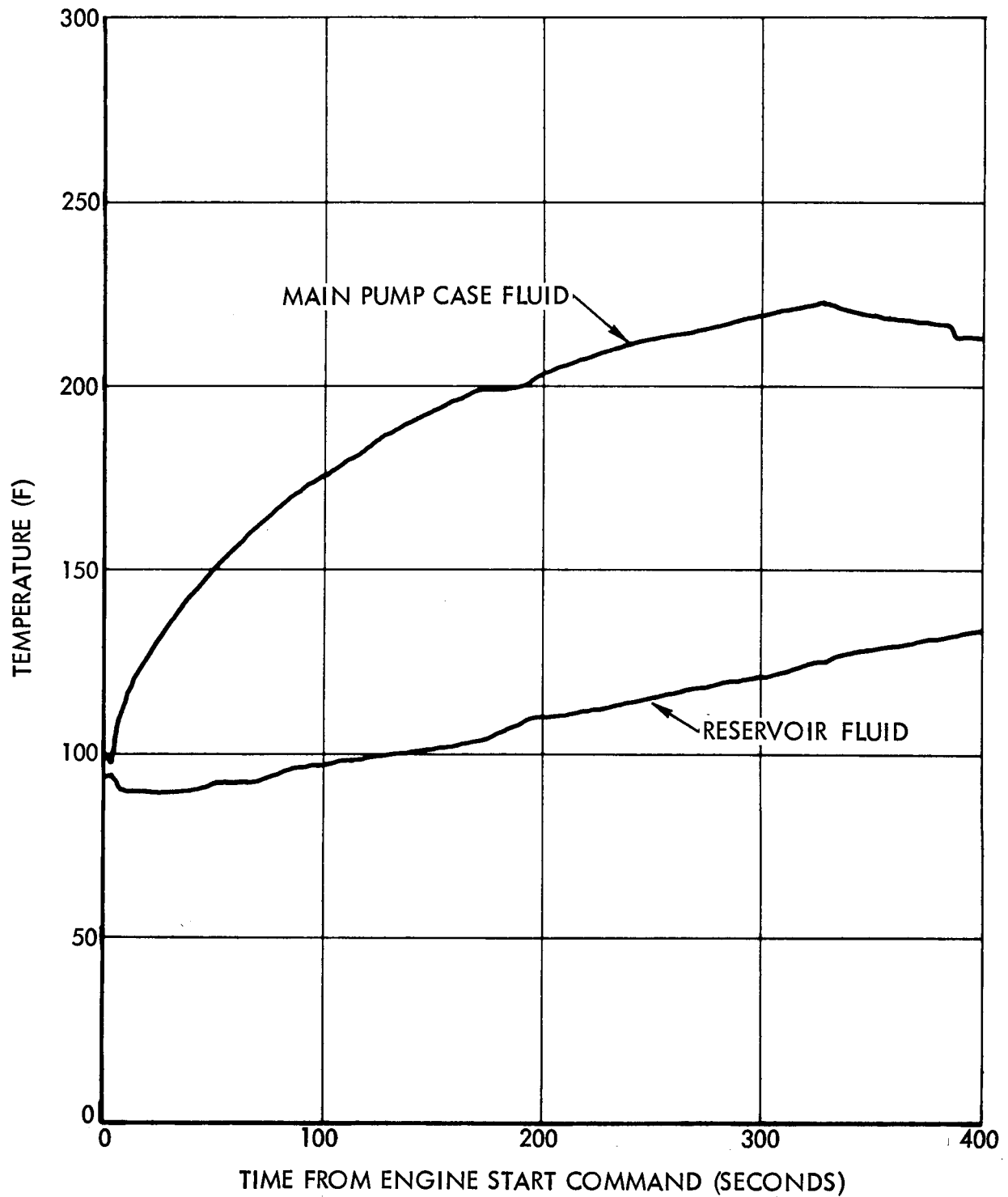
Figure 3-5. Representative EAS Temperatures

4.0 ELECTRICAL SYSTEM

4.1 ELECTRICAL POWER SYSTEM

SYSTEM DESCRIPTION

The stage electrical power system generates and distributes electrical energy to the using systems. The four buses powered in flight are: the main dc bus, supplying primarily the operational sequencing loads; the instrumentation dc bus, supplying primarily the measurement and telemetry loads; the ignition dc bus, supplying J-2 engine ignition loads; and the recirculation dc bus, supplying the LH$_2$ recirculation system static inverter loads. These buses are energized by remote-sensing regulated GSE supplies in both the external and internal power modes of operation for static firing. The transfer to internal or battery simulated power is accomplished by GSE commands at approximately 50 seconds prior to simulated liftoff, using make-before-break, motor-driven power transfer switches. The five static inverters convert 56-vdc power to nominal 42-vac, three-phase, 400-cps power suitable to drive the ac induction motors on the LH$_2$ recirculation pumps. These inverters operate during the interval between 745.9 and 1.4 seconds prior to J-2 engine start. Two buses operated only during ground operations are the heater dc bus, supplying battery and instrument heaters; and the ground dc bus, supplying the system status indicators.

TEST EVALUATION

The stage was transferred to internal power 209.5 seconds prior to engine start and remained on internal power until 386.5 seconds after engine start. The bus transfer switches operated within the procurement specification limit of 200 milliseconds as evidenced by the transfer times shown in Table 4.1-1.

Table 4.1-1. Switch Transfer Parameters

Event	Switch Transfer Times		
	Main (milliseconds)	Instrumentation (milliseconds)	Recirculation (milliseconds)
Transfer to internal	123	125	121
Transfer to external	125	129	129

Stage Bus Voltages and Currents

The main dc bus voltage and current levels achieved during the test are shown in Figure 4.1-1. The bus voltage was within the voltage limits throughout all phases of the test. The bus current varied from 34 to 63 amperes and followed the predicted load profile favorably.

The instrumentation dc bus voltage and current levels reached during the test are shown in Figure 4.1-2. The bus voltage was within the voltage limits throughout all phases of the test. The bus current varied from 28 to 31 amperes and followed the predicted load profile favorably.

The recirculation dc bus voltage and current levels reached during the test are shown in Figure 4.1-3. The bus voltage was within the voltage limits throughout all phases of the test. The bus current varied from 0 to 93 amperes and followed the predicted load profile favorably.

The ignition dc bus voltage and current levels are shown in Figure 4.1-4. The bus voltage was within the voltage limits throughout all phases of the test. The bus current varied from 0 to 30 amperes and followed the predicted load profile favorably.

The heater dc bus voltage was within limits throughout all phases of the test. Current drawn by the instrument heaters was less than 5.0 amperes throughout the autosequence and firing intervals.

Recirculation Inverter Operation

Based on recirculation bus voltage and current and on recirculation motor-pump speeds, satisfactory operation of the inverters was indicated throughout the engine chilldown period of approximately 12.4 minutes.

Flight Predictions

The flight predictions for the S-II-8 stage covering the bus voltages and currents and conforming to Flight Evaluation Working Group (FEWG) format requirements are the same as those contained in SD 68-655 for the S-II-6 stage. The predicted currents are considered to be maximum.
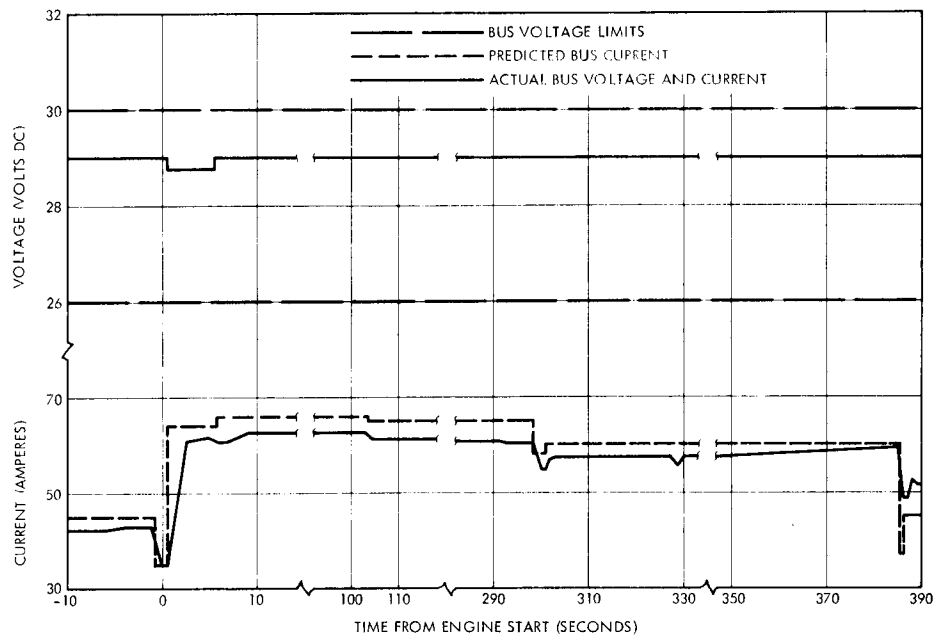
Figure 4.4-1. Main Bus Voltage and Current
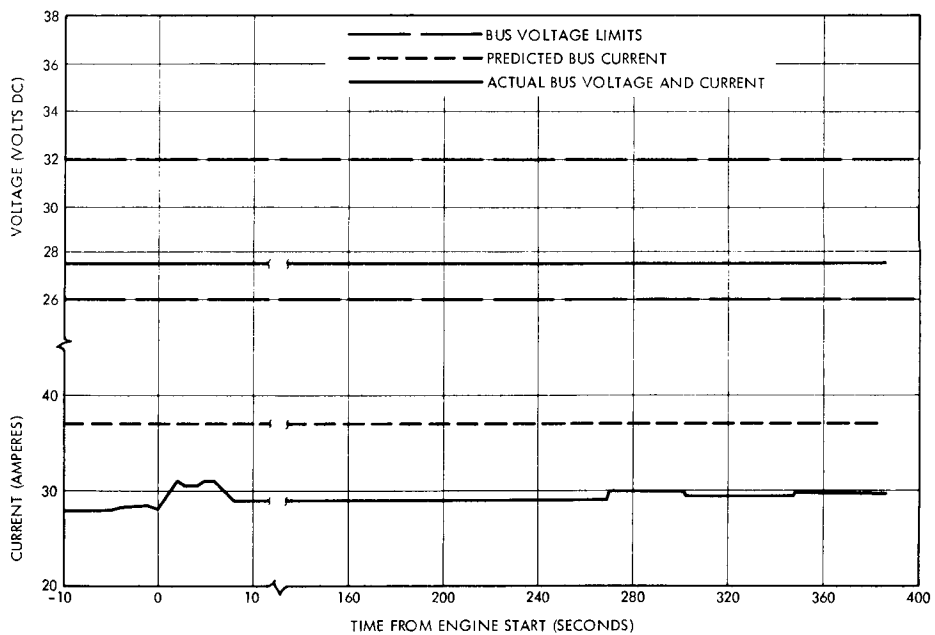
Figure 4.1-2. Instrumentation Bus Voltage and Current
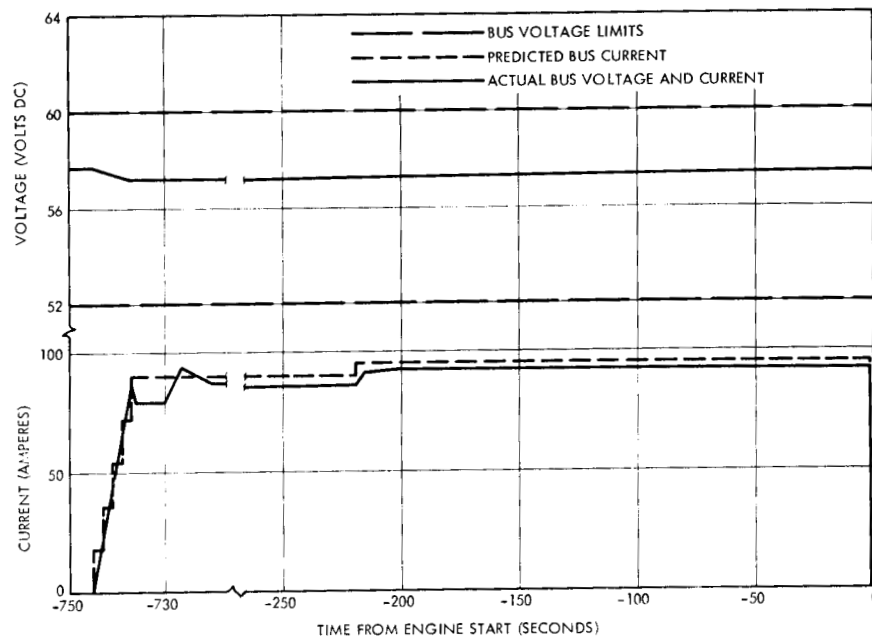
Figure 4.1-3. Recirculation Bus Voltage and Current
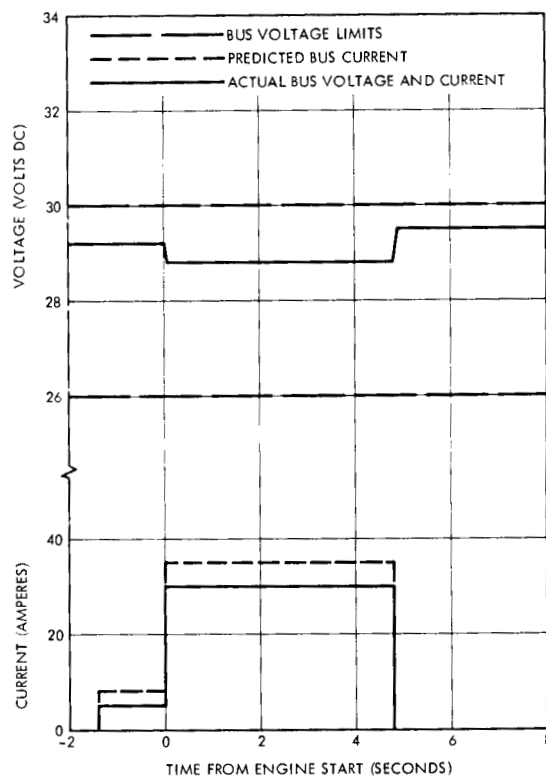
Figure 4.1-4. Ignition Bus Voltage and Current

4.2 ELECTRICAL CONTROL SYSTEM

SYSTEM DESCRIPTION

The electrical control system provides control over various mechanical stage functions associated with both ground and flight operations.

All of the electrical solenoids, switches, connectors, and wire cables integral with the related mechanical systems are components of the electrical control system. Stimuli for the electrical control system are provided from the GSE, propellant sensing transducers, switch selector, instrument unit, and the propellant dispersion and engine systems.

The S-II-8 static firing configuration is the same as that used on the S-II-7 static firing except for a programmed early center engine cutoff, the LOX two-out-of-five dry sensor depletion cutoff for the outboard engines and the ground-controlled engine purges using the helium control solenoids. Drag-on cables were used to replace stage control of the chilldown pump valves. The cables are also used in series with prevalve control circuits to provide GSE closure capability. In all other control areas, the static firing configuration is the same as that used for flight.

TEST EVALUATION

Test evaluation for the electrical control system was included in the evaluation of the mechanical system being controlled.

The early inboard engine cutoff required the presence of additional helium purges in the engine area. To accomplish these purges, certain flight operations were bypassed. A detailed discussion of that situation is contained in Subsection 2.3 of this report.

All other control circuits functioned normally to provide the required mechanical control.

4.3 EMERGENCY DETECTION SYSTEM

SYSTEM DESCRIPTION

    The emergency detection system (EDS) is required to provide data, resulting from certain critical stage measurements, to the spacecraft. The EDS configuration for the S-II-8 stage is the same as that used on previous S-II stages and is identical to the flight configuration.

TEST EVALUATION

    Test evaluation for the EDS consisted of verifying that the redundant EDS measurements were normal, and that the results compared with other stage operational information.

    The engine Thrust-OK pressure switches were activated by variations in pressure in the main oxidizer injection line. The switches are set to close at 500 ± 30 psig and drop out between 20 to 105 psi below the closing pressure. The switches closed during thrust buildup and opened following the engine cutoff signal at the times shown in Table 4.3-1. Comparisons between the closing and opening of redundant pressure switches indicate normal switch operation for Thrust-OK circuits.

Table 4.3-1. Performance Summary of Thrust-OK Pressure Switches

Measurement	Central Standard Time Closed (hr: min: sec:)	Central Standard Time Open (hr: min: sec:)
Engine 1 switch A - K231-201	13:45:02.650	13:51:24.612
Engine 1 switch B - K332-201	13:45:02.675	13:51:24.554
Engine 2 switch A - K231-202	13:45:02.559	13:51:24.604
Engine 2 switch B - K232-202	13:45:02.592	13:51:24.554
Engine 3 switch A - K231-203	13:45:02.725	13:51:24.604
Engine 3 switch B - K232-203	13:45:02.759	13:51:24.637
Engine 4 switch A - K231-204	13:45:02.817	13:51:24.612
Engine 4 switch B - K232-204	13:45:02.859	13:51:24.571
Engine 5 switch A - K231-205	13:45:02.650	13:49:57.620
Engine 5 switch B - K232-205	13:45:02.667	13:49:57.637

4.4 SEPARATION SYSTEM

SYSTEM DESCRIPTION

Flight configuration of the S-II-8 stage separation system is described in SID 62-133, Separation System for the Saturn S-II Stage.

For static firing tests, the stage switch selector is stimulated by the Saturn V instrument unit computer simulator for sequencing the separation system. The separation signals are used to arm and trigger the EBW firing units. Because live ordnance is not used, EBW firing unit pulse sensors are substituted to indicate successful triggering of the firing units, which simulate initiation of S-II ullage motor ignition, S-II second-plane separation, S-II/S-IVB separation, and S-II/S-IVB retrorocket ignition. The C7-210 stage substitute rack was used to simulate the second-plane separation and ullage motor ignition EBW firing units and pulse sensors normally located in the S-II interstage, because the interstage is not installed during static firings.

TEST EVALUATION

The electrical portion of the separation system and the Mod II switch selector were sequenced during the static firing of the S-II-8. They performed within design requirements except that the separation system did not receive the LOX two-out-of-five dry cutoff signal which is used to trigger the two S-II/S-IVB separation and the two S-II/S-IVB retrorocket EBW firing units. This problem is discussed in the paragraph on S-II/S-IVB separation and S-II/S-IVB retrorocket ignition evaluation.

For S-II ullage motor ignition and second-plane separation, the associated firing unit simulators were electrically charged upon command and successfully triggered their associated pulse sensor simulators when the S-II ullage motor ignition and second-plane separation signals were sent. The following measurements were evaluated to verify proper system operation:

Measurement Number	Function
WK228-206	Separation system reset
K0034-206	Instrumentation bus On
K0035-206	Liftoff indication
M0082-206	Ullage motor firing unit 1A monitor
M0083-206	Ullage motor firing unit 1B monitor
M0086-206	Second separation firing unit 1A monitor
M0087-206	Second separation firing unit 1B monitor
K0237-206	Ullage pulse sensor 1A output
K0238-206	Ullage pulse sensor 1B output
K0239-206	Second separation pulse sensor 1A output
K0240-206	Second separation pulse sensor 1B output

For S-II/S-IVB separation and S-II/S-IVB retrorocket ignition, the four associated EBW firing units charged up to 4.4 + 0.5 vdc within 1.5 seconds after the arm signal was received from the switch selector. However, when the S-II/S-IVB separation trigger signal was sent from the switch selector, only S-II/S-IVB separation firing unit 1B and S-II/S-IVB retrorocket firing unit 1B successfully triggered, while S-II/S-IVB separation firing unit 1A and S-II/S-IVB retrorocket firing unit 1A did not trigger as expected. An investigation revealed that the S-II-8 separation system did not receive a LOX two-out-of-five dry cutoff signal, which is utilized for triggering the two S-II/S-IVB separation and the two S-II/S-IVB retrorocket firing units. The LOX two-out-of-five cutoff signal remained on for .589 seconds which was long enough to shutdown the S-II engines but not long enough to provide the cutoff signal for triggering the four S-II/S-IVB firing units. To have accomplished triggering of the firing units the cutoff signal would have had to remain on (dry) for at least 1.060 seconds. The reason S-II/S-IVB separation firing unit 1B and S-II/S-IVB retrorocket firing unit 1B triggered during the static firing was because of the manual application of GSE all-engines-cutoff command K9476-STM which was applied .324 seconds after the LOX two-out-of-five dry signal. The manual application of GSE all-engines-cutoff K9463-STM would have provided the trigger signal for S-II/S-IVB separation firing unit 1A and S-II/S-IVB retrorocket firing unit 1A but this signal was not applied during the S-II-8 static firing. During flight, a switch selector all engine cutoff command (channel 18) is applied as a backup cutoff command to the LOX two-out-of-five dry cutoff signal and would have provided a trigger signal to the four S-II/S-IVB separation and S-II/S-IVB retrorocket firing units. A review of AS-504 and AS-505 flight data indicated that the LOX two-out-of-five dry cutoff signal remained dry (on) until after S-II/S-IVB separation and therefore provided the cutoff signal for triggering S-II/S-IVB separation and S-II/S-IVB retrorocket ignition. Since the S-II-6 and subsequent flight stages have a 1.5 second time delay in the LOX depletion cutoff circuitry as did the S-II-4 and S-II-5 stages (contrasted to a one second time delay for this static firing), it is expected that the LOX depletion cutoff signal in the S-II-6 and subsequent flight stages will also remain dry (on) beyond S-II/S-IVB separation. The following measurements were evaluated to verify system operation.

Measurement Number	Function
M0101-206	S-II/S-IVB separation firing unit 1A monitor
M0102-206	S-II/S-IVB separation firing unit 1B monitor
M0084-206	S-II/S-IVB retrorocket firing unit 1A monitor
M0085-206	S-II/S-IVB retrorocket firing unit 1B monitor
K0243-219	S-II/S-IVB separation pulse sensor 1A output
K0244-219	S-II/S-IVB separation pulse sensor 1B output
K0241-219	S-II/S-IVB retrorocket pulse sensor 1A output
K0242-219	S-II/S-IVB retrorocket pulse sensor 1B output

Switch Selector

The Mod II switch selector was sequenced during the static firing and successfully responded to all input commands. The following measurements were evaluated to verify switch selector operations:

Measurement Number	Function
M136-206	Switch selector telemetry output
WM136-206	Switch selector telemetry output
WK222-206	Switch selector register reset
WK402-206	Switch selector address verification digit 1
WK403-206	Switch selector address verification digit 2
WK404-206	Switch selector address verification digit 3
WK405-206	Switch selector address verification digit 4
WK406-206	Switch selector address verification digit 5
WK407-206	Switch selector address verification digit 6
WK408-206	Switch selector address verification digit 7
WK409-206	Switch selector address verification digit 8

The Mod II switch selector events and event times are listed in Table 4.4-1.

Table 4.4-1. Mod II Switch Selector Events

Real Time (hr:min:sec)	Function	S-II Switch Selector	
		Code	Channel
13:42:12.895	Cutoff S-II J-2 engines	00110011	18
13:44:48.097	Start 1st PAM-FM/FM calibration	00000011	30
13:44:53.096	Stop 1st PAM-FM/FM calibration	00010011	9
13:44:53.296	S-II ordnance arm	01110011	11
13:44:57.595	LH_2 tank high-pressure vent mode	00110001	38
13:44:57.799	S-II ullage trigger	00010010	24
13:44:57.937	S-II hydraulic accumulator unlock	01001101	12
13:44:58.204	S-II LH_2 recirculation pumps off	00101100	48
13:44:58.398	S-II engines cutoff reset	00100011	31
13:44:58.597	Engines ready bypass	01101110	20
13:44:58.797	Prevalves lockout reset	01010010	19
13:44:59.614	S-II engine start	00011100	33
13:45:00.195	Engines ready bypass reset	00001100	49
13:45:04.796	Chilldown valves close	01011100	88
13:45:05.100	S-II start phase limiter C/O arm	00111101	25
13:45:05.237	High (5.5) engine mixture ratio on	01101011	59
13:45:06.098	S-II start phase limiter C/O arm reset	00101101	6
13:45:06.298	Prevalves close arm	01010110	99
13:45:29.098	S-II aft interstage separation	00100010	23

Table 4.4-1. Mod II Switch Selector Events (Cont)

Real Time (hr:min:sec)	Function	S-II Switch Selector	
		Code	Channel
13:46:42.767	S-II LOX step pressurization	00001101	14
13:47:03.397	Start 2nd PAM-FM/FM calibration	00000011	30
13:47:08.397	Stop 2nd PAM-FM/FM calibration	00010011	9
13:48:43.395	Start 3rd PAM-FM/FM calibration	00000011	30
13:48:48.396	Stop 3rd PAM-FM/FM calibration	00010011	9
13:49:57.397	S-II inboard engine cutoff	01101111	15
13:49:58.396	S-II LH$_2$ step pressurization	00011101	7
13:50:24.597	High (5.5) engine mixture ratio off	00111001	58
13:50:24.795	Low (4.5) engine mixture ratio on	01010100	56
13:50:46.395	S-II/S-IVB ordnance arm	00111111	8
13:50:47.195	S-II LOX depletion sensors C/O arm	01100010	3
13:50:47.398	S-II LH$_2$ depletion sensors C/O arm	01011110	42
13:51:25.402	S-II/S-IVB separation	00000010	5

4.5 PROPELLANT DISPERSION SYSTEM

SYSTEM DESCRIPTION

The propellant dispersion system (PDS) is that portion of the flight termination system downstream of the range safety command receivers. The PDS must be capable of thrust termination (engine cutoff) and propellant dispersion by radio command and must also be capable of being turned off (safed) by radio command. Functionally, the PDS is the same as that used on the S-II-7 static firing. The complete description of the PDS is described in SID 62-134, Propellant Dispersion System for the Saturn S-II.

TEST EVALUATION

The electrical portion of the PDS that was sequenced during the static firing performed within design requirements with no malfunctions. The safe command was sent approximately 32 seconds after engine start. This command removed power from the range safety command decoders and receivers. The safe command was removed and power was restored to the decoders and receivers, approximately four seconds after application of the safe command, by the manual GSE application of system 1 and system 2 receiver internal power transfer commands.

5.0 MEASUREMENT, TELEMETRY, AND RF SYSTEMS

5.1 SYSTEMS DESCRIPTION

MEASUREMENT SYSTEM

The flight measurement system contains all the transducers, signal conditioners, power supplies, and patch panels to measure and supply suitably scaled signal inputs to the telemetry system for all measurement requirements defined in the S-II-8 Instrumentation Program and Components List (IPCL), (V7-976408). The onboard remote automatic calibration system (RACS) that interfaces with the ground automatic checkout equipment is also a part of the measurement system.

Measurements are categorized by the type of variable being measured, the rate of change of the variable with respect to time, the amplitude or signal level of the measured quantity, and other considerations. Table 5.1-1 lists the number of measurements, under each code name and parameter contained in the IPCL for the S-II-8 flight configuration.

Table 5.1-1. S-II-8 Flight Measurements

Measurement Code*	Measurement Parameter	Total
A	Acceleration	-
B	Acoustics	-
C	Temperature	95
D	Pressure	111
E	Vibration	-
F	Flowrate	10
G	Position	44
K	Discretes	254
L	Liquid level	4
M	Voltage and current	33
N	Miscellaneous	2
R	Angular velocity	-
S	Strain	-
T	Tachometer	10
IPCL total**		563

*Part of measurement number that denotes parameter
**Includes 43 measurements taken hardwire through umbilical.

The configuration of the S-II-8 stage measurement system was the same as that defined in SD 68-655 for the S-II-6 static firing.

TELEMETRY AND RF SYSTEM

The telemetry (TM) system contains the equipment for data gathering, time or frequency multiplexing and signal conversion to the formats required for transmitter modulation. This equipment is interspersed throughout the vehicle and interconnected to provide separate data links to the radio frequency (RF) transmitters. The three data links consist of two frequency modulation (FM) links and one pulse-code modulation (PCM) link.

The RF system contains the equipment necessary for range safety; i.e., provides positive control of engine cutoff, arming, and propellant dispersion. Also included in the RF system are the transmitters and a telemetry antenna subsystem required for conditioning and transmission of telemetry data signals to the receiving ground stations.

A detailed description of the TM and RF equipment is contained in the Instrumentation Subsystem Report, SID 62-136. The configuration of the TM and RF equipment for this test was the same as that defined in SD 68-655 for the S-II-6 static firing.

5.2 TEST EVALUATION

Acceptance test specifications for S-II-8 static firing at MTF are contained in MA0201-4368 (S-II-6 and Subs RL). System performance data for test 546 and applicable test specification requirements are contained in Section 5.0 of Volume 1 of this report.

MEASUREMENTS EVALUATION

Active stage measurements performance was satisfactory for this test. Reasonable ambient condition data were received on 98.6 percent of all active measurements throughout the static firing test.

Volume I of SD 69-329 identifies all of the flight measurement system problems associated with the S-II-8 static firing. The problems were associated with the failure of the following measurements:

C004-202	E2 LOX turbine inlet T
C012-202	E2 Helium tank gas T
C329-201	E1 Thrust chamber jacket T
C329-205	E5 Thrust chamber jacket T
C648-219	H_2 Pressure regulator out T
F001-203	E3 Main fuel flow
F001-205	E5 Main fuel flow

The transducers for all of the above temperature measurements have been replaced. The failure of the fuel flow measurements has been attributed to the motherboard/harness assembly in the flow and tach chassis. This chassis will be replaced when a new chassis is made available.

The RF and Telemetry Systems as indicated in Volume I experienced no problems during this test.

RF transmitters and telemetry antenna subsystems performance was satisfactory and within specification limits throughout the static firing test. The RF power output of the three telemetry transmitters exceeded the minimum required power level of 28 watts. Voltage standing wave ratio (VSWR) calculations were satisfactory as determined in Volume 1.

TELEMETRY SUBSYSTEM EVALUATION

Performance of the two FM/FM telemeters and the PCM/FM telemeter was as expected and within specification limits set for this test. PCM encoding accuracies, five-volt dc reference power supplies and low-level temperature bridge power supplies performances were as determined in Volume I. The inflight calibration levels (5 voltage steps) levels were received within specification limits on BF1 and BF2 IRIG channels and on all calibrating AO and BO TOM channels.

SPACE DIVISION of NORTH AMERICAN ROCKWELL CORPORATION

6.0 INSULATION AND PURGE SYSTEMS

SYSTEM DESCRIPTION

The S-II-8 stage was the first S-II stage to utilize spray foam insulation for the forward bulkhead, forward skirt, sidewall, and bolting ring areas. S-II-6 and S-II-7 used spray foam insulation only on the forward bulkhead and the bolting ring. The use of spray foam insulation also eliminated the need for purging these areas. Additionally, the maturing status of the stage structure permitted deletion of the leak detection system. The forward bulkhead uninsulated area, common bulkhead, and J-ring voids were purged.

The change in the LH$_2$ feedline elbow configuration from the flange heel fillet weld to the butt weld eliminated the requirement for both purge and leak detection.

Based upon results of tests on S-II-6 and S-II-7 stages, the forward bulkhead seal drain system was deleted and all seal drain test ports were capped on the S-II-8 stage. The purge circuit for the five engine cutoff sensor flanges was supplied with helium from facility sources by a temporary hard line.

TEST EVALUATION

The S-II-8 stage was subjected to two cryogenic operations at the Mississippi Test Facility. A cryogenic proof-pressure test was performed on 28 March 1969 and was followed by the 385-second full duration acceptance static firing on 8 April 1968.

The purge system performed satisfactorily during both the cryoproof test and the acceptance firing. All pressure traces indicated that purge gas flows were within design limits and operational expectations. The performance of each individual circuit is described in the following paragraphs. Further details are contained in Volume I of this report.

Forward Bulkhead Uninsulated Area

The circuit was set up to a flow rate of 6.4 scfm of helium at an inlet pressure of 0.8 psig. During operation the inlet pressure remained well within the circuit requirements, which indicated that the system operated satisfactorily.

J-Ring Circuit

The inlet and outlet pressures of the J-ring circuit indicated satisfactory operation during both cryogenic operations.

Common Bulkhead

Evacuation began about 28 minutes prior to starting LOX loading. Figure 6-1 shows the pumpdown curve. The internal bulkhead pressure was below 1 psia throughout the test. The specification requirement is 3 psia maximum at the time of engine ignition. The vacuum decay rate of 2 mm Hg/hour before and after cryotesting indicates a very tight bulkhead.

Engine Cut-off Sensors

During set-up for static firing, the flow rate of 3.5 scfm exceeded the minimum specification allowable of 1.1 scfm. During cryo-operation the inlet pressure was steady.

Insulation Evaluation

The spray foam insulation performance was excellent during both cryogenic operations. No unpredictable problems occurred as a result of either tanking. Inspection of 42 discrepancies in the insulation showed all defects would be easily repaired with existing specifications and procedures. The types of discrepancies that were identified have been experienced in prior spray foam development tests.

The principal problems concern the following:

1. Debonds occurred between the cork facing sheet and the spray foam in the feedline elbow cavities 3, 4, and 5. These were caused by cryopumped gases which leaked in liquid form into foam voids. These revaporized and formed bubbles under the scrim cloth after LH_2 depletion. Figure 6-2 shows the approximate location of the discrepancies in the lower cylinder bolting ring and cylinders 2 and 3. Engineering direction has been released which will seal all suspect areas.

2. Debonds occurred between the aluminum tank wall and the adhesive bond of the honeycomb rail which supports the corks outer facing sheet on the right side of feedlines 2 and 5. The principal cause of the failure was the thick adhesive bond line.

Inspections of 33 areas on the S-II-8 have included the integrity of bond lines. Similar inspections have been planned for subsequent stages.
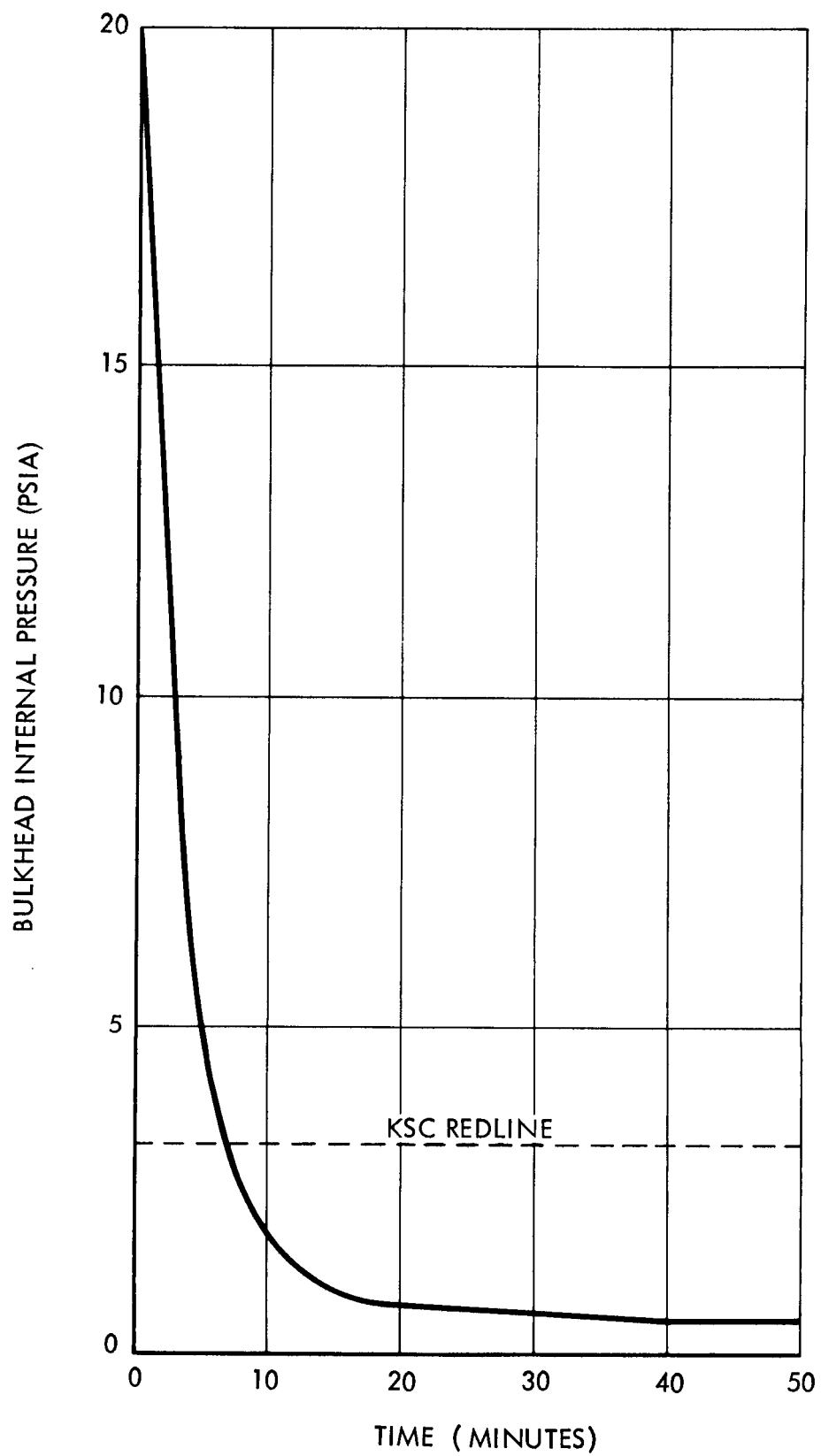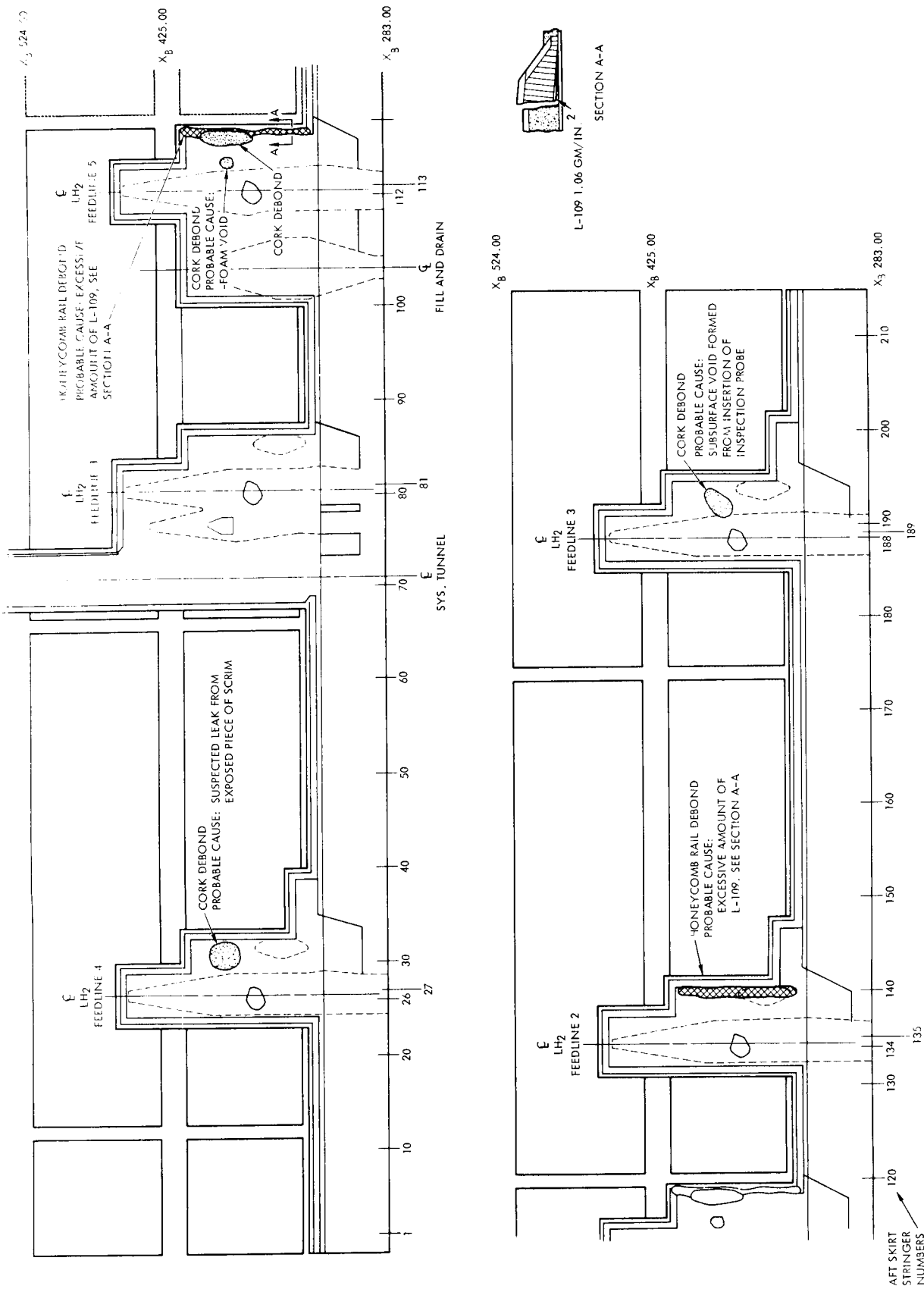
Figure 6-1. Common Bulkhead Evacuation

Figure 6-2. Discrepancies in Cork/Foam Insulation System in S-II-8 After Cryoproof and Static Firing

SD 69-329

7.0 VIBRATION AND ACOUSTIC ENVIRONMENT

An extensive hardwire vibration instrumentation system, capable of measuring dynamic responses in the frequency range from 5 to 10,000 Hertz, was used on all previous S-II stage acceptance firings. Except for the engine vibration safety cutoff transducers, this hardwire system has been eliminated from S-II-8 and all subsequent stages.

The S-II-8 acceptance firing did, however, employ a special, limited hardwire vibration measurement system. The purpose was to obtain data on the effects of early center engine cutoff, which was tested for the first time on this acceptance firing.

A thorough evaluation of the vibration data was made at Mississippi Test Facility, immediately after the firing. The results are reported in Volume I of this report. Review of that data at Seal Beach revealed no further information for inclusion in this section. Section 2.3 of this report includes a comparison of S-II-8 dynamic pressure and vibration data processed by the Seal Beach data station.

8.0 THRUST STRUCTURE COMPLIANCE

SYSTEM DESCRIPTION

Thrust Structure

The thrust structure for stages S-II-4 through S-II-10 have undergone design changes (from configuration of S-II-1, -2, -3) on two separate occasions.

The initial changes were brought about as part of the S-II stage weight reduction program. The two principal means of reducing weight were the use of thinner materials and the substitution of 2020-T6 aluminum alloy extrusions in structural members designed primarily by consideration of compression loads. The S-II-4 and S-II-5 stages were static fired with these structural modifications. Engine deflections due to thrust structure compliance were evaluated and reported in SD 68-104, Volume 2, S-II-4 Static Firing Final Test Report, dated 26 April 1968, and in SD 68-377, Volume 2, S-II-5 Static Firing Final Test Report, dated 1 November 1968.

Subsequent to the static firings of the S-II-4 and S-II-5 stages, ECP 5644 authorized further changes to the thrust structure for stages S-II-4 through S-II-10. Primary changes were the addition of a reinforcing bar to the thrust structure engine mount frame outer cap (station 112) in the area of the four thrust blocks and reinforcement of the center engine thrust beam webs and end fittings. As a consequence of these modifications, a reevaluation of compliance was performed from data obtained during the static firing of the S-II-8 stage per ECP 6304. The results are presented in this section.

Engine Deflection Measurement System

The measuring system was comprised of four motion picture cameras stationed in the pitch and yaw planes of engines 1 and 3, eight wall-mounted target illumination lamps (two for each camera), and engine targets in a vertical array mounted on the engine hatbands. The targets were a 1-inch by 2-inch highly reflective surface contiguous to a 1-inch by 2-inch dull black surface. The reflective surface is on the left as seen by the camera. The cameras were arranged as shown in Figure 8-1. The motion picture films were evaluated with a Telereadex film data reader. Accuracy of the angular measurements was 0.1 degree. A minimum of 12 readings per camera was obtained for each of the test conditions listed in Table 8-1. The purpose in making several readings during each test condition was to get an average deflection during the interval. This minimizes random effects of engine vibrations and film reading errors.

TEST EVALUATION

J-2 engine alignment on the Saturn S-II stage changes when engine thrust conditions change because of compliance in the thrust structure. The outboard engine's pre-cant angle is set to minimize the effects on payload, base heating and second-plane separation clearances of these alignment changes.

The cameras photographed changes in engine alignment due primarily to thrust changes. Four test conditions were measured. These are defined in Table 8-1 in terms of thrust state of the outboard and center engines (on-off), and engine mixture ratio (EMR).

The results of the motion picture evaluation are summarized in Table 8-1 for all four camera monitoring stations. The principal results are shown in column 7 of the table. These are the in-plane alignment changes corresponding to a change from a thrust-on condition at maximum (i.e. at high EMR) thrust for all five engines to a thrust-off condition. The average or nominal in-plane alignment change (average of pitch and yaw alignment changes of engines 1 and 3) for this condition is seen to be 0.64 degrees. The resulting nominal cross-corner engine deflection is therefore 0.9 degrees.

The ratio of thrust at altitude to thrust at sea level for S-II flights is approximately 1.4:1, so the nominal cross-corner engine deflection predicted for the S-II-8 at altitude (vacuum) conditions is 1.3 degrees. This prediction applies to stages S-II-6, -7 and to S-II-9 and -10 as well because the thrust structure design is common to each of these stages. This prediction is a significant change from the 1.9 degrees quoted for these stages in SD 68-377. The difference (0.6 degree) is attributed to rework of the station 112 frame (see System Description) and was expected to be about 0.4 degree. Therefore, reasonable agreement is evident between these measurements and the expected values.

The data presented in columns 8, 9, and 10 are also of interest. Column 8 indicates the change in alignment (0.45 degree) contributed by the thrust of four outboard engines at the maximum thrust condition. Column 9 indicates the change in alignment (0.42 degree) with four outboard engines at minimum thrust condition (i.e., at low EMR). The expected change in alignment between the high EMR and the low EMR thrust conditions was about 0.07 degrees, or about twice the difference shown in the table. However, the film data reader cannot resolve differences this small because of the limit accuracy of the equipment. Column 10 indicates the contribution from the center engine thrust to the alignment changes of the outboard engines. This is seen to average 0.2 degree in a plane, which results in an average cross-corner alignment change at CECO of 0.3 degrees at sea level and an estimated 0.4 degrees at altitude.

Based on the foregoing evaluation, the outboard engine's pre-cant angle for stages S-II-7 through S-II-10 shall be 1.3 degrees (was 2.3 degrees). This change has been authorized by ECP 6348.

8-2

Table 8-1. Summary of Average Engine Compliance Deflections From S-II-8 Stage Static Firing Test A2-546

		Test Conditions Identification				Compliance Deflection in Pitch or Yaw Planes			
Outboard engines Thrust condition		On	On	On	Off	Five Engines Thrusting at EMR = 5.5 (Absolute value of difference between conditions 1 and 4)	Four Engines Thrusting at EMR = 5.5 (Absolute value of difference between conditions 2 and 4)	Four Outboard Engines Thrusting at EMR = 4.7 (Absolute value of difference between conditions 3 and 4)	Change in Compliance Due to Center Engine Shut-off (Absolute value of difference between conditions 1 and 2)
Center engine Thrust condition		On	Off	Off	Off				
Engine Mixture Ratio (EMR)		5.5	5.5	4.7	-				
Nominal thrust levels* (Engines 1 and 3)		166,000	166,000	123,000	0				
Test condition numbers		1	2	3	4				
Engine	Camera Station	Averages of Measured Pitch Plane Deflections** (Degrees)							
1 Pitch	4A	-0.08	0.06	0.08	0.42	0.50	0.36	0.34	0.14
3 Pitch	3A	-0.38	-0.13	-0.06	0.12	0.50	0.25	0.18	0.25
		Averages of Measured Yaw Plane Deflections** (Degrees)							
1 Yaw	1A	0.85	0.62	0.53	-0.06	0.91	0.68	0.59	0.23
3 Yaw	6A	0.27	0.10	0.18	-0.39	0.66	0.49	0.57	0.17
AVERAGE IN-PLANE DEFLECTIONS***						0.64	0.45	0.42	0.20

*Center engine high EMR thrust = 164,900 pounds
**Relative to an arbitrary reference set before reading the measurements. Positive angles represent clockwise rotation from reference.
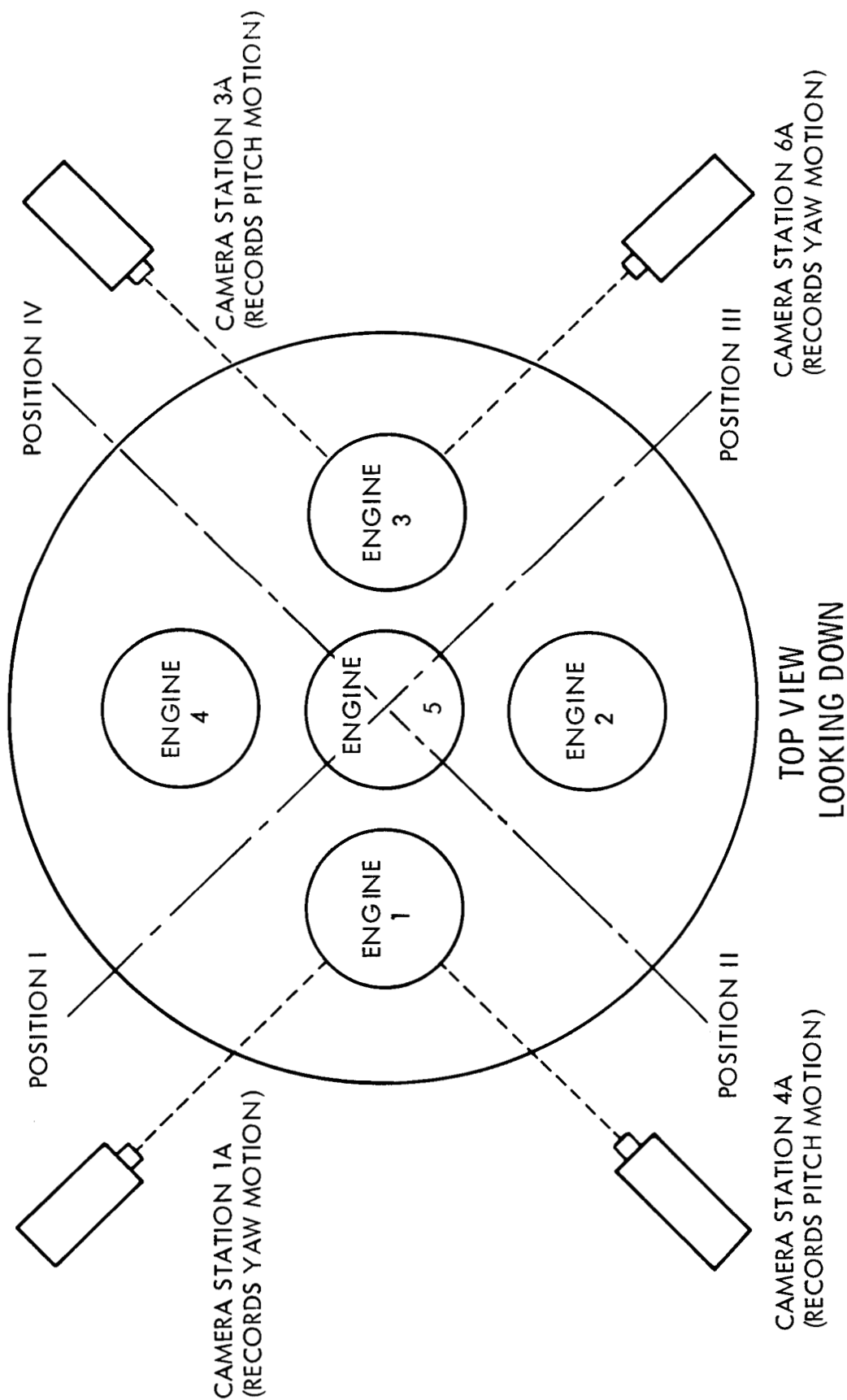***Motion causes engine to move inboard toward stage centerline if thrust change is positive and outboard if negative.

Figure 8-1. S-II-8 Static Firing Camera Layout Diagram

SD 69-329